Title
Numerical Simulation of Land Subsidence in the Los Banos-Kettleman City Area, California

Authors
Larson, Keith J
Basagaoglu, Hakan
Marino, Miguel A

Publication Date
1999-10-01

Numerical Simulation of Land Subsidence in the Los Banos-Kettleman City Area, California

By
Keith J. Larson[1], Hakan Basagaoglu[1] and Miguel A. Mariño[2]
[1]Department of Civil & Environmental Engineering
[2]Department of Land, Air, and Water Resources and
Department of Civil & Environmental Engineering
University of California, Davis
Davis, CA 95616

TECHNICAL COMPLETION REPORT

Project Number UCAL-WRC-W-892

October 1999

University of California Water Resources Center

The research leading to this report was supported by the University of California Water Resources Center, as part of Water Resources Center Project UCAL-WRC-W-892.

ABSTRACT

Land subsidence caused by the excessive use of ground water resources has traditionally caused serious and costly damage to the Los Banos-Kettleman City area of California's San Joaquin Valley. Although the arrival of surface water from the Central Valley Project has reduced subsidence in recent decades, the growing instability of surface water supplies has refocused attention on the future of land subsidence in the region. This report develops a three-dimensional, numerical simulation model for both ground water flow and land subsidence. The simulation model is calibrated using observed data from 1972 to 1998. A probable future drought scenario is used to consider the effect on land subsidence of three management alternatives over the next thirty years. Maintaining present practices virtually eliminates unrecoverable land subsidence, but with a growing urban population to the south and concern over the ecological implications of water exportation from the north, it does not appear that the delivery of surface water can be sustained at current levels. The two other proposed management alternatives reduce the dependency on surface water by increasing ground water withdrawal. Land subsidence is confined to tolerable levels in the more moderate of these proposals, while the more aggressive produces significant long-term subsidence. Finally, an optimization model is formulated to determine maximum ground water withdrawal from nine water sub-basins without causing irrecoverable subsidence over the forecasted period. The optimization reveals that withdrawal of ground water supplies can be increased in certain areas in the eastern side of the study area without causing significant subsidence.

KEY WORDS: Subsidence, ground water and ground water hydrology, optimization, systems modeling, environmental impacts

TABLE OF CONTENTS

LIST OF TABLES

LIST OF FIGURES

1. INTRODUCTION

The San Joaquin Valley is an important agricultural region in California, contributing billions of dollars to the state's economy and providing jobs and food for the state's growing population. As such, providing affordable water for agriculture has traditionally been a high priority for water managers in the region. In recent years, however, a limited water supply has created economic and environmental concerns that threaten the viability of agriculture in portions of the Valley.

One of the more subtle of these concerns is land subsidence. Land subsidence is defined as a lowering of the land surface elevation. Although this geological/hydrological hazard progresses slowly, it can result in significant economic losses over time (Hua et al., 1993). In the San Joaquin Valley, land subsidence has caused serious and costly damage to highways, water-transport structures and deep water wells (Ireland et al., 1984). Although there are several causes of land subsidence, the majority of subsidence in the Valley can be attributed to overpumping of the aquifer system underlying the region.

Prior to 1967, the main source of irrigation water was ground water. As unregulated pumping accompanied rapid agricultural development, dramatic drawdown occurred in the aquifers underlying the region. One result of this drawdown was severe land subsidence throughout much of the Valley. In 1967, the completion of the California Aqueduct provided a new source of water for irrigation. As canals and delivery systems were completed, the demand for ground water was reduced and land subsidence rates correspondingly decreased. However, the inevitability of drought and the continued growth of urban areas to the south made the aqueduct a less than reliable alternative. This was made evident in 1977 and the early 1990s as drought forced a renewed dependence on ground water and the return of subsidence.

The goal of this research is to evaluate the effects of existing and proposed water management plans on land subsidence in the Los Banos-Kettleman City region of the San Joaquin Valley. This will be accomplished through: (1) employment of existing numerical models to simulate ground water flow and land subsidence over the Los Banos-Kettleman City region; (2) calibration of the overall model using observed ground water and compaction data for the years 1972 to 1999; (3) identification of the most influential aquifer parameters and their roles in model calibration; (4) construction of future water availability scenarios; and (5) implementation of the calibrated model to estimate future land subsidence to test the existing and proposed management alternatives.

2. BACKGROUND

2.1 Subsidence in the San Joaquin Valley

California's San Joaquin Valley (Figure 1) is one of the most productive and intensely farmed agricultural areas in the world (American Farmland Trust, 1995). The Valley has been experiencing land subsidence and its negative implications as early as the 1920s (Ireland et al., 1984). Intense abstractions of ground water in excess of natural recharge caused ground water storage depletion and resulting land subsidence across the Valley. In 1969, subsidence reached nearly 29 feet in one location with a total volume of 15.5 MAF (Poland, 1981).

Subsidence can have several negative economic, social, and technical implications. Problems associated with land subsidence include: (1) changes in ground water and surface water flow patterns (e.g., Lofgren, 1979); (2) ground water quality deterioration and salt-water encroachment (e.g., Belitz and Philips, 1995); (3) decline in aquifer storage capacity; (4) flooding (e.g., Hua et al., 1993); (5) failure of well casings and changes in channel gradient (e.g., Holzer, 1989); and (6) damage to highways, buildings, and other structures (e.g., Ireland et al.,

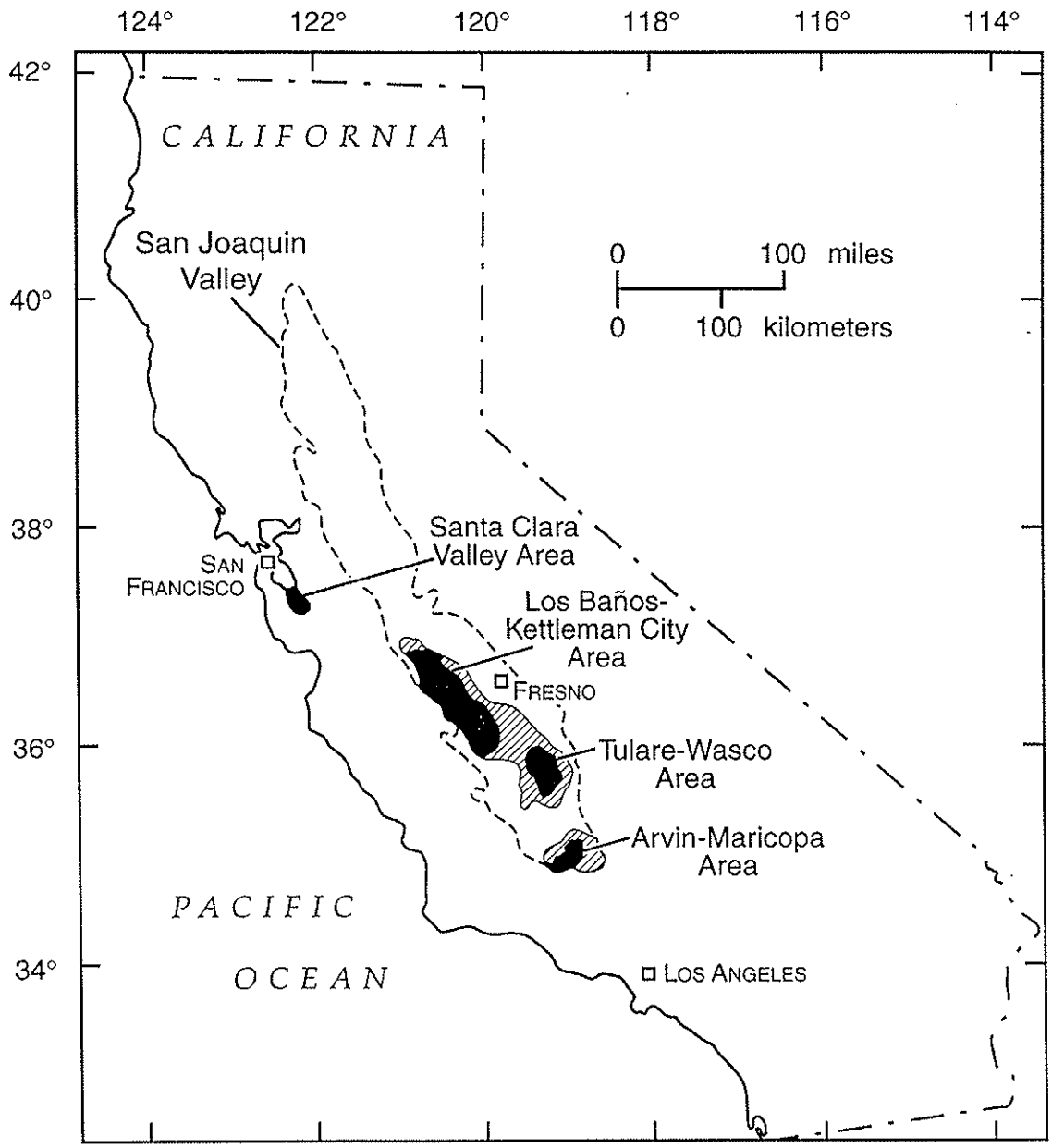

Figure 1 - Areas of observed land subsidence in California

1984). By the mid-1960s, several regions in the San Joaquin Valley were facing many of these problems (e.g., Ireland, 1986).

The arrival of surface water supplies in the late 1960s greatly reduced the amount of ground water withdrawn from the region. With the reduction in pumpage, the rate of land subsidence slowed down. During droughts in 1976-77 and 1990-1992, however, ground water supplies were pumped heavily to meet demand as surface water deliveries were reduced. In the Los Banos-Kettleman City area, pumpage increased to 470,000 acre-feet in 1977 compared to a yearly average of less than 100,000 acre-feet from 1974 to 1976 (Ireland et al., 1984). The result was a return to subsidence rates comparable to those before the arrival of surface water.

In addition to drought, several other factors threaten future surface water supplies to the San Joaquin Valley. The growth of urban populations to the south places an increasing strain on existing imported water supplies. There is also growing concern over the ecological impact of exportation of water from the north. The surface water for the Valley remains precariously balanced between competing urban, environmental, and agricultural interests. Although recent measurements reveal that annual average land subsidence rates have declined over the last three decades, the volatile future of surface water in the region maintains land subsidence as a serious concern to local and state water agencies (California Department of Water Resources, 1998).

2.2 The Los Banos-Kettleman City Region

Three areas of the San Joaquin Valley exhibit especially severe subsidence: the Los Banos-Kettleman City area, the Tulare-Wasco area, and the Arvin-Maricopa area. The area chosen for this research comprises the northern portion of the Los Banos-Kettleman City area. This 550-square-mile region of western Fresno County (Figure 2) has been chosen because of the large amount of ground water and land subsidence data available. Additionally, several previous

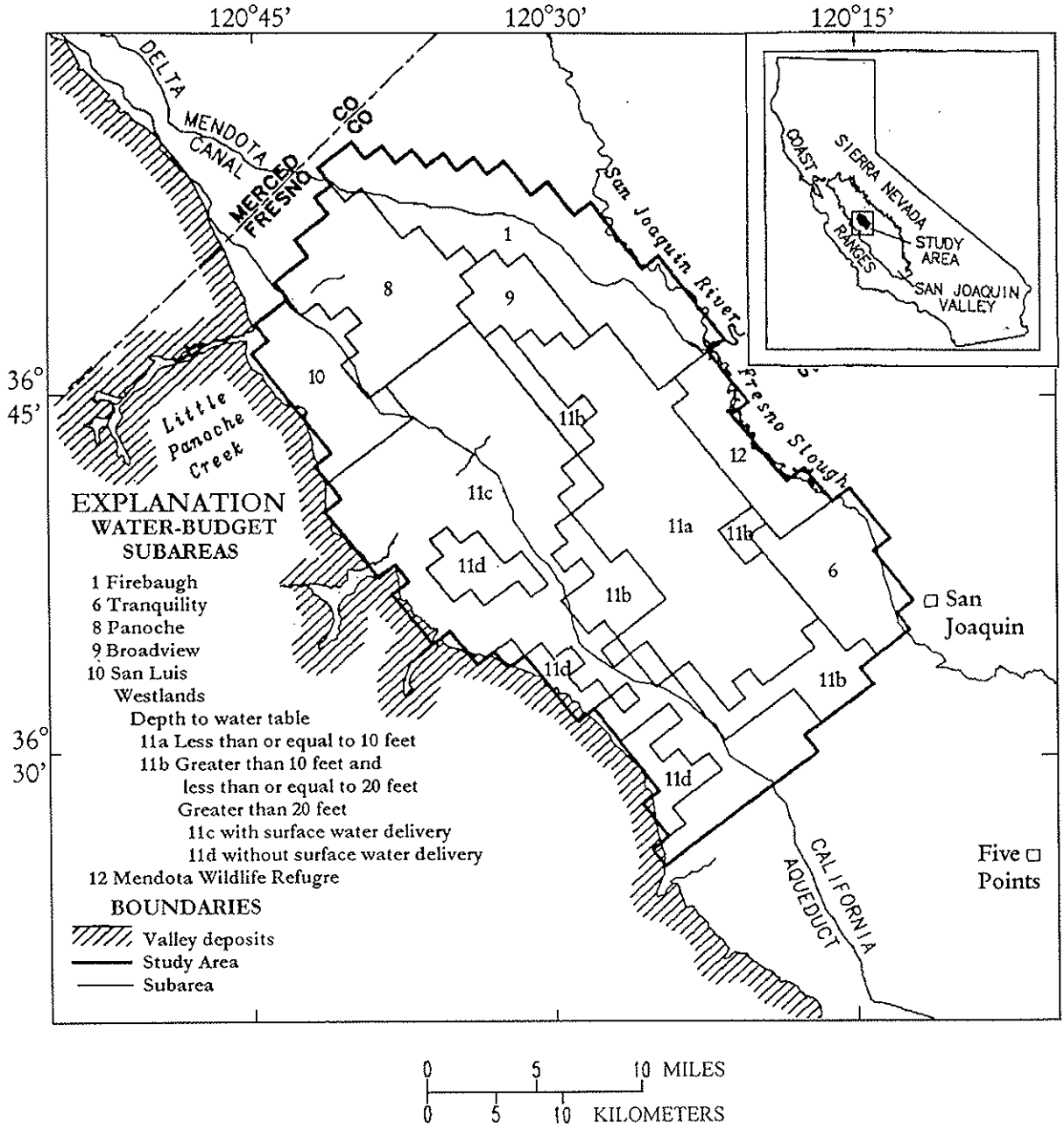

Figure 2 - Location of Study Area and Water Budget Subareas
(Modified from Gronberg and Belitz, 1992)

studies have been conducted in the region, providing important insight into several aspects of this research.

2.2.1 Hydrogeology

The hydrogeology of the Los Banos Kettleman City area was previously documented by Miller et al. (1971) and Belitz and Heimes (1990). From their reports, the subsurface flow system is divided into upper and lower water-bearing zones, which are separated by the Corcoran Clay Member of the Tulare Formation (Figure 3). The thickness of the Corcoran Clay Member ranges from 20 to 120 ft (Page, 1986) and consists of low-conductivity lacustrine deposits (Johnson et al., 1968).

The unconfined to semi-confined zone above the Corcoran Clay member consists of Coast Ranges alluvium, Sierran sand, and flood basin deposits. The Coast Ranges alluvium reaches a thickness of more than 800 ft near the western edge of the valley. It is composed of sand and gravel along the stream channels and at the fan heads, and of clay and silt in the distal fan areas (Laudon and Belitz, 1991). The Coast Ranges alluvium is interfingered laterally with the Sierran sand, which consists of well-sorted medium to coarse-grained fluvial sand reaching a thickness of 400-500 ft in the valley trough (Miller et al., 1971). Flood-basin deposits, with a thickness of 5-35 ft, overlie the Sierran sand at the center of the valley (Laudon and Belitz, 1991). The quality of ground water of the upper water-bearing zone is generally poor with high concentrations of calcium, magnesium, and sulfate, except near Fresno Slough (Bull and Miller, 1975).

The lower water-bearing zone is locally less permeable than the upper-water bearing zone. It is also much thicker, ranging from 570 to 2460 ft (Williamson et al., 1989). In general, it is composed of poorly consolidated flood-basin, deltaic, alluvial-fan, and lacustrine deposits of

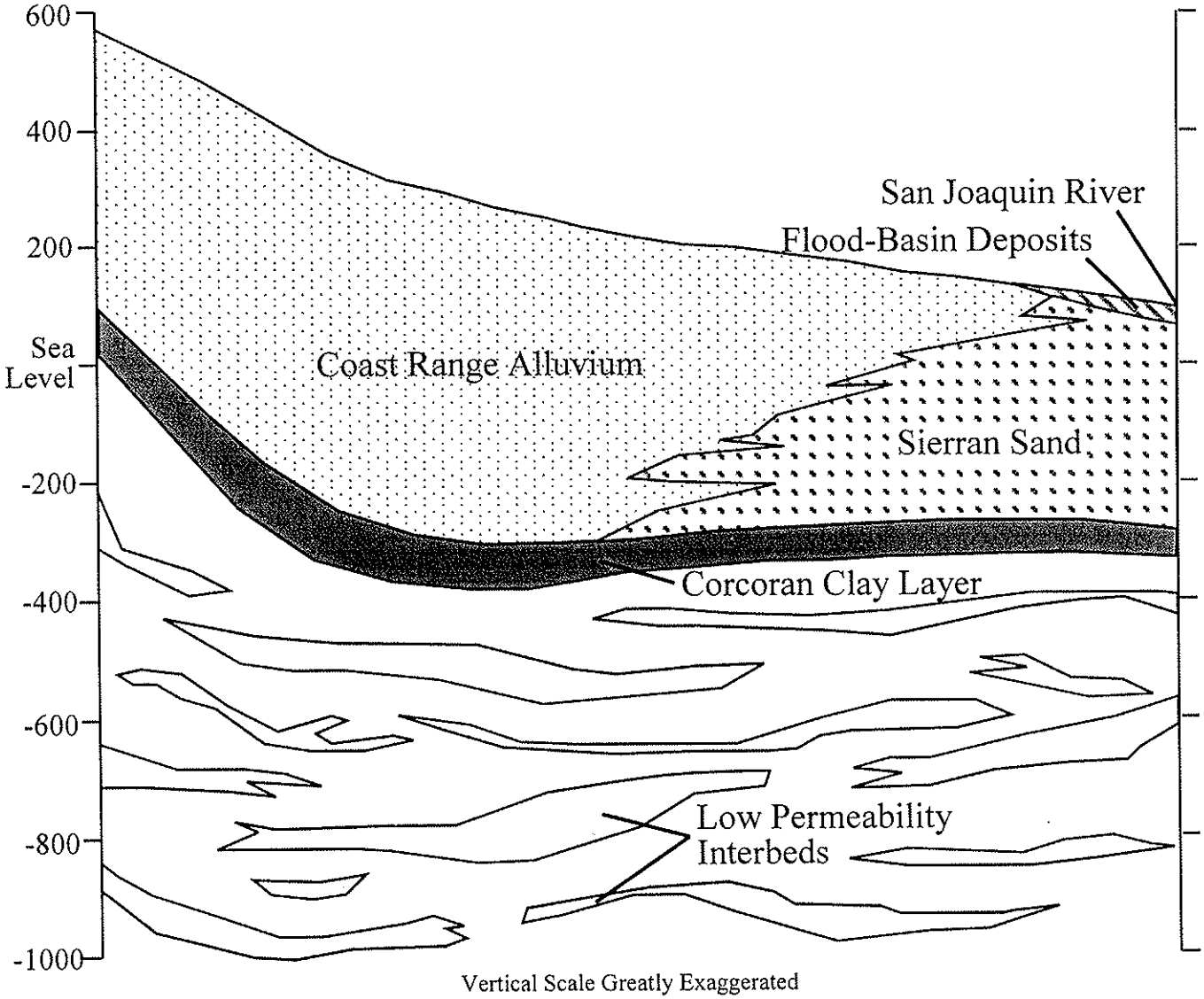

Figure 3 - Hydrogeologic Cross-section of the Study Area
(Modified from Belitz et al.,1992)

Tulare formation (Bull and Miller, 1975) characterized by discontinuous clay lenses embodied with sand and gravel deposits. Before surface water supplies were made available to the Los Banos-Kettleman City area through aqueducts and irrigation channels, 75-80% of irrigation water was pumped from the lower water-bearing zone due to its greater thickness and better water quality (Bull and Miller, 1975; Ireland et al., 1984).

2.2.2 Water Budget

Gronberg and Belitz (1992) performed an analysis of ground water pumpage, recharge, and irrigation efficiency for the Los Banos-Kettleman City region. This analysis resulted in two water budgets for the years 1980 and 1984. The Los Banos-Kettleman City area is divided into nine water-budget subareas based on water district boundaries and depth to water table (Figure 2). An area-weighted average irrigation efficiency is calculated for each subarea as a function of depth to water table. The irrigation efficiency is subsequently used to compute the irrigation requirement in each water budget subarea. If the computed irrigation requirement exceeds surface water delivery, the unmet water requirement is supplied from the ground water reservoir; otherwise no pumpage takes place. The required ground water pumpage volume is spread uniformly over each subarea.

Gronberg and Belitz (1992) did not consider drought in their water budget analysis. However, drought will have a substantial influence on the rate and magnitude of land subsidence. During normal water years, this report will adopt the same pumping rates and spatial distribution between subareas as that computed by Gronberg and Belitz (1992) for the year 1980 (Table 1). For drought periods, however, ground water pumping rates will be a function of available surface water supplies. This will be discussed in greater detail in subsequent sections.

Table 1 - Revised Water Budget for 1980
(Modified from Gronberg and Belitz, 1992)

Subarea	Area (mi^2)	Surface Water Delivery (ft/yr)	Ground Water Pumpage (ft/yr)	Ground Water Recharge (ft/yr)
Firebaugh	73	2.63	0.0	0.75
Panoche	48	2.48	0.0	0.96
Broadview	16	2.75	0.0	0.78
Tranquility	30	2.51	0.30	0.84
San Luis	30	1.86	0.40	0.79
WestLands				
Depth to Water < 10 ft	97	1.90	0.40	0.46
10 ft < Depth to Water < 20ft	42	2.19	0.46	0.74
Depth to Water > 20 ft				
with suface water	163	2.43	0.25	0.94
without surface water (1980)	30	0.0	2.46	0.86

2.2.3 Surface Water Supplies

The State Water Resources Control Board (SWRCB) issued the first water rights to the U.S. Bureau of Reclamation (USBR) for operation of the Central Valley Project (CVP) in 1958 and to the California Department of Water Resources (DWR) for operation of the State Water Project (SWP) in 1967. Principal facilities of the SWP include Oroville Dam, Delta facilities, the California Aqueduct, and North and South Aqueducts. The principal facilities of CVP include Shasta, Trinity, Folsom, Friant, Clair Engle, Whiskeytown, and New Melones dams, Delta facilities, and the Delta Mendota Canal. Joint SWP/CVP facilities include San Luis Reservoir and Canal and various Delta facilities (California Water Plan Update, 1998). Although it arrives through an SWP facility (the California Aqueduct), all of the surface water used in the study region is contracted through the CVP and delivery rates are determined by the USBR.

2.3 Numerical Models

2.3.1 The Ground Water Flow Model

Ground water levels for the Los Banos-Kettleman City area were previously modeled by Belitz et al. (1992) using MODFLOW, a modular finite-difference flow model developed by McDonald and Harbaugh (1988). MODFLOW is a three-dimensional ground water simulation model that has been successfully used in real world problems involving aquifer simulation (e.g., Sophocleus and Perkins, 1993; Reynolds and Spruill, 1995; Bumb et al., 1997; Hubbel et al., 1997). It can simulate anisotropic and heterogeneous aquifer systems with various boundary conditions.

MODFLOW's structure is described as modular because it consists of one main program surrounded by a group of "modules" or packages. Each package considers different aspects of ground water flow. Packages are available to evaluate evaporation, recharge, drains, and land

subsidence to name a few. A modular structure is advantageous because it allows for the addition of new features without much alteration of the existing code.

The focus of the research by Belitz et al. (1992) was drainage and water quality problems in the aquifer above the Corcoran layer. Although it does not simulate land subsidence, their model provides a calibrated estimate of ground water flow in the Los Banos-Kettleman City area. This report adopts the Belitz et al. (1992) ground water model to simulate flow in the upper and lower aquifer, however, modifications are made to the model in order to: (1) consider ground water flow and subsidence in the aquifer system's low-conductivity layers; and (2) account for the time delay of consolidation. The inclusion of land subsidence simulation is accomplished by coupling the modified ground water simulation model of Belitz et al. (1992) with the Interbed Storage Package-1 (IBS1) of Leake (1991).

2.3.2 The Land Subsidence Model

The relationship between ground water movement and land subsidence was not well understood at the beginning of the century. In the 1920s, Karl Terzaghi began investigating the relationship between stress and the compression of soils. His one-dimensional consolidation theory (Terzaghi, 1925) became the foundation for almost all current subsidence models, including the IBS1 model (Leake, 1991) used for this report. This theory encompasses the following principles (Holtz and Kovacs, 1981).

As a saturated soil is loaded, it can change volume through three mechanisms: (1) compression of the soil particles; (2) compression of the water within the soil; and (3) expulsion of water from the soil and the resulting deformation of the soil matrix. The first two processes can easily be explained using simple stress-strain relationships, but their contribution to overall compression is small. The third process, the release of water from the soil matrix,

dominates the compression of soil. Consequently, the rate of soil compression is governed by the rate at which water can leave the soil matrix. Low-conductivity soils such as clays can continue to compress for years after being loaded because the water in the clay escapes very slowly.

Underlying this observation is the concept of effective stress. As a load is applied to a low-conductivity soil, the water towards the middle of the soil is unable to escape and pore water pressure develops. The pressure that remains supports the soil matrix and is called residual pore pressure. No compression will occur until the pore pressure dissipates as the water flows out of the soil. To account for the presence and effects of pore pressure, Terzaghi (1925) defined an effective stress. This is the stress "felt" by the soil matrix and can be written as:

$$\sigma' = \sigma - u \tag{1}$$

in which σ' is the effective stress; σ is the total stress; and u is the pore water pressure.

The principle of effective stress provides the link between ground water withdrawal and subsidence. Within an aquifer, the pore water pressure is equivalent to the pressure head. As water is withdrawn from the aquifer and piezometric head drops, the effective stress on the aquifer increases even though the total stress remains constant. It is this increase in effective stress that causes the compression of the soil leading to subsidence.

Further study of compression revealed a highly nonlinear relationship between effective stress and the compression of clays. Fine-grained soils exhibit a "memory" of past exposure to stress (Casagrande, 1932). The past maximum stress is recorded in the soil's structure and is called its preconsolidation stress, σ_p'. At stresses less than the preconsolidation stress, the magnitude of compression is much smaller than it is for stresses that exceed this past maximum. Additionally, compression is elastic (recoverable) at stresses less than the preconsolidation stress

while the compression beyond the preconsolidation stress is inelastic (unrecoverable). This inelastic compression of clay is called consolidation. It is the consolidation of the fine-grained aquifer interbeds that causes the vast majority of subsidence problems in the San Joaquin Valley.

Several models have been created to calculate compaction based on changes in effective stress according to Terzaghi's one-dimensional consolidation theory (1925). The IBS1 package used for this report is one such model. The package assumes that a change in piezometric head produces an equal but opposite change in effective stress in the aquifer. In other words, even as the piezometric head fluctuates, the total stress (i.e., geostatic load) remains constant. This assumption introduces error in shallow unconfined aquifers (e.g., Leake, 1991), but holds for deep or confined aquifers.

The package also assumes that the inelastic and elastic storage coefficients are constant. The values of these coefficients are actually functions of effective stress, however, the assumption introduces little error if changes in effective stress are small in relation to the overall effective stress. Again, this assumption is problematic for shallow aquifers, but satisfactory for deeper ones (e.g., Leake, 1991).

An alternative land subsidence package, IBS3 (Leake, 1991), eliminates the above assumptions by calculating changes in the storage coefficients and geostatic load. Although this would be a valuable improvement for a shallow aquifer, the subsidence model only considers compaction occurring in the Corcoran clay layer and the lower confined aquifer. Subsidence in the upper aquifer is neglected. Extensometer data have shown that almost all the consolidation-induced subsidence in the valley occurs at depths between 350 and 2000 feet (Ireland et al., 1984). This roughly corresponds to the range of depths for the Corcoran clay layer and confined aquifer and justifies the exclusion of subsidence occurring in the unconfined aquifer. Thus, the

additional complexity of the IBS3 package is not merited because it would perform very similarly to the IBS1 model.

Using the above assumptions, the IBS1 package calculates the compaction of each model layer as:

$$\Delta b_e = S_{ske} b_0 \Delta h \tag{2}$$

$$\Delta b_i = S_{skv} b_0 \Delta h \tag{3}$$

in which Δb_e and Δb_i are the elastic and inelastic compaction, respectively; Δh is the change in head at the center of the layer; b_0 is the original thickness of the layer; and S_{ske} and S_{skv} are the elastic and inelastic storage coefficients, respectively.

For all layers included in the IBS1 package, the preconsolidation stress is actually recorded as a preconsolidation head, $h_p = \sigma_p' / \gamma_{water}$. Inelastic subsidence occurs when the head in a model layer drops below its preconsolidation head. The amount of each type of compaction is based on the change in head in relationship to the preconsolidation head. For each time step, the total elastic and inelastic compaction is recorded and the amount of water released due to compaction is returned to the model water balance. Finally, if inelastic compaction has occurred, a new value of preconsolidation head is recorded.

The major weakness of the IBS1 package is its inability to directly consider the time delay of compaction. The IBS1 package assumes that compaction occurs instantaneously with change in head (Leake, 1991). This approach is sufficient for aquifer systems with very thin compressible units and large model time steps, but thicker clay layers require a significant amount of time for pore pressures to dissipate.

Figure 4 illustrates the role of pore pressure in the time delay of consolidation. The line to the left represents the pressure in the aquifer system at a point of equilibrium before any

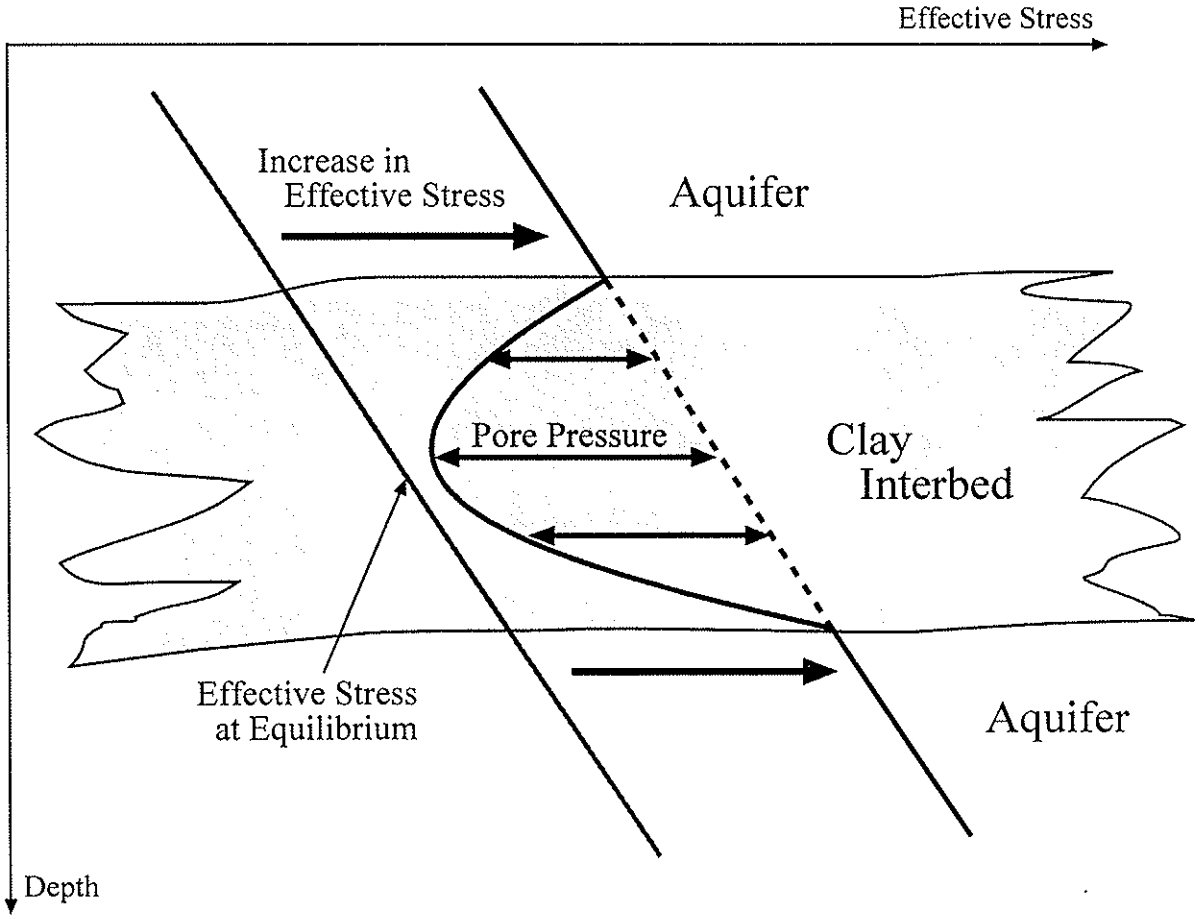

Figure 4 - Role of Pore Pressure in the Time Delay of Consolidation

change in stress occurs. As the effective stress in the aquifer increases, the low hydraulic conductivity of the clay layer results in a parabolic profile of residual pore pressure. Complete consolidation will not occur until all of the pore pressure dissipates and equilibrium is again achieved.

There are two viable techniques for representing the time delay of consolidation. The first is to consider the delay in the analytical derivation of the land subsidence model as illustated by Shearer and Kitching (1994). In their Interbed Drainage Package (IDP), each model element is split into two sub-elements; one for the coarse aquifer material and one for the fine-grained interbeds. Flow between them is controlled by: (1) a parameter called vertical interbed conductance, which is analogous to the conductance term in the stream-routing package of MODFLOW (McDonald and Harbaugh, 1988); and (2) the head difference between the sub-elements. Similarly, Leake's (1998, personal communication) IBS2 package allows for the delayed release of water from compressible, discontinuous clay beds within an aquifer. However, confining clay beds between aquifers must be simulated with individual model layers as they are in the IBS1 package (Wilson and Gorelick, 1996; Leake, 1998, personal communication).

The same result can be achieved numerically by dividing the larger low-conductivity units vertically into a number of smaller units. The residual pore pressure is then represented discretely across each compressible unit (Leake, 1990; Onta and Gupta, 1995). This second approach has been employed in this model and allows for representation of the time delay using the IBS1 package. The actual implementation of this method will be discussed in further detail in the following section.

It should be emphasized that the IBS1 subsidence model only considers compaction due to increased effective stress caused by changing ground water levels. It does not consider

subsidence due to hydrocompaction, withdrawal of gas and oil, deep-seated tectonic movement, or the dewatering of organic soils. Of these alternative causes of subsidence, only hydrocompaction has been significantly observed in the study area.

Hydrocompaction is subsidence that occurs as shallow, low-density soils are wetted for the first time. In the Los Banos-Kettleman City area hydrocompaction has resulted from the arrival of the California Aqueduct. Two sections of the California Aqueduct within the study region, miles 98-103 and 114-129, appear to be especially sensitive to hydrocompaction. Water was applied to these areas in the mid-1960s to exhaust the majority of hydrocompaction before the aqueduct was constructed. It has been assumed that all significant hydrocompaction occurred at that time and that it does not significantly contribute to subsidence during the modeling period (1972-2028).

3. APPLICATION OF THE MODEL

3.1 Modification of the Belitz et al. (1992) Model

3.1.1 Geometry

The model used in this research is an adaptation of the Belitz et al. (1992) model. Modifications have been made in order to simulate land subsidence due to ground water withdrawal. No changes were made to the horizontal dimensions, model grid, and boundary conditions as shown in Figure 5. Each grid cell represents a one-square-mile area with uniform hydrologic and hydrogeologic parameters. The only significant change in geometry occurs in the representation of the vertical model layers. Figure 6 shows the conceptual modifications made to the Belitz et al. (1992) model. Most notably there is a change in how the low-conductivity layers (the Corcoran clay layer and clay interbeds) are represented. In the Belitz et al. (1992) model,

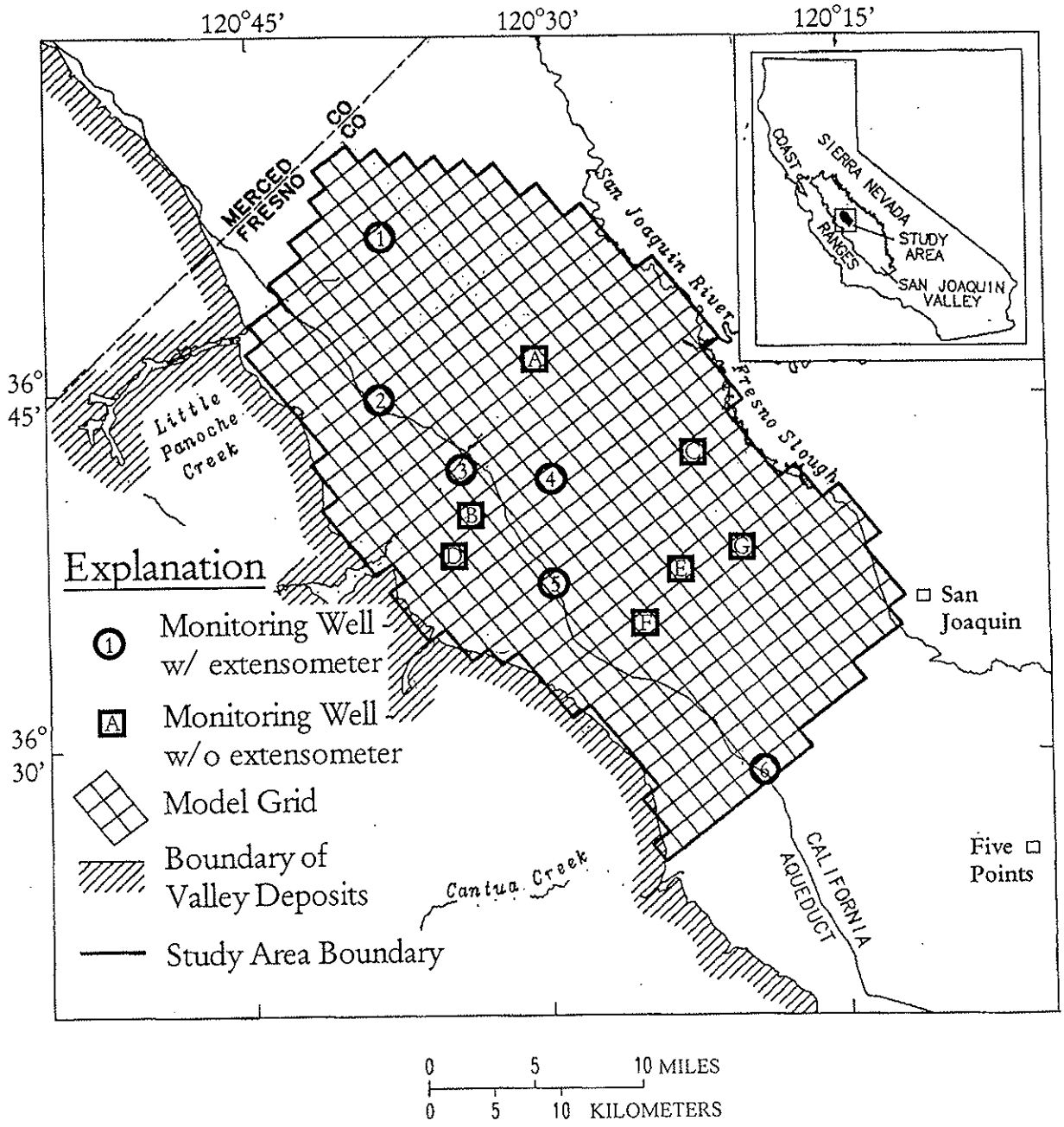

Figure 5 - Model Grid and Location of Observation Wells

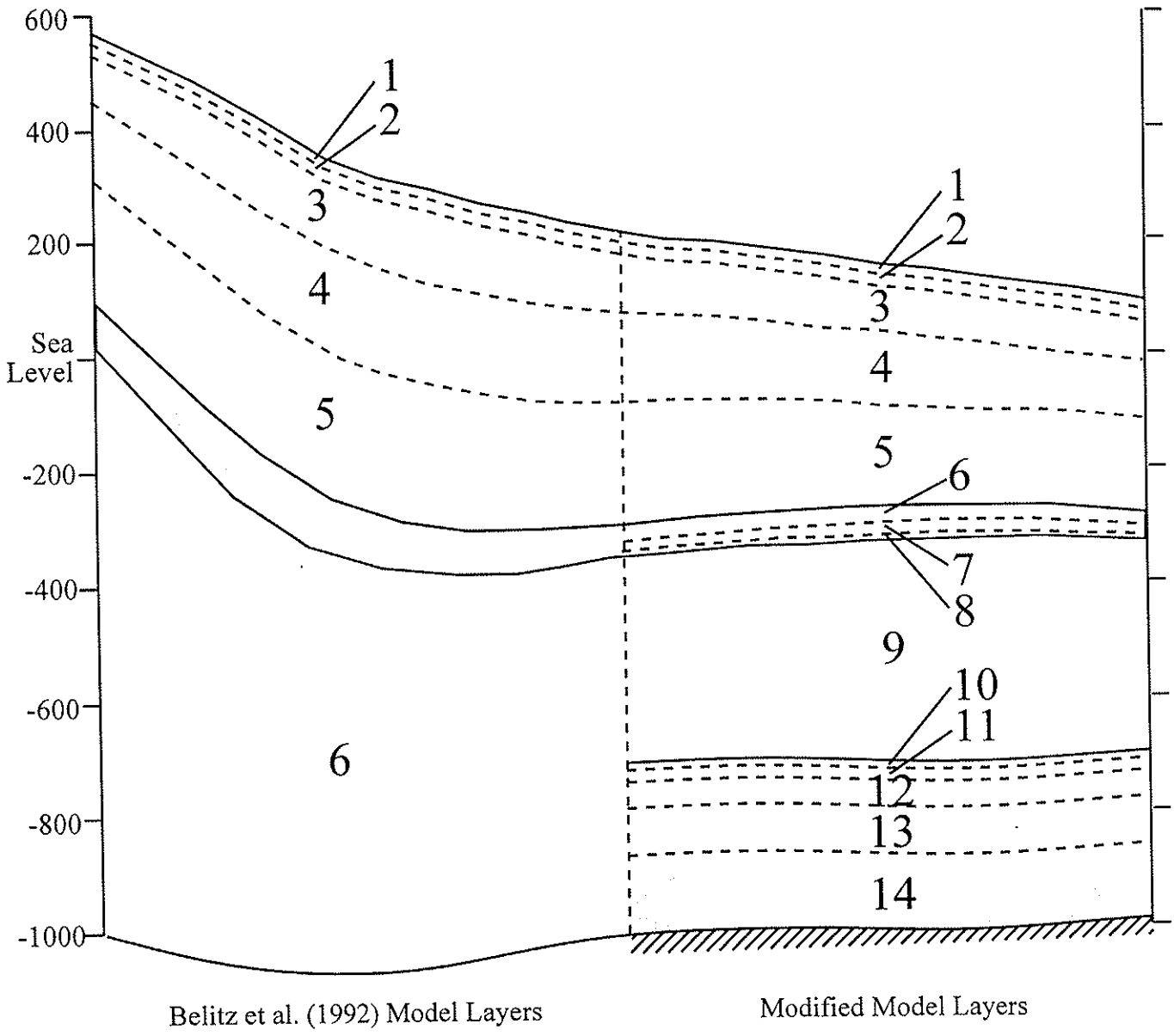

Figure 6 - Modifications to Belitz et al. (1992) Model Layers

both the high-conductivity deposits as well as the clay interbeds in the confined aquifer system have been represented as one composite unit. Additionally, the Corcoran clay layer has not been directly included in the Belitz et al. (1992) model. Instead, its presence is accounted for by reducing the vertical conductivity between layers 5 and 6. The model was satisfactory for assessing the alternatives to agricultural drains, but is inadequate for modeling land subsidence.

In order to model subsidence, two major changes have been made regarding the compressible, low-conductivity layers. First, the larger clay layers have been divided into several smaller modeling layers. As discussed previously, this modification allows a head gradient to develop between each clay modeling layer to mimic the presence of pore pressure and capture the time delay of consolidation. The Corcoran layer is represented in this way. It was divided into three modeling layers comprising 55, 30, and 15 percent of the layer thickness (layers 6, 7, and 8, respectively). The thickness of the layers decreases with depth because the largest head changes occur in the confined aquifer. As head in the aquifer changes, the steepest head gradients in the Corcoran clay layer occur near the outer edge. The thinner layers are better able to capture this gradient.

The Corcoran layer can be easily modeled this way because both its depth and thickness are known. However, for the interbed layers of the confined aquifer, far less information is available. Even if the location of each interbed was known, the large number of interbeds makes modeling each separately a computationally impractical approach. The second major modification to the model incorporates a possible solution to this problem suggested by Ireland (1986). Instead of trying to map all the major interbeds in the confined aquifer, the interbeds are removed from the confined layer and replaced by one large low-permeability layer at the bottom of the aquifer.

This bottom layer is assumed to have a uniform thickness of 310 feet, located 1000 ft below the Corcoran. It is divided into five modeling layers with thicknesses (for increasing depth) of 10, 20, 40, 80, and 160 ft. There is a no-flow boundary at the bottom of the layer, allowing drainage to occur only in the direction of the confined aquifer. Calibration will focus on choosing parameters for the layer such that its effect on land subsidence is equivalent to the composite effect of the actual interbeds.

The main limitation of the strategy is that since the bottom layer is an artificial representation of the interbeds, characteristics of the layer such as storage coefficients (elastic and inelastic) and vertical hydraulic conductivity cannot be verified by any field measurements. This means the validity of the layer parameters can only be measured by their ability to predict subsidence.

3.1.2 Pumping

The other major modification to the Belitz et al. (1992) model occurs in the representation of ground water pumping. The pumping of ground water from the aquifer system is one of the most important components of the ground water model, affecting piezometric head in the confined aquifer more than any other single variable. It is also one of the most difficult components to model because it has never been directly measured.

The Belitz et al. (1992) model estimated pumping magnitudes using the same nine subareas designated in the water budget by Gronberg and Belitz (1992). Pumping rates are allowed to vary between subareas, but are uniform within each subarea. Well depths and perforation lengths were used to determine the percentage of pumping from upper and lower water-bearing units. The 1980 water budget values (Gronberg and Belitz, 1992) were adopted for all model years.

This model adopts the spatial distribution of pumping in the Belitz et al. (1992) model, but alters the yearly magnitude estimates. The major limitation of Belitz et al. (1992) approach is that the magnitude of pumping for all model years was assumed to be exactly the same. This was satisfactory for the purposes of their report (Belitz et al., 1992; Belitz and Phillips, 1995), but does not capture the pore pressure fluctuation necessary to model land subsidence.

There are two major sources of water in the Las Banos-Kettleman City region, surface water from the CVP and ground water. Although ground water pumping has not been measured, some records of water delivery from the CVP are available. Records from the Westlands and Panoche Water Districts are summarized in Table 2. These rates have been used to construct an estimation of the pumping rate for each model year. Figure 7 illustrates the relationship adopted between CVP water delivery and ground water pumping rates.

Several assumptions have been made in creating this figure. First, it is assumed that the Gronberg and Belitz (1992) water budget is appropriate for years in which 100 percent of the CVP contract water is available. During years of reduced surface water availability, the shortage can be met by reducing demand (land retirement), increasing irrigation efficiency, procuring other sources, or increasing ground water pumping. The line of combined ground water and CVP water use is assumed to be concave up. This is because increasing efficiency and the use of other sources are inexpensive alternatives for years with small reductions in CVP water. For increasing levels of drought, however, these options become very costly or unavailable. Thus, an increasing amount of the shortage must be met with ground water. The actual shape of the line of combined ground water and CVP water use was determined through trial and error

Table 2 - Yearly CVP Deliveries for Westlands and Panoche Water Districts

Water Year	Westlands CVP Delivery (acre-ft)	Panoche CVP Delivery (acre-ft)	Model Percent
1972	*1,150,000**	*104,600*	100%
1973	*1,150,000*	*104,600*	100%
1974	*1,150,000*	*104,600*	100%
1975	*1,150,000*	*104,600*	100%
1976	*230,000*	*20,920*	20%
1977	*1,150,000*	*104,600*	100%
1978	*1,150,000*	*104,600*	100%
1979	*1,150,000*	*104,600*	100%
1980	*1,150,000*	*104,600*	100%
1981	*1,150,000*	*104,600*	100%
1982	*1,150,000*	*104,600*	100%
1983	*1,150,000*	*104,600*	100%
1984	*1,150,000*	*104,600*	100%
1985	*1,150,000*	*104,600*	100%
1986	**1,150,000**	**101,600**	100%
1987	**1,150,000**	**111,800**	100%
1988	**1,150,000**	**107,000**	100%
1989	**1,150,000**	**97,900**	100%
1990	**575,000**	**63,600**	51%
1991	**287,500**	**36,900**	26%
1992	**287,500**	**41,100**	26%
1993	**575,000**	**80,500**	52%
1994	**402,500**	*52,500*	36%
1995	**1,150,000**	*104,600*	100%
1996	**1,092,500**	*98,200*	94%
1997	**1,035,000**	*94,100*	90%
1998	**1,150,000**	*104,600*	100%

*Recorded values in bold, approximations italicized

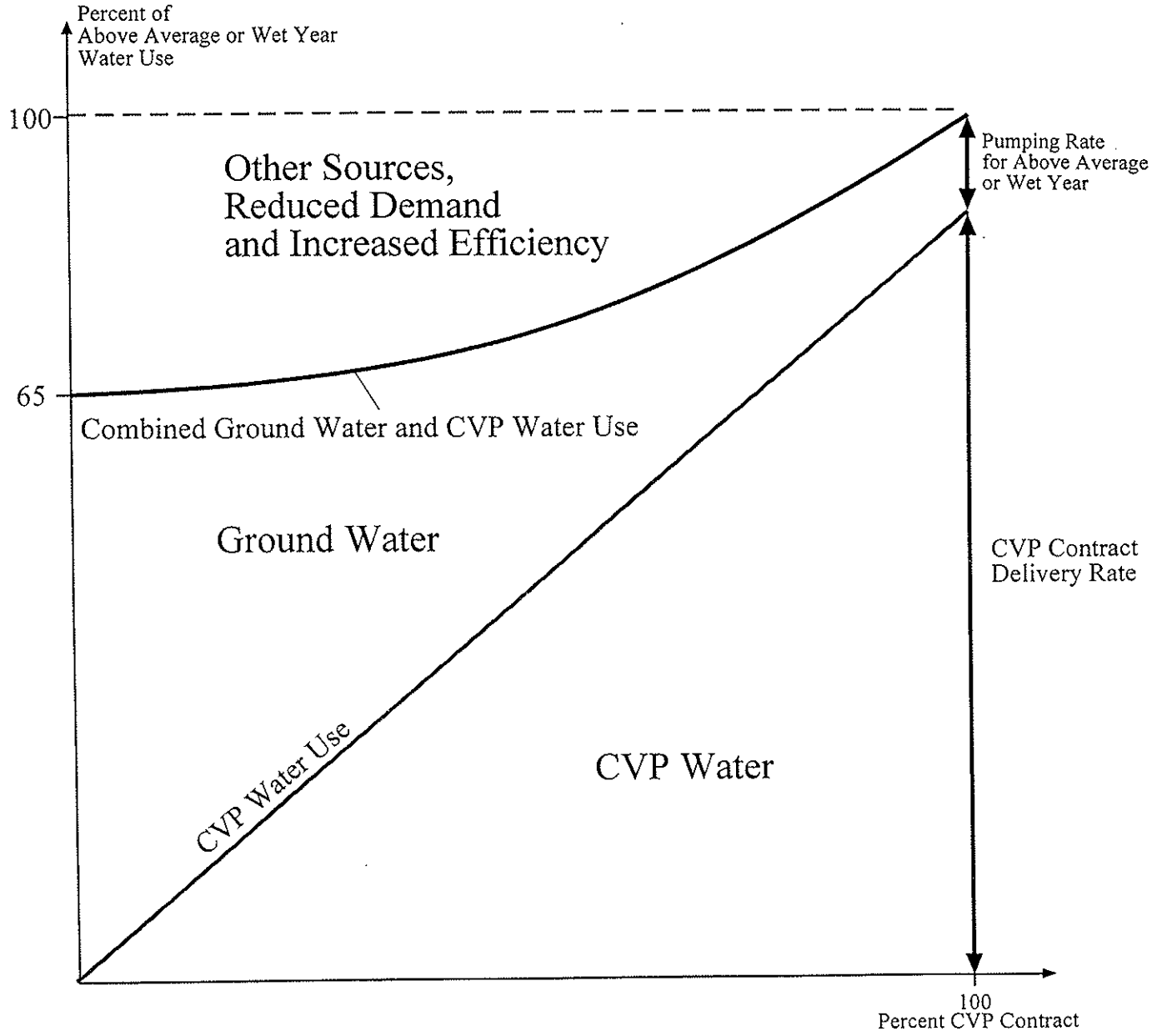

Figure 7 - Relationship between CVP Delivery and Ground Water Pumping Rates

during the model calibration and can be mathematically described as:

$$\Phi_c = 0.0022\Phi_s^2 + 0.13\Phi_s + 65 \quad (4)$$

in which Φ_c is the percent of normal, combined ground water and surface water use; and Φ_s is the percent of contracted surface water.

This relationship not only assures consistent estimation of pumping rates for the calibration period, but also provides an estimate for future pumping rates based on the availability of surface water.

3.1.3 Initial and Preconsolidation Heads

The IBS1 package requires the entry of a preconsolidation head for each element of the model for which subsidence will be monitored. Since the Belitz et al. (1992) model did not include any consideration of subsidence, all preconsolidation files are original to this model. Additionally, the initial heads for both the Corcoran and the clay interbed layers are newly generated. The estimates for both initial and preconsolidation heads in the clay layers are the result of each layer's pressure history.

From the historical record it is apparent that piezometric head levels were dropping prior to the arrival of the California Aqueduct. This suggests that when head levels were at a minimum in the aquifers, some amount of residual pore pressure probably remained in the thicker clay layers. The extensometer record supports this observation. It shows inelastic subsidence occurring even as heads in the confined layer recover, evidence that pore pressure is still dissipating from the clay layers at the beginning of the modeling period.

Given this information, it is possible to create a schematic drawing of heads in the model for the time of maximum drawdown (Figure 8). Heads in the aquifers are based on water table

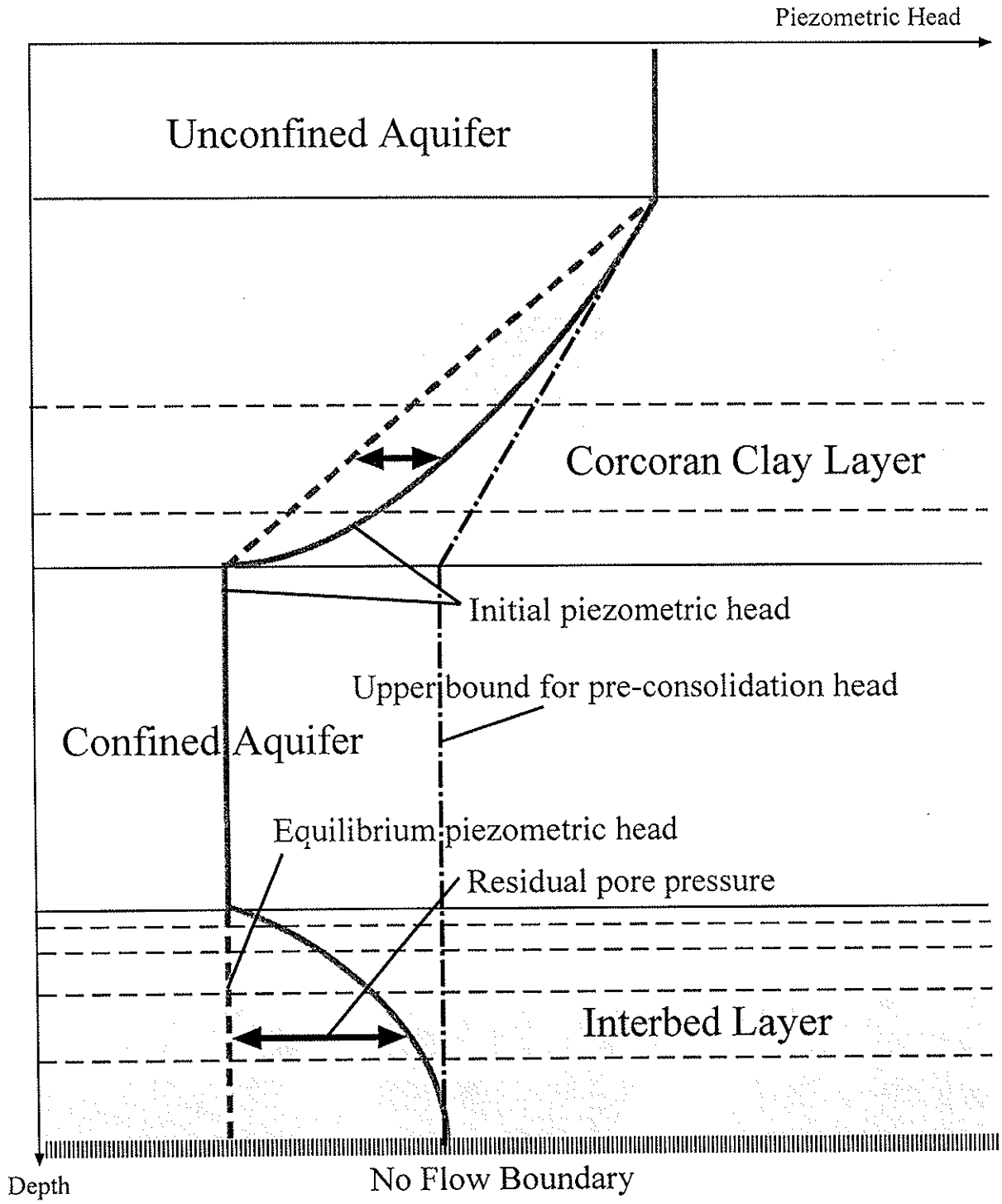

Figure 8 - Schematic Drawing of Initial Heads

and potentiometric surface maps from 1972 (after Belitz et al., 1992). Heads in the low-conductivity layers will be equal to the equilibrium piezometric head plus the residual pore pressure. The equilibrium head is determined from the initial heads in each aquifer. The shape of the residual pore pressure profile is assumed to be parabolic. The magnitude of the residual pore pressure will be a function of past changes in piezometric head and the thickness and hydraulic conductivity of the clay layers. Since this information is unknown, the magnitude of residual pore pressure is treated as a calibration parameter.

Because of the relatively small changes in the water table, only residual pore pressure from changes in piezometric head in the confined aquifer is considered. Additionally, Figure 8 shows the upper bound for pore pressure being equivalent for both the Corcoran and interbed layer. This is not necessarily true. The rate at which each fine-grained geological unit will dissipate pore pressure will be a function of its thickness and hydraulic conductivity. Even though the pressure history for the confined aquifer is the same for both the Corcoran and the interbed layers, the amount of pore pressure remaining from these changes need not be equal. For this model, the best results were produced with residual pore pressure being two times greater in the interbed layer than in the Corcoran.

The above observations are only applicable for the time of maximum drawdown. The time of maximum drawdown is also a convenient time period to consider head levels because initial and preconsolidation heads will be equal to each other. For this reason, it is assumed that the initial heads for the model are equal to the maximum historical drawdown. Although some amount of recovery has occurred between the arrival of the aqueduct (approximately 1967) and the beginning of the model (1972), the initial heads in the confined aquifer are sufficiently close to the historic minimum for this assumption to produce acceptable results. Additionally, the

assumption affects only the outermost portions of the Corcoran and clay interbed layers, resulting in minimal effect to overall land subsidence.

Finally, initial heads in the aquifers remain largely unchanged from the Belitz et al. (1992) model. Modifications were made only where large jumps were observed in the initial time steps indicating that the head values were inconsistent with the rest of the model. This was particularly prevalent in the bottom layer of the unconfined aquifer (Belitz and Phillips, 1995). Such inconsistencies usually stabilize in the first few time steps. Although they have little effect on the long-term accuracy of the ground water flow portion of the model, they cause large fictional jumps in land subsidence. For this reason, model head values for the bottom layer of the unconfined aquifer were chosen after four time steps (1974) in the generation of initial and pre-consolidation heads in the Corcoran clay layer. This allowed sufficient time for any transient instability to dissipate. A small number of other changes to initial head in the aquifers occurred near the edges of the model grid, but were not aerially extensive.

3.1.4 Other Modifications

All other aspects of the model have not been significantly changed from the model developed by Belitz et al. (1992). For information on the selection of parameters for drainage, evapotranspiration, recharge processes, and boundary conditions, the reader should consult Phillips and Belitz (1991), Belitz et al. (1992), and Belitz and Phillips (1995).

As in the Belitz et al. (1992) model, the model formulated in this study uses yearly stress periods. This has been done because most of the data (water table levels, subsidence rates, CVP deliveries, etc.) are only available at yearly intervals. The major weakness of this approach is its effect on pumping. By averaging the pumping out over the entire year, the higher drawdowns occurring during the summer months are lost. This is significant for the land subsidence portion

of the model because most of the subsidence actually occurs during these periods of high drawdown. This can be compensated for by altering some of the other model parameters, but it should be noted that the piezometric heads predicted by the model will be artificially high during the summer months.

It should also be noted that, in addition to the temporal averaging of pumping rates, pumping is also averaged spatially over the grid cells. During calibration, measured ground water levels were assigned to the center of the grid cells and compared with the spatially and temporally averaged model-computed ground water levels. In short, although spatial and temporal averaging of parameters causes the loss of some information, it is unavoidable in numerical modeling efforts, mainly due to the scarcity of data and/or budget and time restrictions for more detailed data gathering.

3.2 Calibration

3.2.1 Piezometric Head

Calibration of the model encompasses matching simulated piezometric head levels and land subsidence with corresponding observed values across the study area. The California Department of Water Resources (DWR) monitors piezometric head levels at observation wells throughout the San Joaquin Valley. Figures 9-21 show the model results following calibration plotted against the observed piezometric head for thirteen monitoring locations. Each location is shown on Figure 5, while the actual well numbers are given in Table 3. Some of the locations include more than one monitoring well and each well may be located anywhere within the model cell. Since the model simulates head at the middle of the grid cell, it is possible for observation wells to be more than a half-mile away from the location of simulated head. Thus, small

Table 3 - Well Numbers for Extensometers and Monitoring Wells

	Observation Location	Well Number
Extensometer and Monitoring Wells		
	1	12/12-16H2
	2	13/12-20D1
	3	14/12-12H1
	4	14/13-11D6
	5	15/13-11D2
	6	16/15-34N1
Monitoring Wells Only		
	3b	14/12-01Q1
	3c	14/13-07E3
	4b	14/13-11R1
	5b	15/13-02N2
	6b	16/15-33J1
	6c	17/15-03E1
	A	13/13-10R1
	B	14/12-25D1
	C	14/14-02N2
	D	15/12-01R1
	E	15/14-02B1
	F	15/14-21E1
	G	14/15-32N3

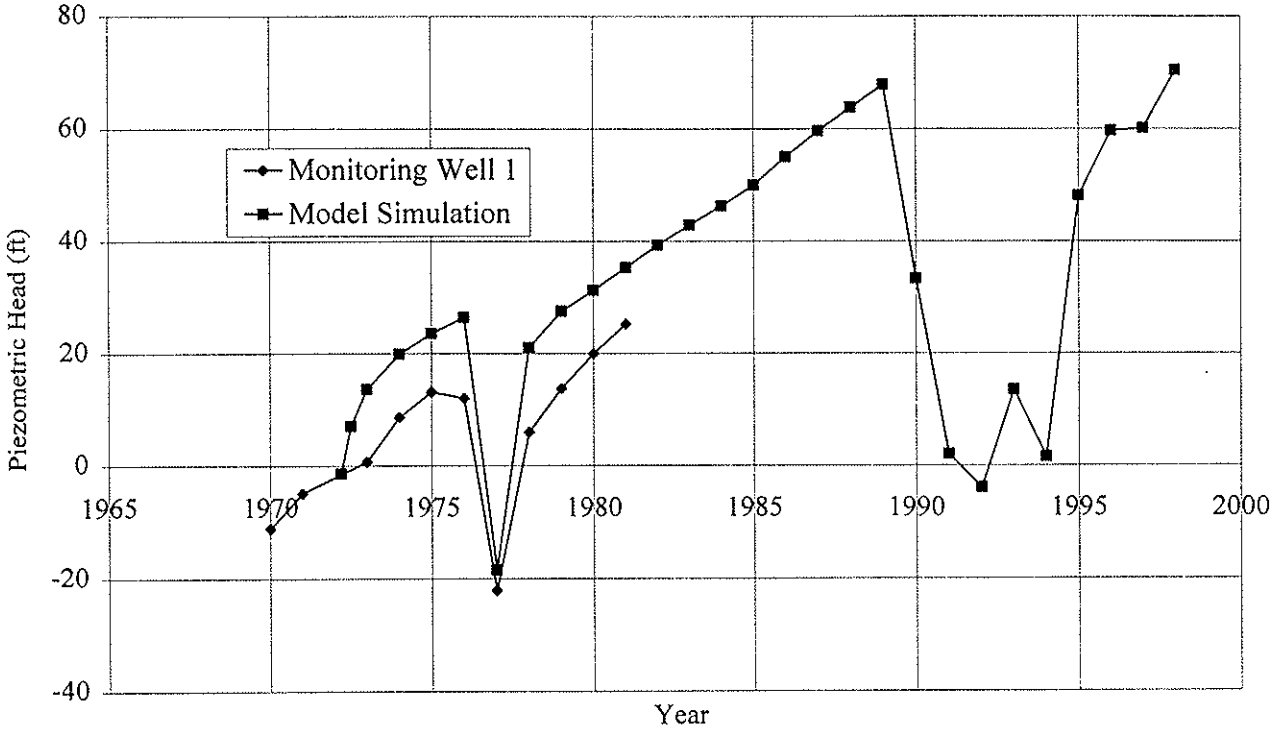

Figure 9 - Observed and Simulated Piezometric Head for Observation Location 1

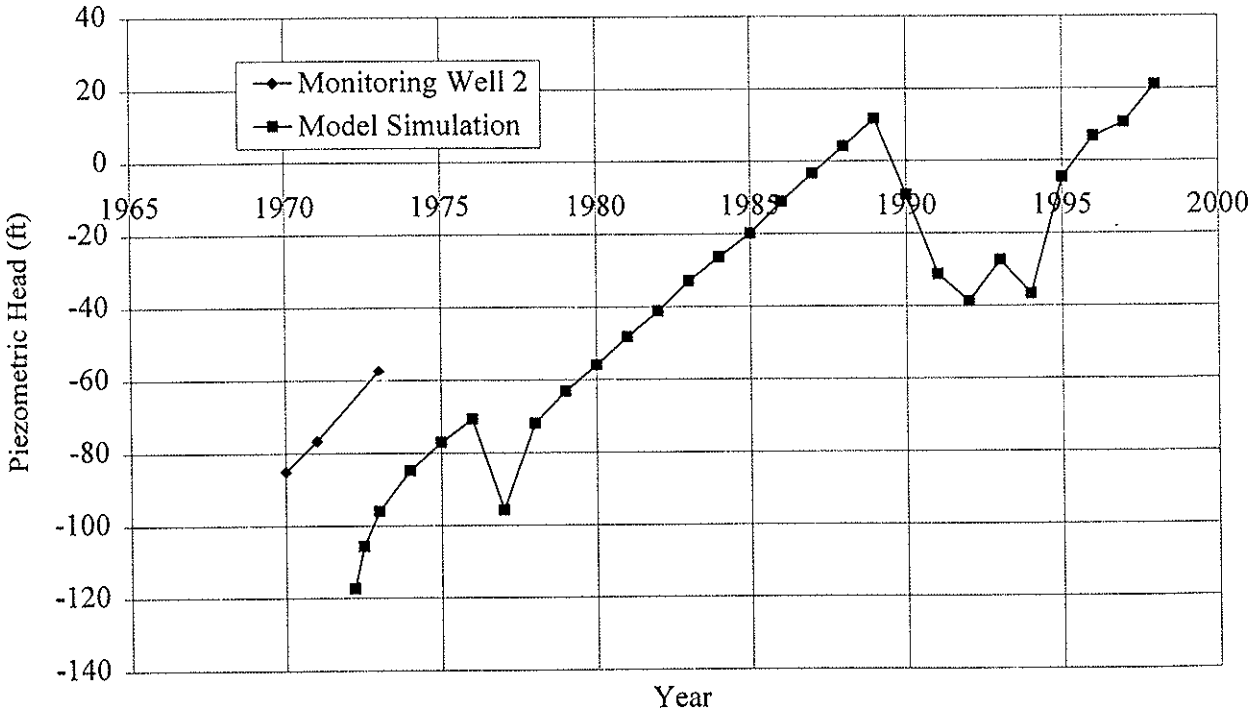

Figure 10 - Observed and Simulated Piezometric Head for Observation Location 2

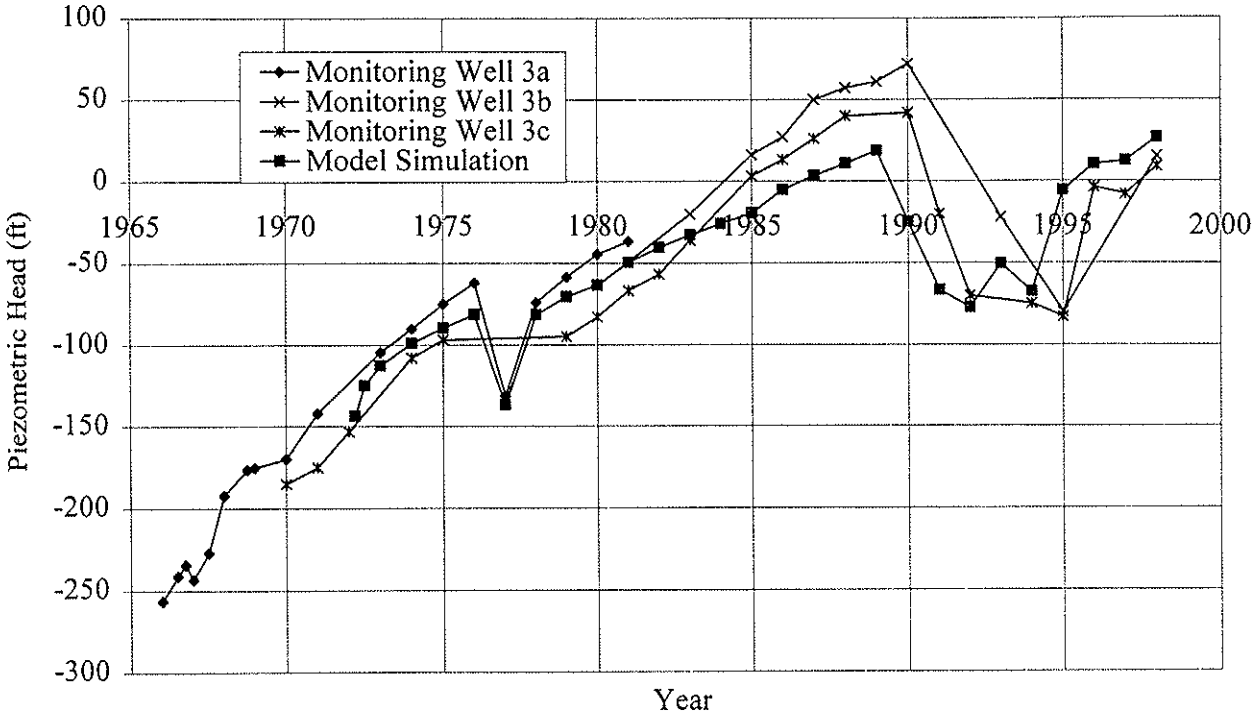

Figure 11 - Observed and Simulated Piezometric Head for Observation Location 3

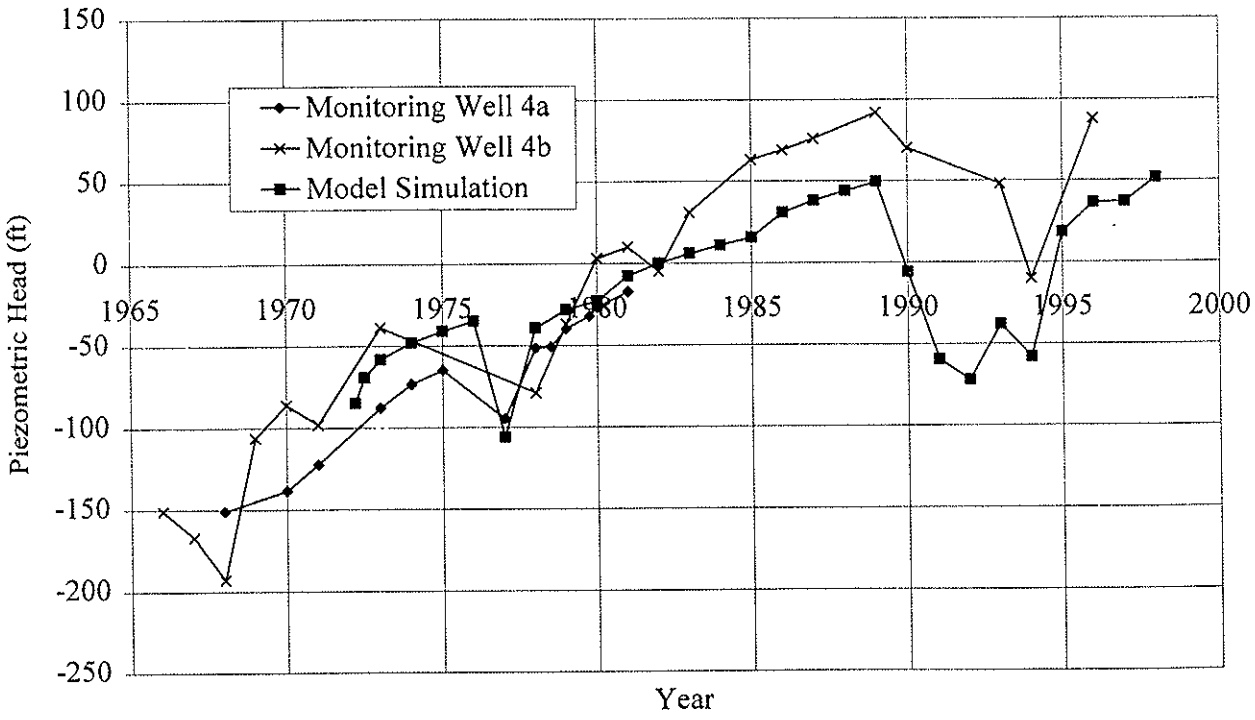

Figure 12 - Observed and Simulated Piezometric Head for Observation Location 4

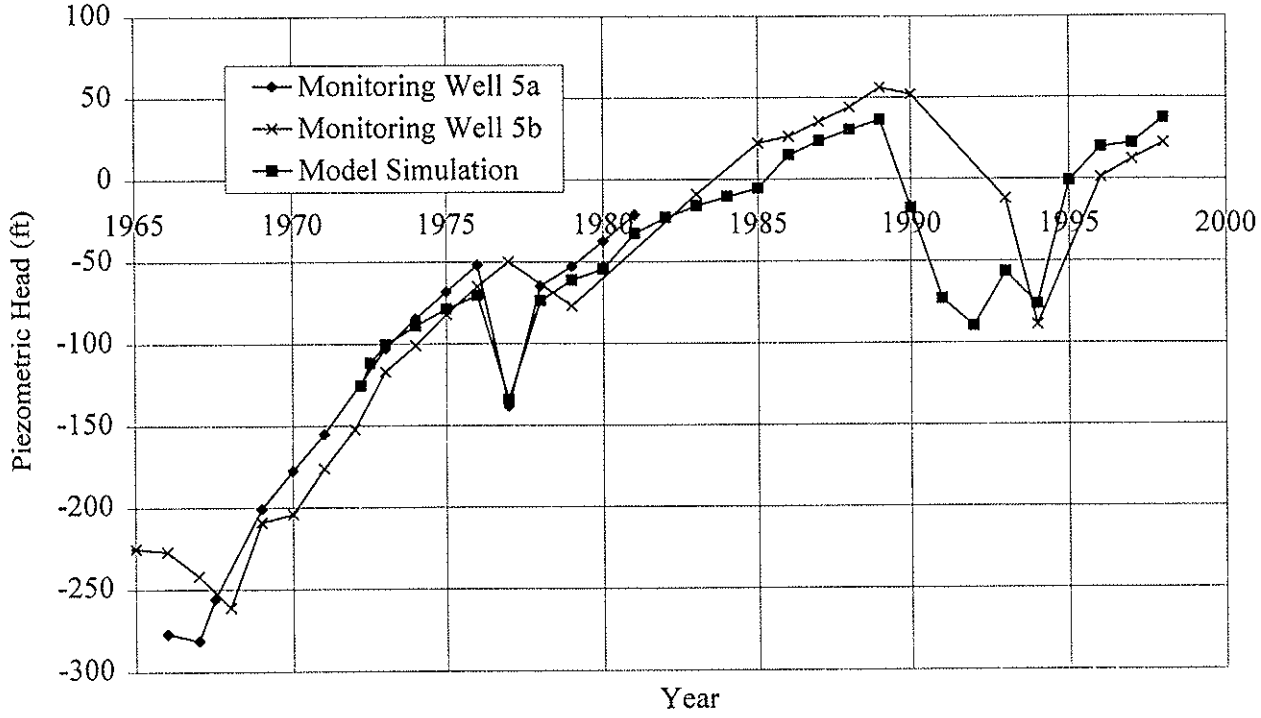

Figure 13 - Observed and Simulated Piezometric Head for Observation Location 5

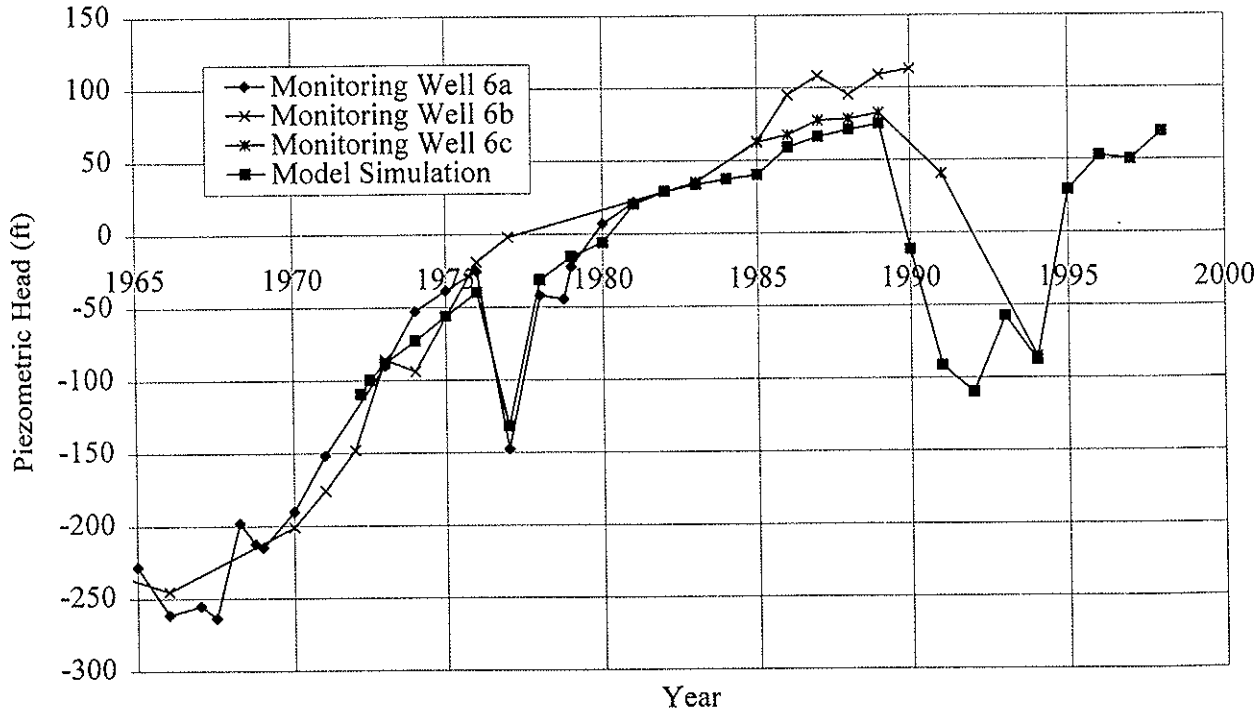

Figure 14 - Observed and Simulated Piezometric Head for Observation Location 6

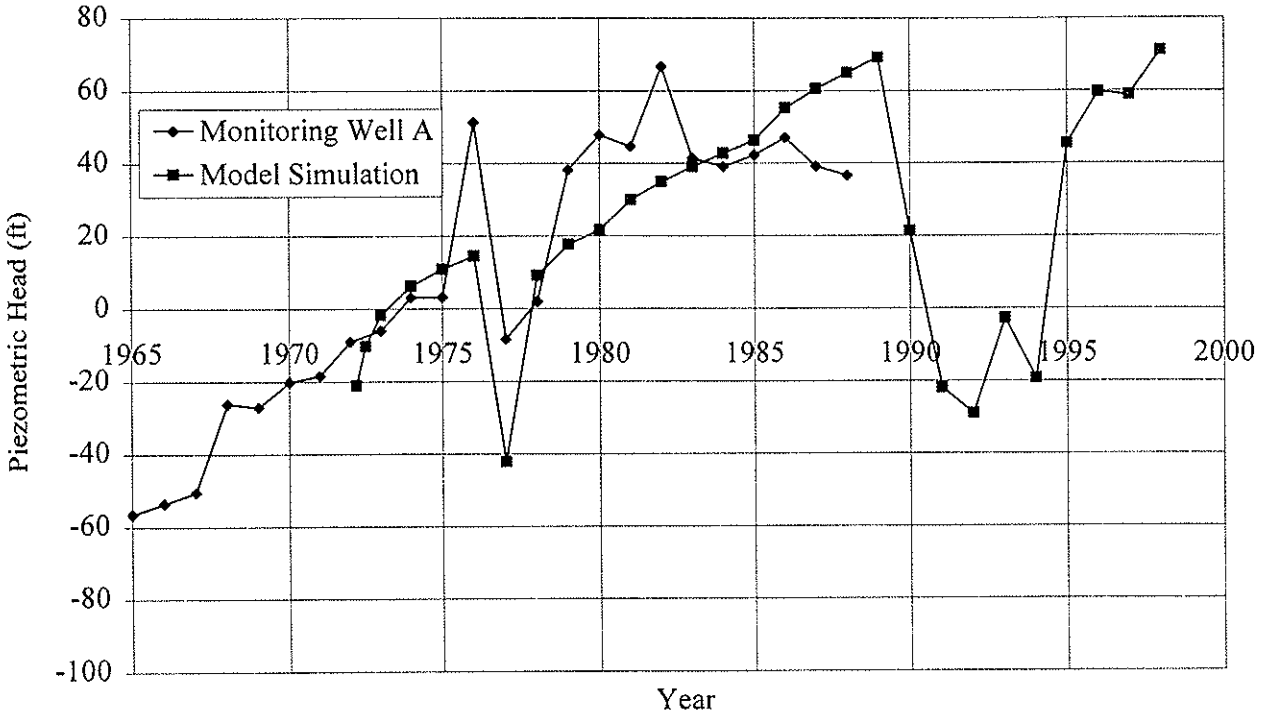

Figure 15 - Observed and Simulated Piezometric Head for Observation Location A

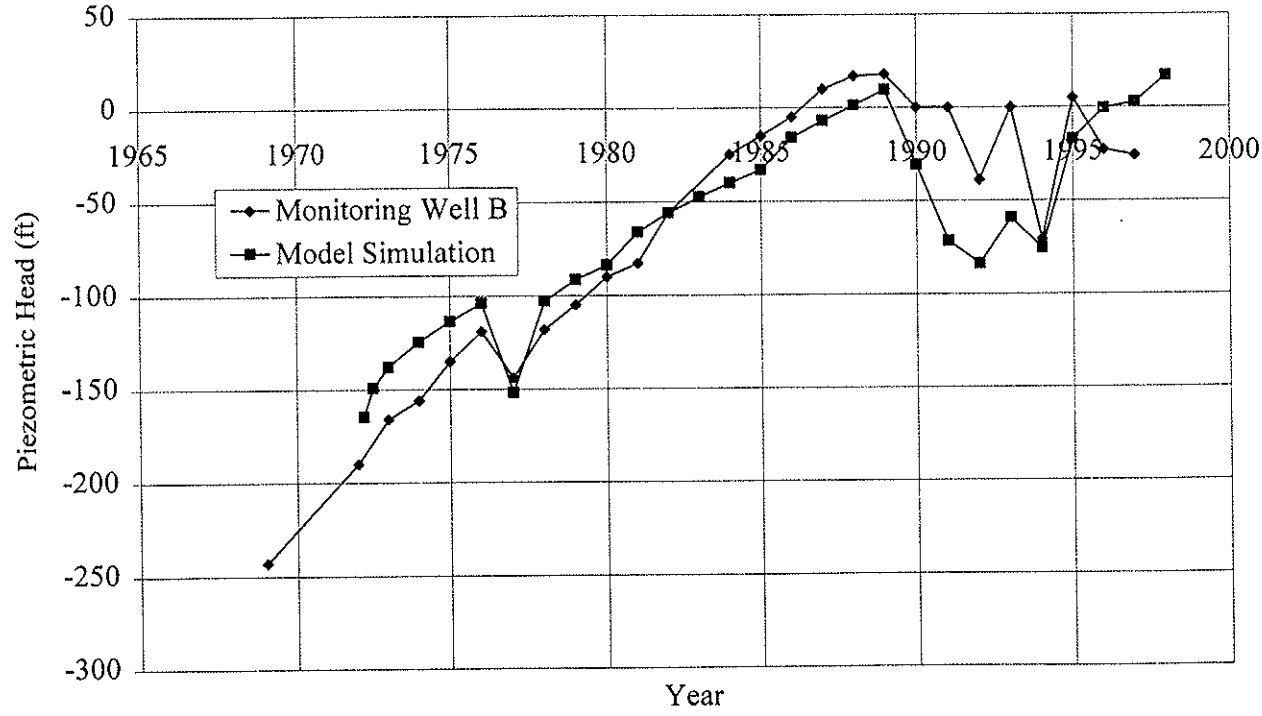

Figure 16 - Observed and Simulated Piezometric Head for Observation Location B

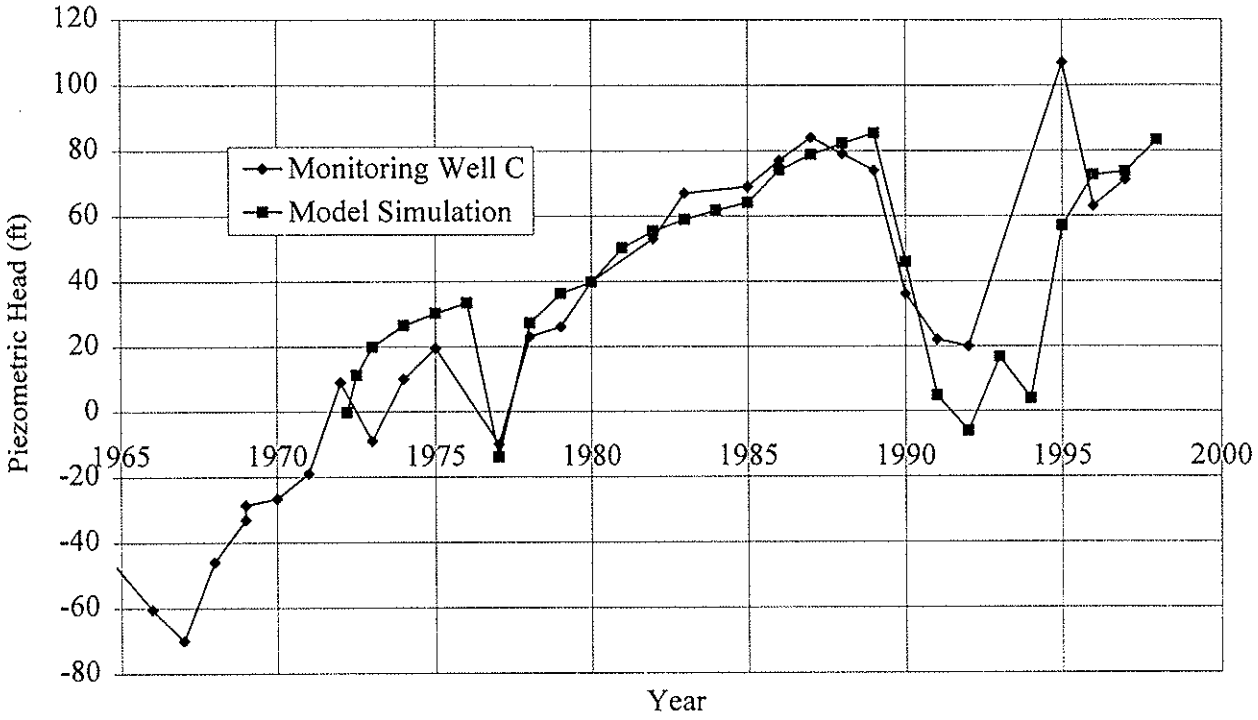

Figure 17 - Observed and Simulated Piezometric Head for Observation Location C

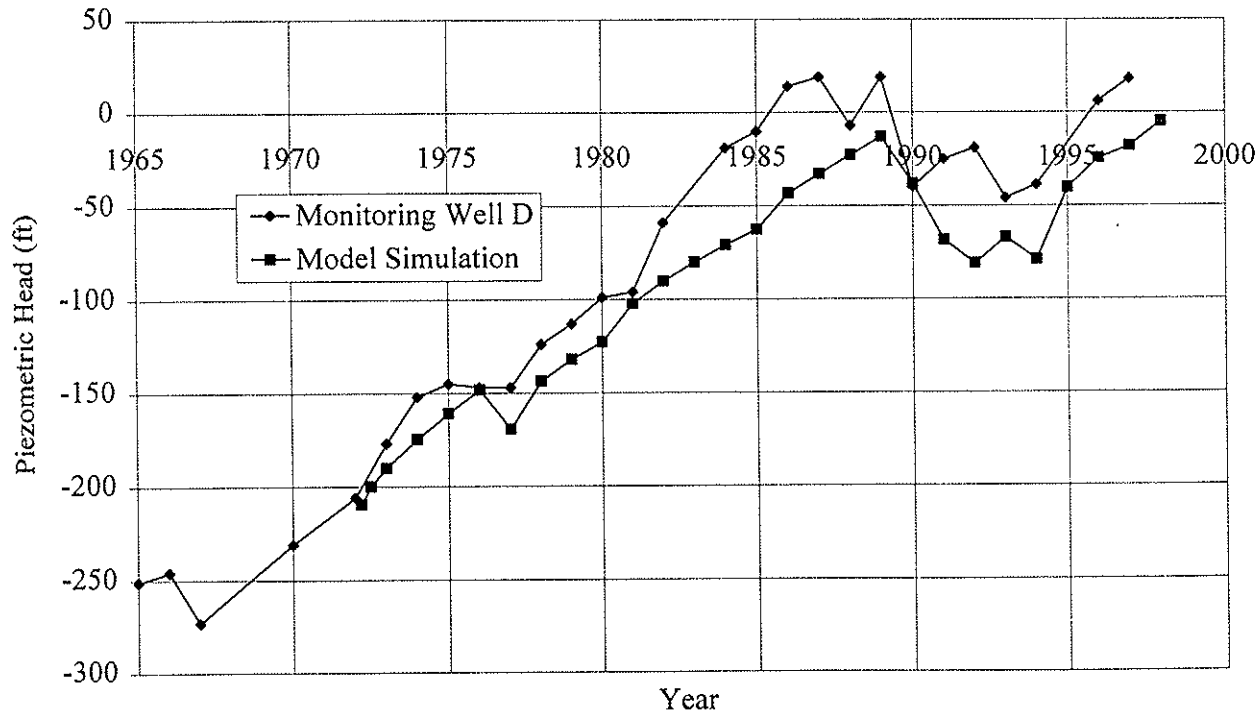

Figure 18 - Observed and Simulated Piezometric Head for Observation Location D

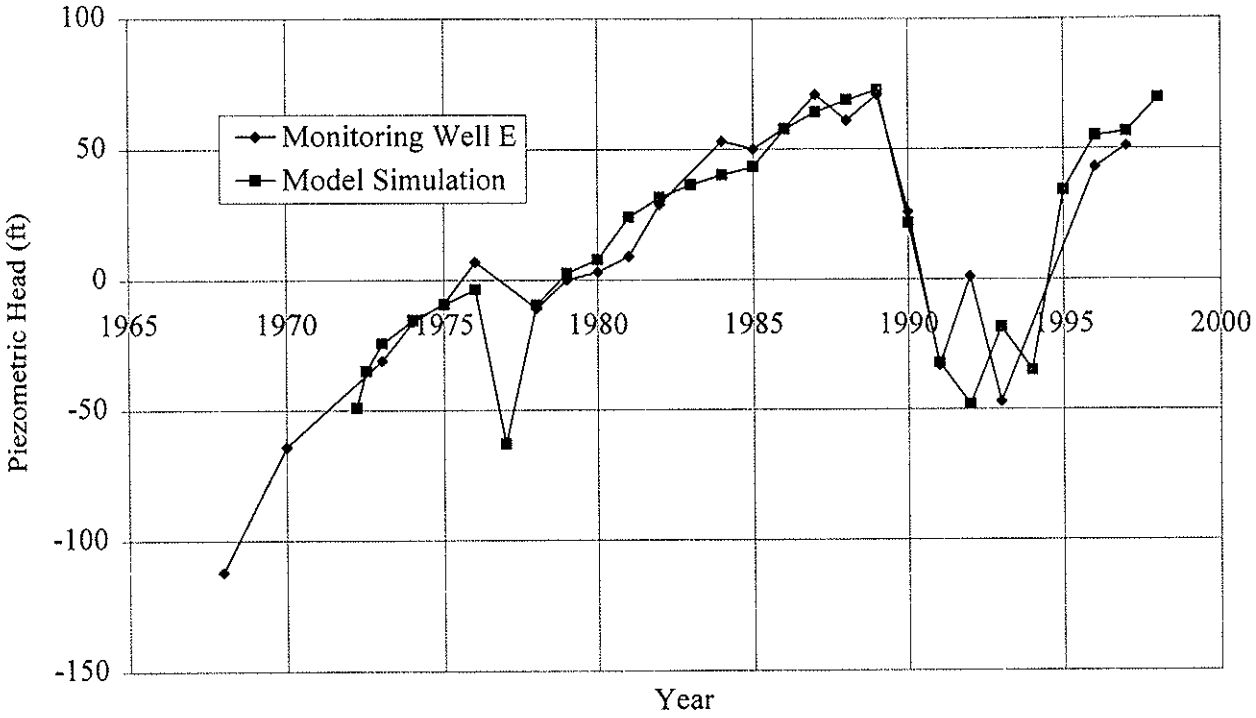

Figure 19 - Observed and Simulated Piezometric Head for Observation Location E

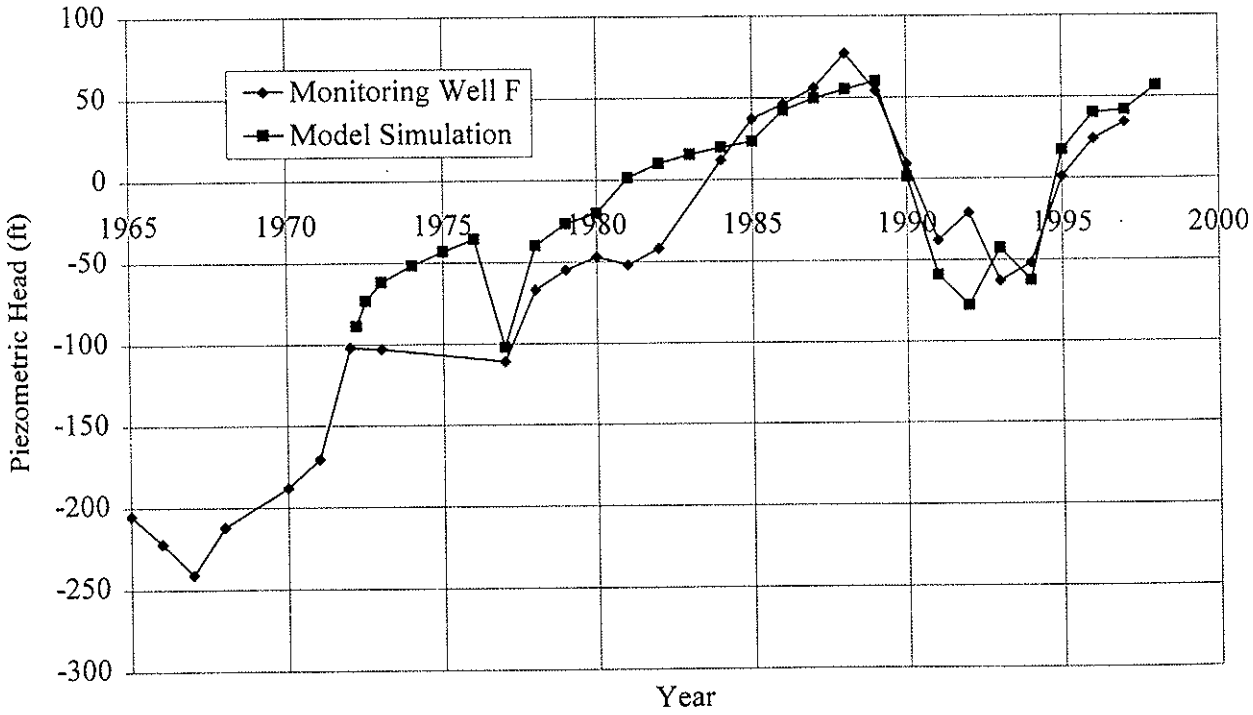

Figure 20 - Observed and Simulated Piezometric Head for Observation Location F

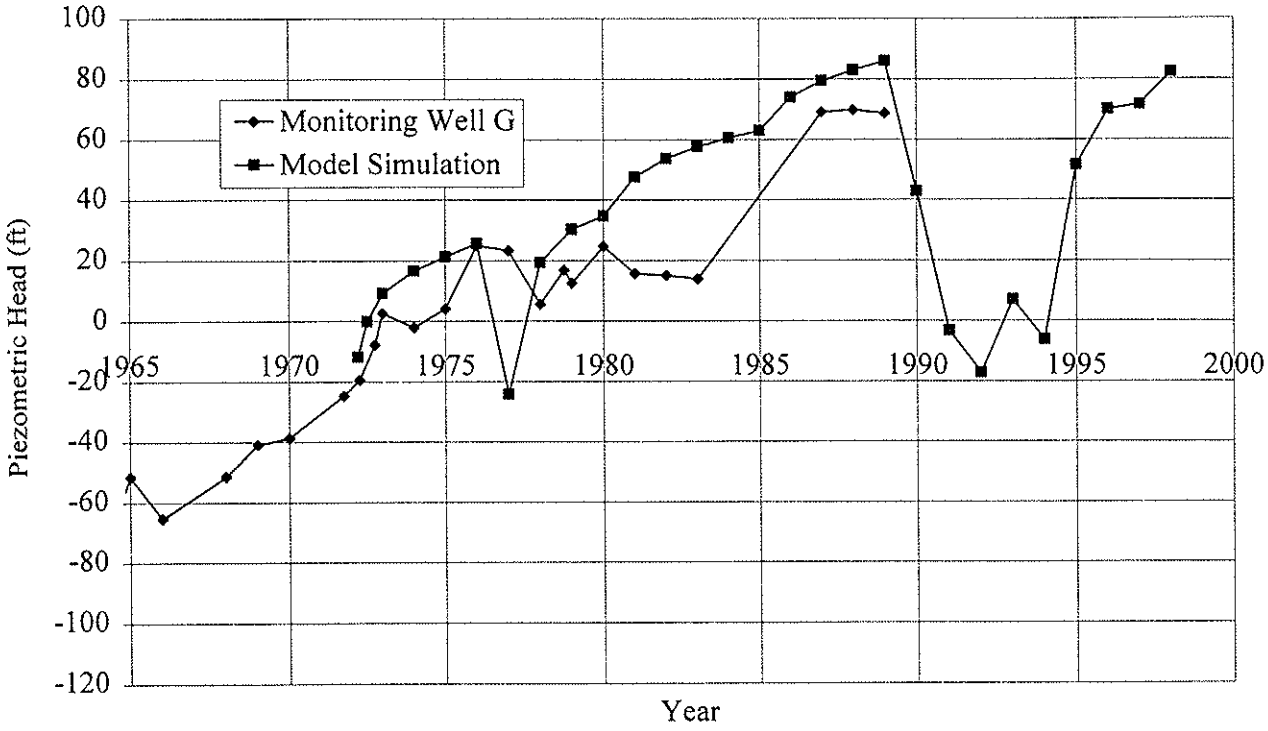

Figure 21 - Observed and Simulated Piezometric Head for Observation Location G

differences should be expected between observed and simulated piezometric head values, as well as between head values at different observation wells within the same grid cell.

By using the aquifer parameters found by Belitz et al. (1992), it was possible to produce relatively accurate results for piezometric head with modification to the pumping rates only. Proper drawdown during years of drought was achieved using the scheme described in Section 3.1.2. In addition to determining the best equation to define combined ground water and surface water use (see equation 4), the calibration dictated two other significant changes.

The water budget for the Belitz et al (1992) model includes a portion of the Westlands Water District that relies strictly on ground water. Following construction of the water budget, however, improvements were made in the delivery system to bring CVP water to portions of this area. This was evident during the calibration trials when predicted head levels were significantly below those observed in these portions of the Westlands Water District. To address this problem, the original water budget is retained for the model years up to 1980, but it is assumed that CVP water replaces 25 percent of the pumping in 1981 and replaces 50 percent in 1986.

The second significant change to the pumping scheme occurs along the southern edge of the study area. Observed head values suggest that more ground water is removed from this area during periods of drought than predicted by the model. By increasing the pumping 150 percent during periods of drought, the head levels in the model appear to better match the observed data in the region.

3.2.2 Land Subsidence

Land subsidence in the San Joaquin Valley has been documented using both extensometers located at wells throughout the Valley and level runs along the California Aqueduct. Extensometers provide the most detailed measurement of compaction. Annual

extensometer measurements can be plotted directly versus model predictions. Unfortunately, each extensometer only records subsidence at one point, and only six are located in the study area. Level runs provide a better indication of subsidence trends spatially. Although they are conducted only once every four years, they measure subsidence along a path line.

The six extensometers included in this study (Figure 5) were installed by the U.S. Geological Survey (USGS) and are now monitored by the San Joaquin district of the California DWR. Three of the extensometers were abandoned in the 1970s and thus provide only a partial record for the calibration period. For those extensometers that continue through the entire time interval (1972-1998), a small portion of the data is missing from the record (1979-1984). Fortunately, the missing portion corresponds to a time of relatively uniform rebound. For this portion, rebound is assumed at a rate equal to the average of the rebound in the years 1978 and 1985.

Extensometers only measure compaction across a monitored depth. As a result, additional compaction can occur below the monitored interval and surface subsidence will usually be greater than the compaction measured by the extensometer. Compaction is tranformed to subsidence by multiplying the observed compaction by the average ratio of subsidence to compaction found for each extensometer (Ireland et al., 1984). Figures 22-27 show the model results following calibration plotted directly against the transformed extensometer data.

Extensive level runs were conducted for the Los Banos-Kettleman City region throughout the 1950s and 1960s. Although more recent data could not be accessed for this project, the previous level runs give a good indication of subsidence trends for the area. Figure 28(a) is a contour map of the measured subsidence from 1926 to 1972, while Figure 28(b) shows the

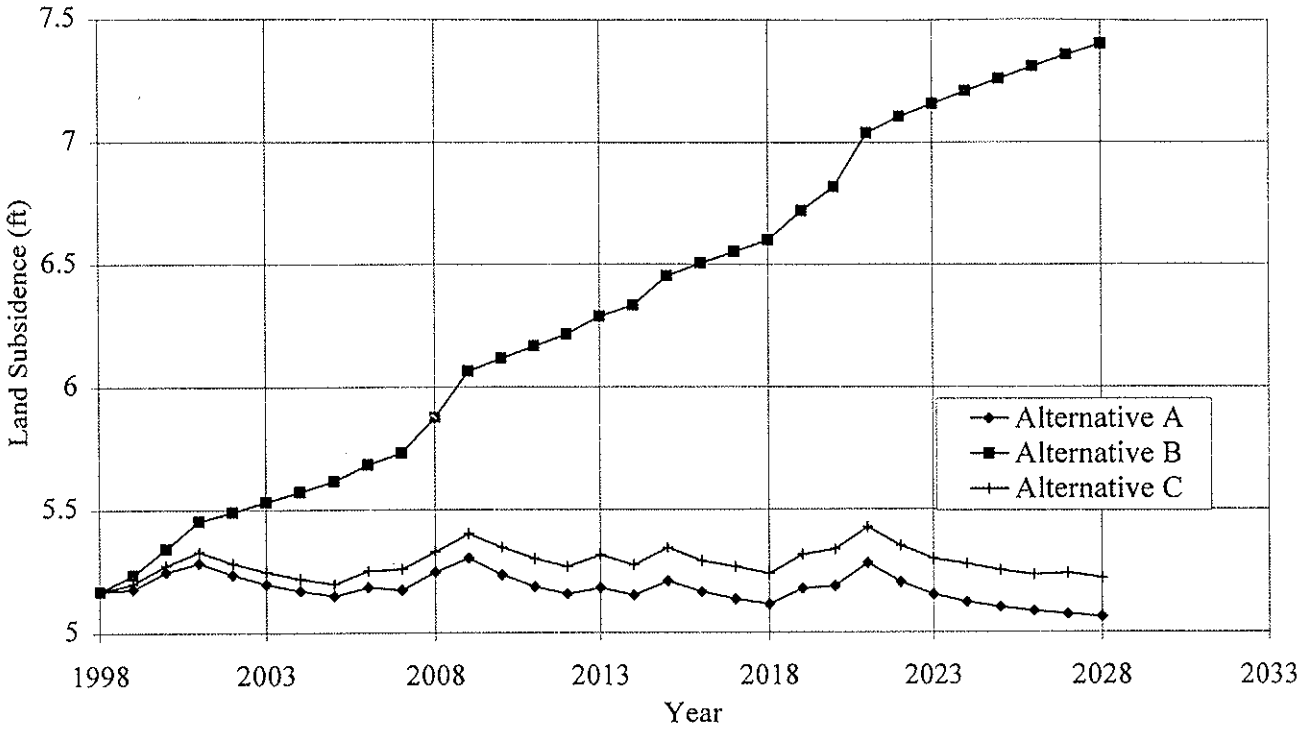

Figure 37 - Model Predictions of Total Subsidence for 1999-2028 at Extensometer 1

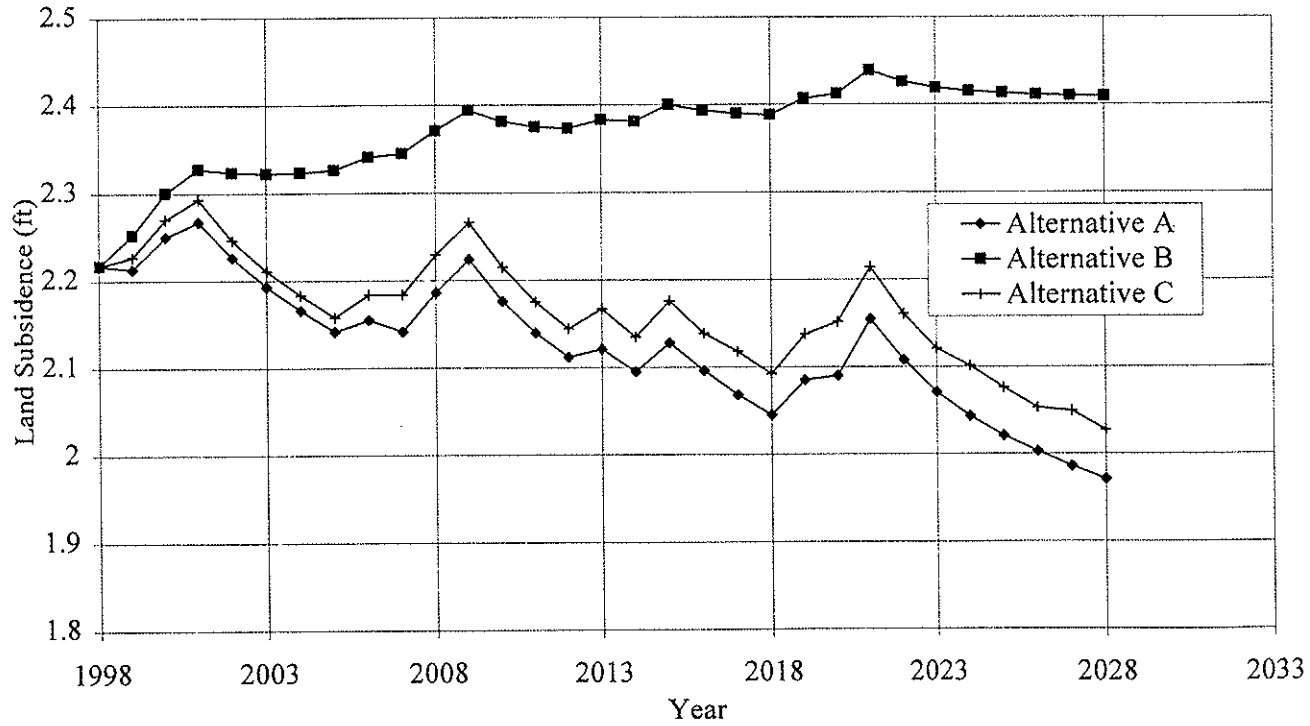

Figure 38 - Model Prediction s of Total Subsidence for 1999-2028 at Extensometer 2

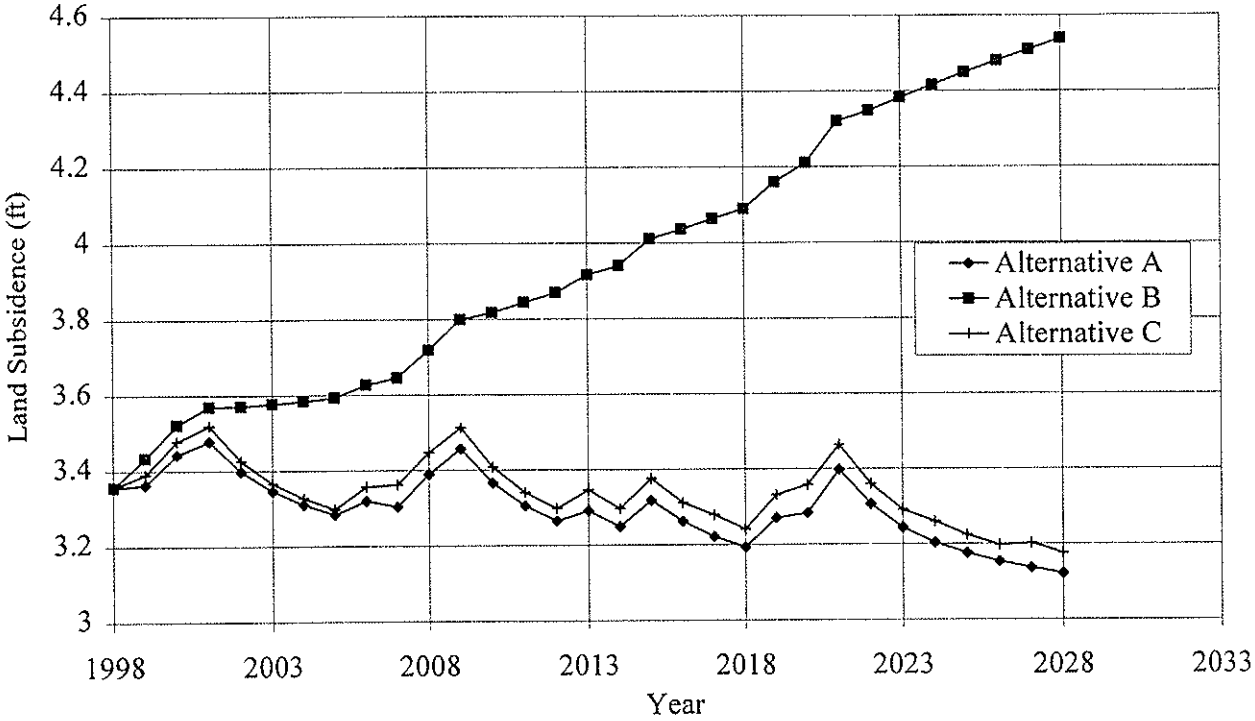

Figure 39 - Model Predictions of Total Subsidence for 1999-2028 at Extensometer 3

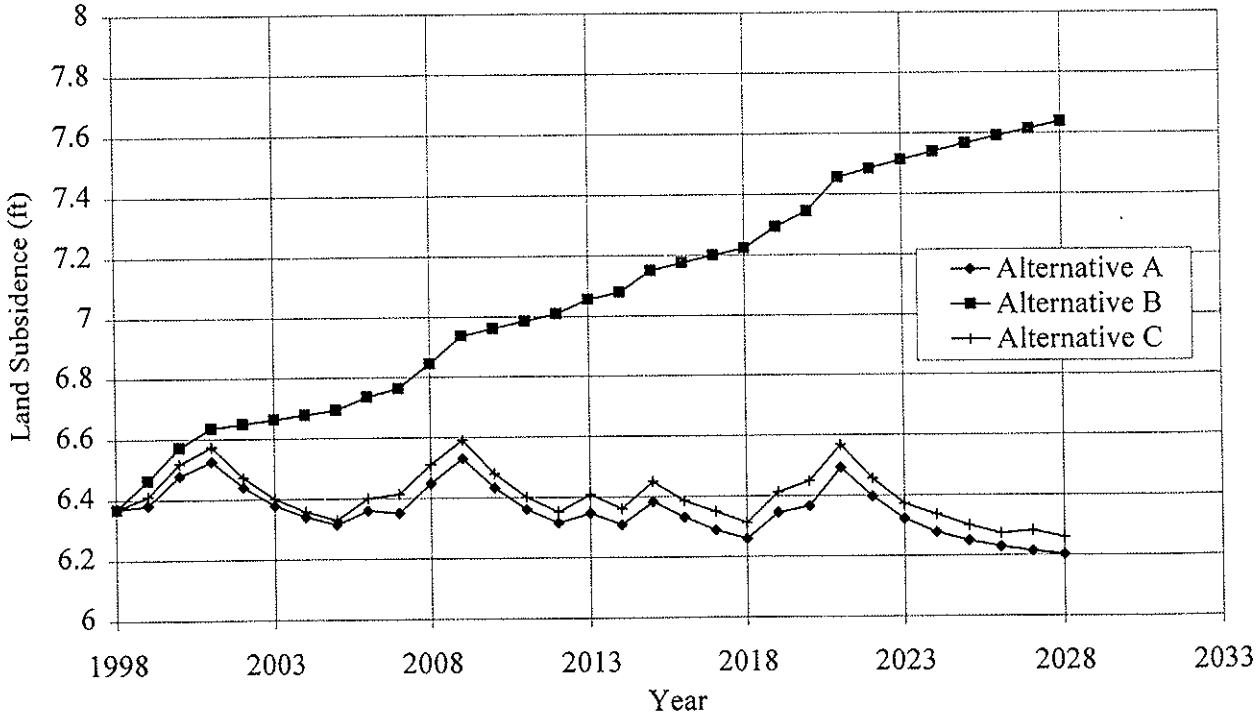

Figure 40 - Model Predictions of Total Subsidence for 1999-2028 at Extensometer 4

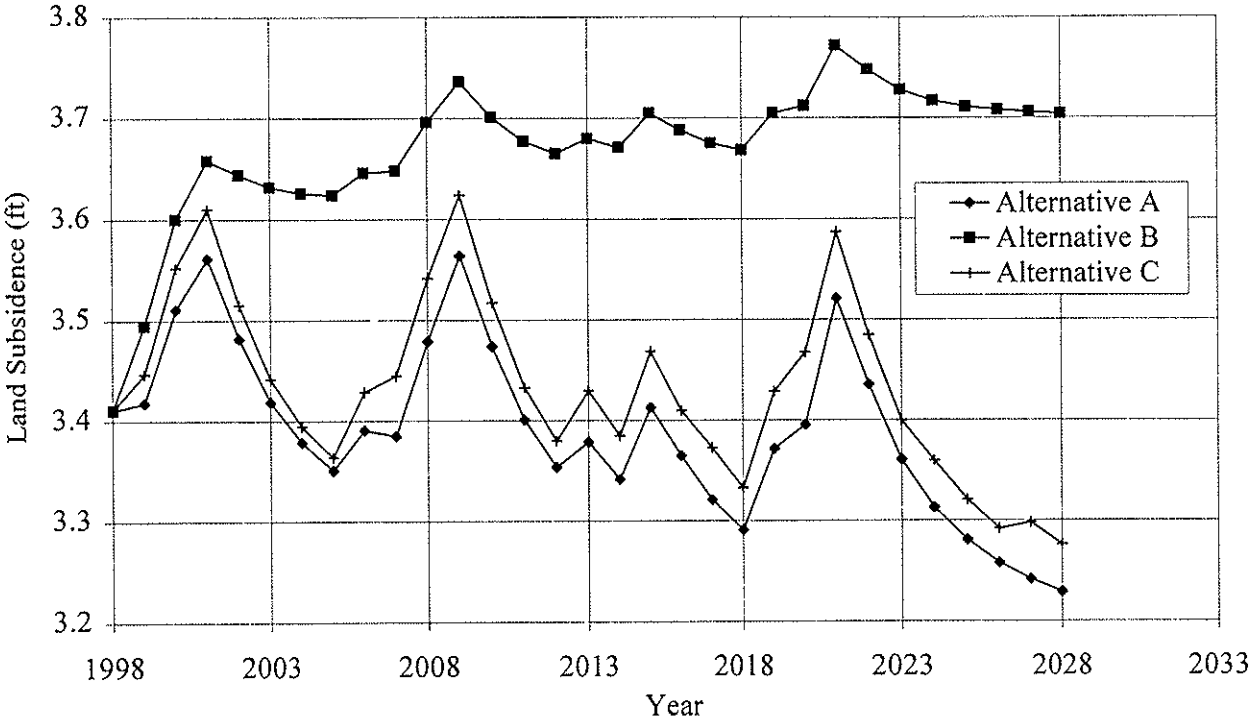

Figure 41 - Model Predictions of Total Subsidence for 1999-2028 at Extensometer 5

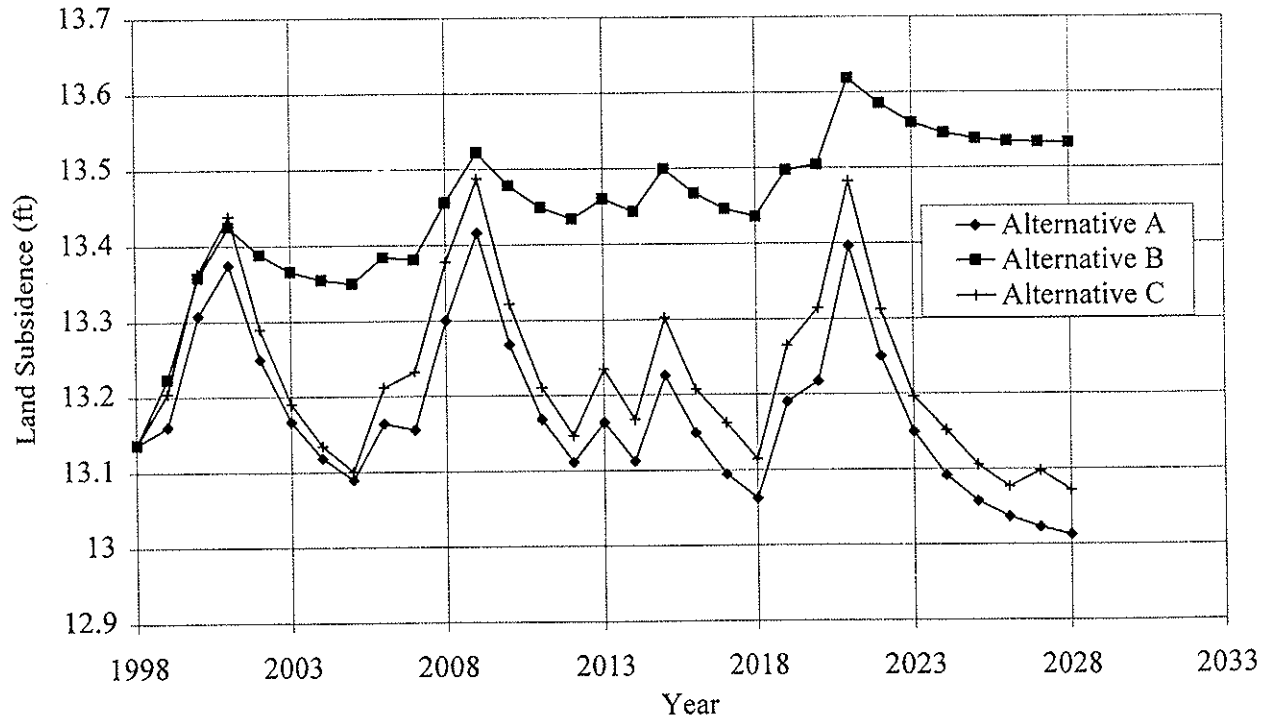

Figure 42 - Model Predictions of Total Subsidence for 1999-2028 at Extensometer 6

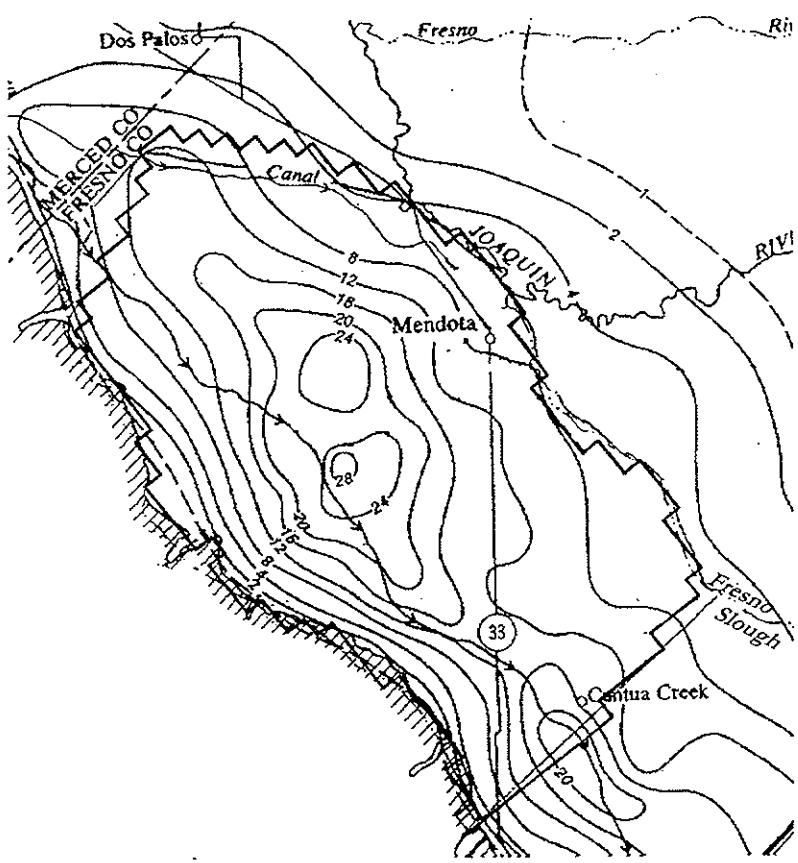

Figure 28A - Observed Subsidence for
Los Banos-Kettleman City, 1926-72
(Ireland et al., 1984)

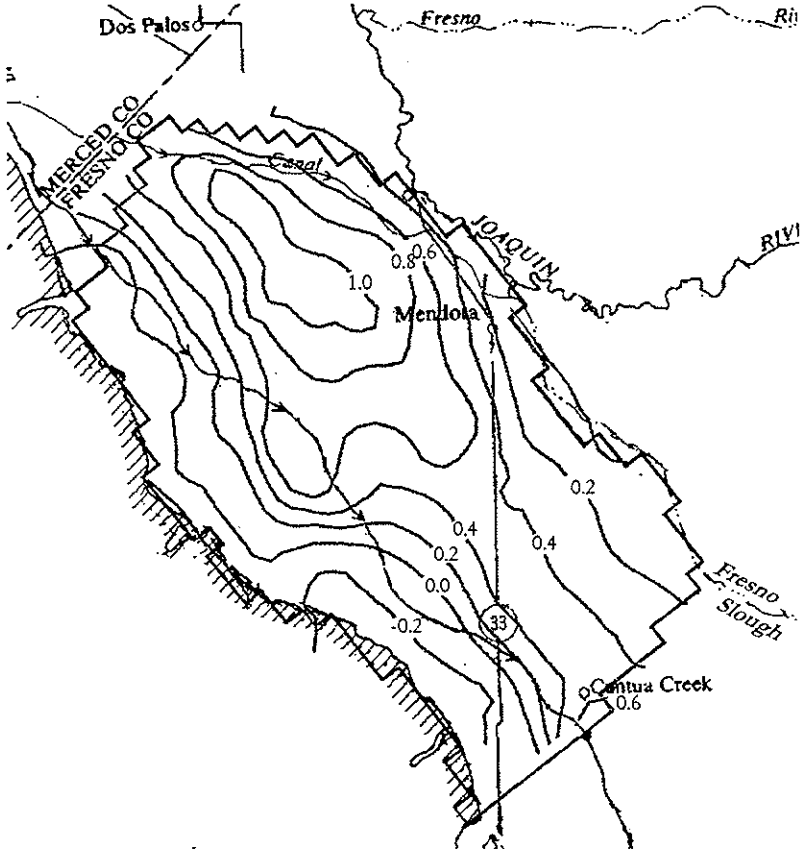

Figure 28B - Simulated Subsidence for
Los Banos-Kettleman City, 1972-98

predicted subsidence from 1972 to 1998. Although the different time periods do not allow for direct comparison, the subsidence trends for each period are similar. There appears to be a small shift in the peak of subsidence to the east. Additional data would be required to verify if this represents a real shift in subsidence or is related to the choice of calibration parameters.

There are four major subsidence parameters determined during the calibration process: hydraulic conductivity, elastic storage coefficient, inelastic storage coefficient, and preconsolidation head. For the Corcoran layer, the storage and conductivity parameters are taken as the average of measured values from Ireland et al. (1984). They remain unchanged and only the preconsolidation heads are modified during calibration. Because of the fictional nature of the interbed layer, however, there is no correlation between its storage parameters and values measured in the field. All four major parameters for this layer can only be determined through calibration.

For both the Corcoran and the interbed layer, the hydraulic conductivity and storage coefficients are assumed to be constant in space and time. Since the thickness of the interbed layer is also assumed to be constant in space, this leaves preconsolidation head alone as the main mechanism for spatial variation. Preconsolidation head is given this distinction because there is a large amount of well data to aid in its selection while there is very little information available on the spatial variation of the other parameters.

The final subsidence parameters (i.e., vertical hydraulic conductivity, storage coefficients, and preconsolidation head) were achieved through trial and error. Although the computational effort required to run the model makes a statistically rigorous calibration numerically impractical, a sensitivity analysis has been performed to aid in the selection of model parameters.

3.3 Sensitivity Analysis

3.3.1 Hydraulic Conductivity

Hydraulic conductivity is represented in two directions, vertical and horizontal. The horizontal conductivity is of little interest in the interbed layers because small head gradients and long flow paths result in insignificant horizontal flow. Additionally, the horizontal flow should not be significantly changed by the new model arrangement. Hence, it is acceptable to adopt the average horizontal hydraulic conductivity in the interbed layers as measured in the field by Ireland et al. (1984).

Conversely, the vertical conductivity greatly affects the performance of the model. It determines the rate pore pressure leaves the fine-grained layers and hence, the rate of subsidence. Figure 29(a)-(f) shows the model results obtained using fourfold and one-forth of the calibrated hydraulic conductivity values. As predicted, the rate of consolidation is very dependent upon the hydraulic conductivity while the general trend of the subsidence is not greatly affected.

3.3.2 Elastic and Inelastic Storage Coefficients

The elastic and inelastic storage coefficients determine the magnitude of subsidence for a given change in hydraulic head. The elastic coefficient can be examined independently of the inelastic coefficient during periods of rebound. The small volume of water flowing from the low-conductivity layers during elastic compaction means there is much less time delay associated with rebound than with consolidation. Hence, the rate of subsidence during rebound is almost exclusively determined by the elastic storage coefficient. This makes the elastic coefficient the easiest parameter to calibrate because it can be chosen, virtually independent of the other parameters, to match the observed rebound rate.

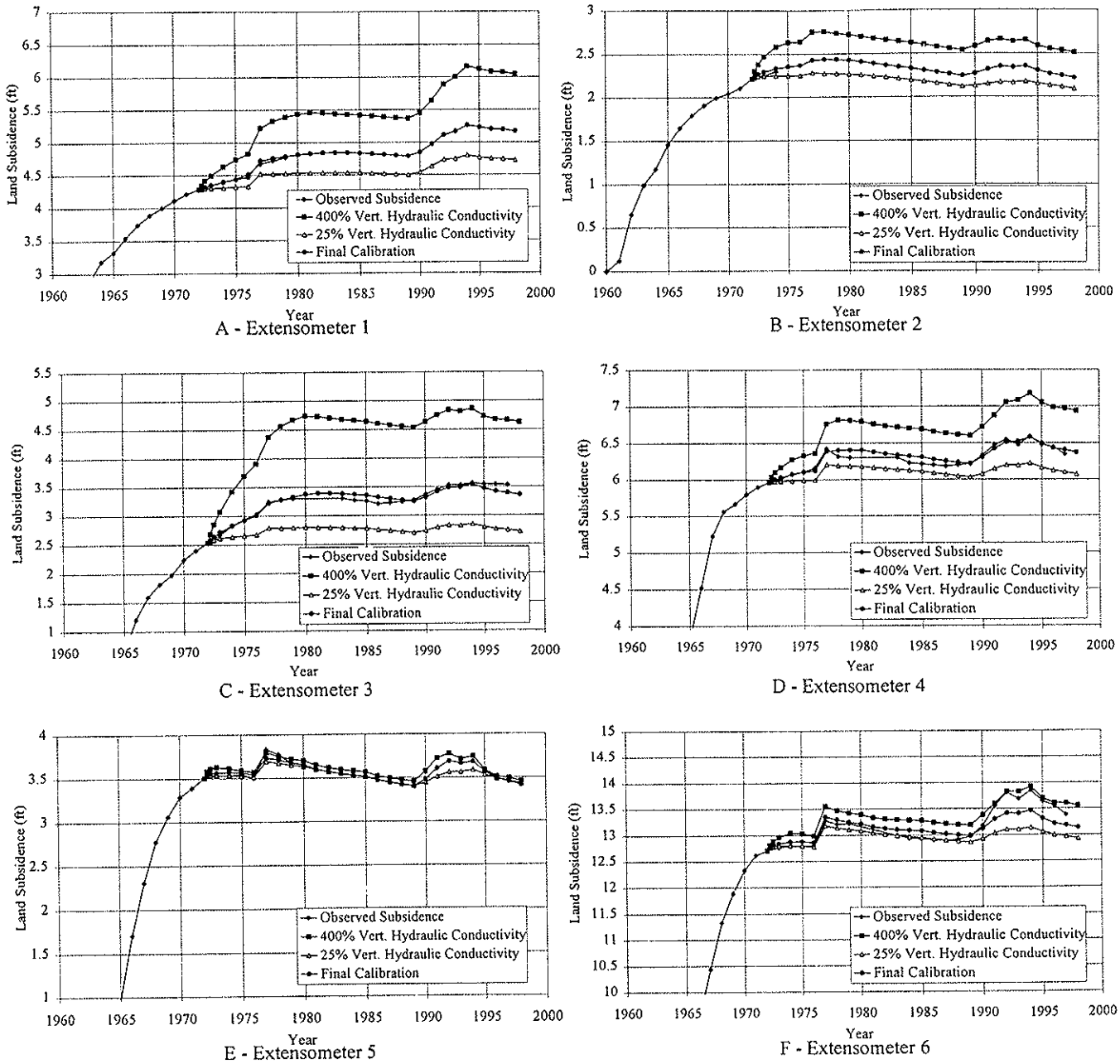

Figure 29A-F - Simulated Subsidence for 400, 100 and 25 Percent of Final Calibrated Value of Vertical Hydraulic Conductivity at Six Extensometer Locations

The contribution of the inelastic coefficient is much more difficult to isolate. It has the least visible effect on the performance of the model. During inelastic compaction a significant volume of water is expelled from the compressible model layers. Because the rate of this expulsion is governed by the vertical hydraulic conductivity, the rate of inelastic consolidation is dominated by the vertical conductivity, not the inelastic storage coefficient. Instead, the latter coefficient determines how quickly the preconsolidation head falls in each layer as consolidation occurs. Thus, it is an important parameter in determining when inelastic compression starts and stops. Figures 30(a)-(f) show the model results obtained using fourfold and one-forth of the calibrated elastic storage coefficients, while Figures 31(a)-(f) present the same information for inelastic storage coefficients.

3.3.3 Preconsolidation Heads

The preconsolidation heads for the Corcoran and interbed layers are determined using the process described earlier (section 3.1.3). Grids of the final preconsolidation heads for each layer can be found in the appendix of this report. If a parabolic profile is assumed as shown in Figure 8, only the upper bound of residual pore pressure need be determined through calibration. This upper bound of residual pore pressure was first approximated using the 1943 head values in the confined aquifer. The year 1943 was chosen because it was approximately this time when intense ground water withdrawal began to cause the most serious subsidence. These values were then adjusted during the calibration process to match observed subsidence.

Preconsolidation head has two effects on the model. First, an increase in preconsolidation head (and corresponding increase in initial head) results in an increased rate of subsidence because of the larger gradient between heads in the aquifers and in the compressible layers. Second, an increase in preconsolidation head results in longer periods of subsidence

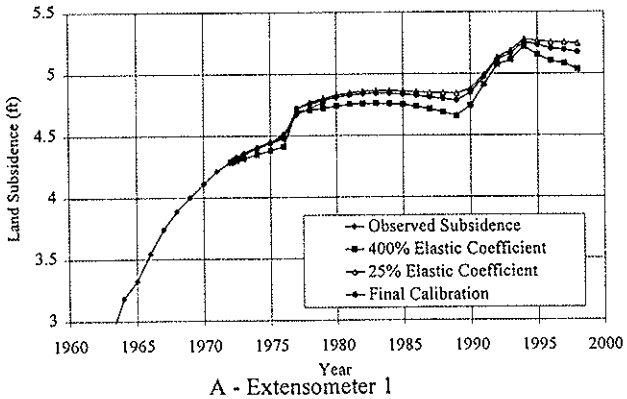

A - Extensometer 1

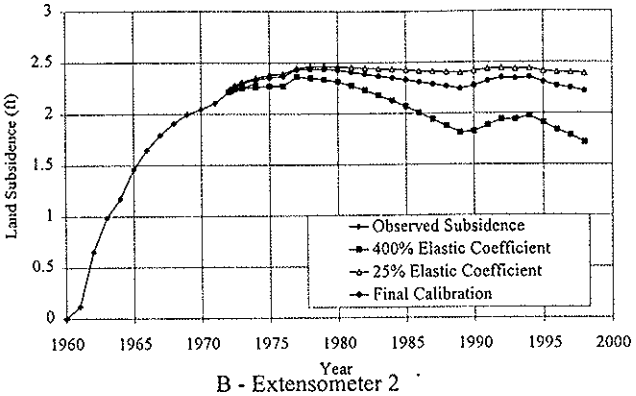

B - Extensometer 2

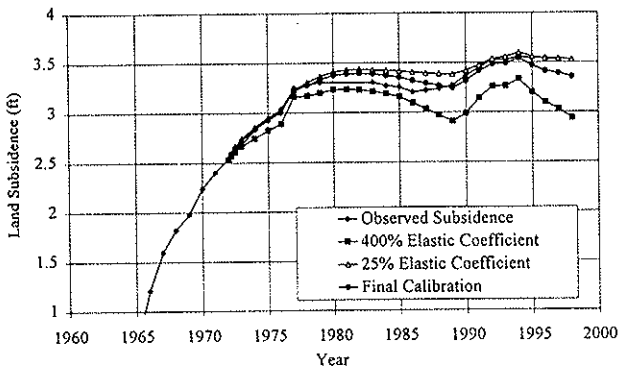

C - Extensometer 3

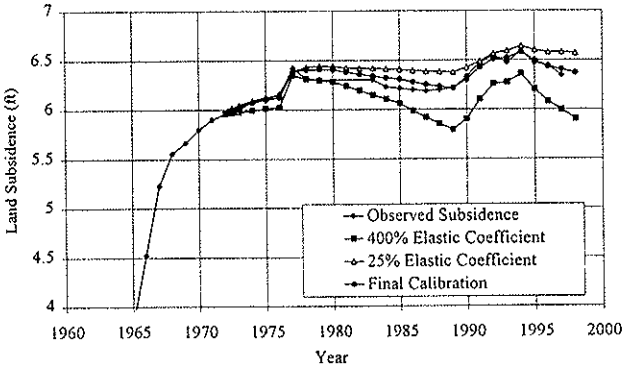

D - Extensometer 4

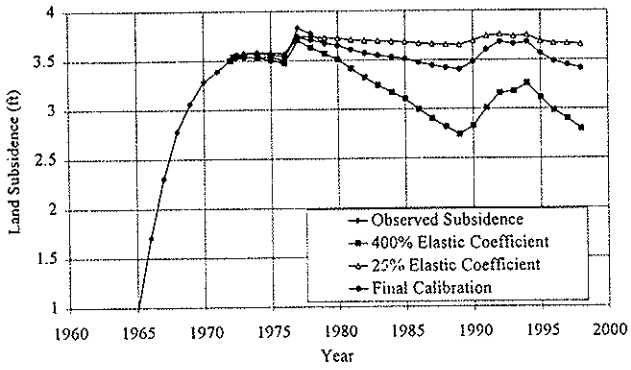

E - Extensometer 5

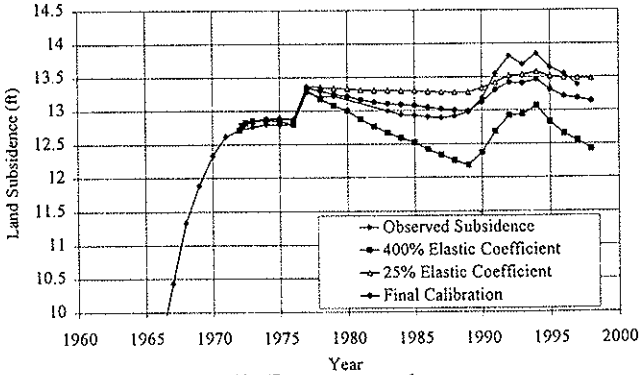

F - Extensometer 6

Figure 30A-F - Simulated Subsidence for 400, 100 and 25 Percent of Final Calibrated Value of Elastic Storage Coefficient at Six Extensometer Locations

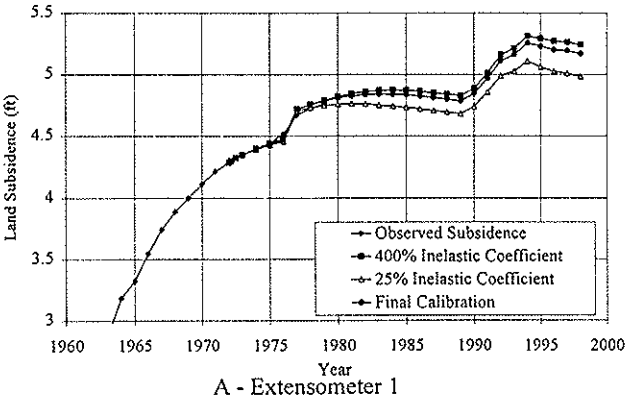

A - Extensometer 1

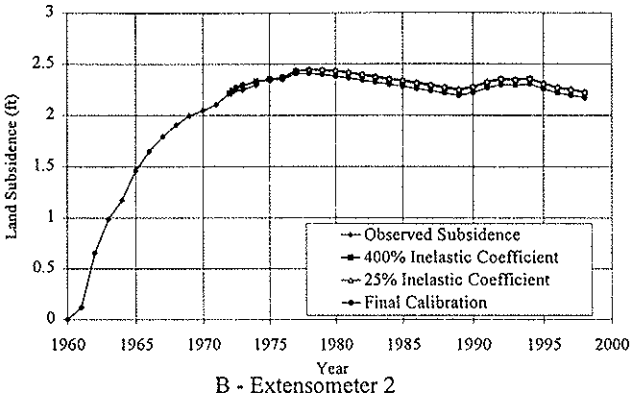

B - Extensometer 2

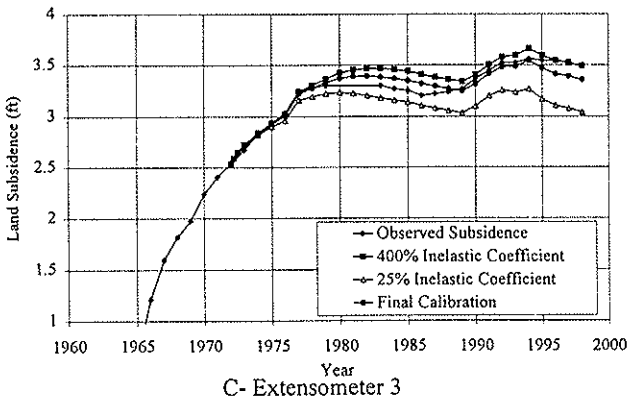

C- Extensometer 3

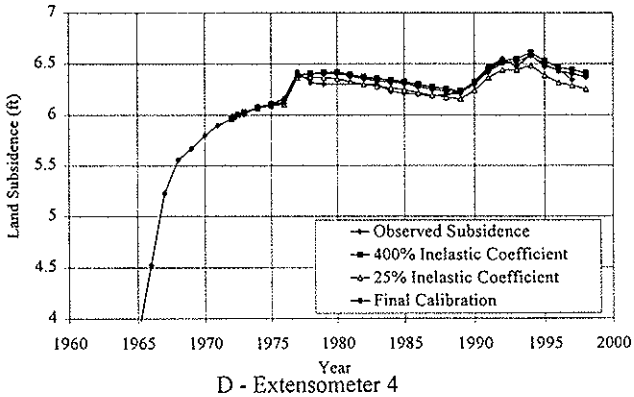

D - Extensometer 4

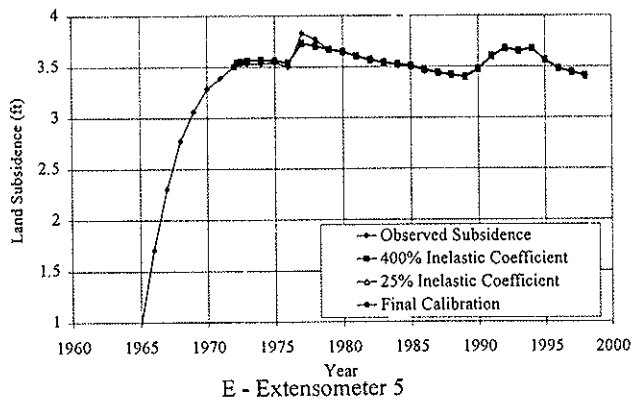

E - Extensometer 5

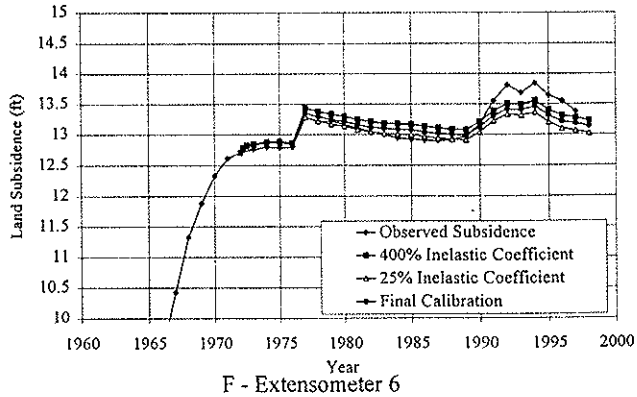

F - Extensometer 6

Figure 31A-F - Simulated Subsidence for 400, 100 and 25 Percent of Final Calibrated Value of Inelastic Storage Coefficient at Six Extensometer Locations

since head levels must rise higher for rebound to begin. This second characteristic makes it possible to differentiate between the effects of an increase in preconsolidation head and an increase in vertical conductivity. Figure 32(a)-(f) shows the model results obtained using fourfold and one-forth of the calibrated residual pore pressure values.

4. PREDICTING FUTURE SUBSIDENCE POTENTIAL

4.1 Development of Future Drought Scenarios

It is not currently possible to predict land subsidence for the Los Banos-Kettleman City area. As illustrated during the calibration process, ground water levels and subsidence are highly dependent upon the rate of pumping. Because pumping rates are dependent on surface water availability, reliable long-range weather forecasting is required before true subsidence prediction is possible. Instead of predicting subsidence, this model estimates subsidence potential by evaluating subsidence for possible CVP water delivery scenarios.

Unfortunately, the CVP water delivery system has been in place for only 30 years. This does not provide sufficient data to statistically generate future CVP delivery rates. However, two river indices for water year classification, the Sacramento Valley 40-30-30 and the San Joaquin Valley 60-20-20, were developed by the State Water Resources Control Board (SWRCB) as part of the SWRCB's Bay-Delta regulatory activities (California DWR, 1998). Since the majority of the Los Banos-Kettleman City CVP water comes from the Sacramento Valley, the Sacramento 40-30-30 index can be used to estimate future surface water supplies in the Los Banos-Kettleman City area.

The Sacramento 40-30-30 index, also known as the Sacramento Four-Rivers Index (SFRI), is calculated from measurements of unimpaired runoff for four major rivers in the Sacramento Valley: American, Feather, Sacramento, and Yuba. The SFRI is computed as the

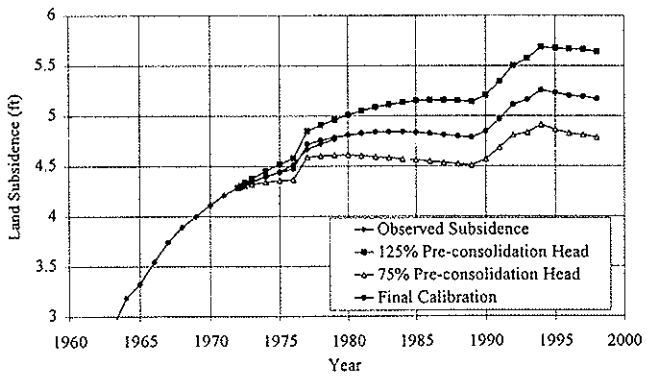

A - Extensometer 1

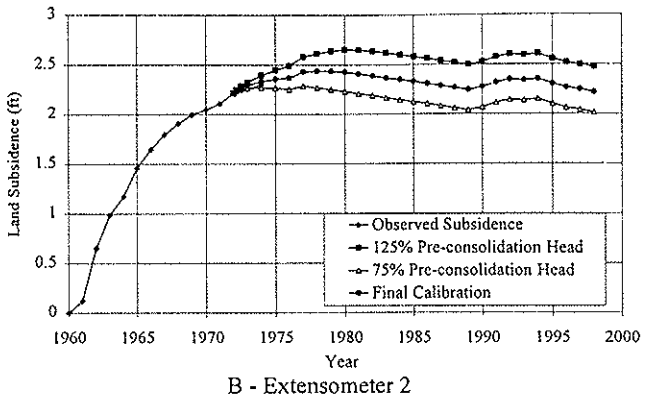

B - Extensometer 2

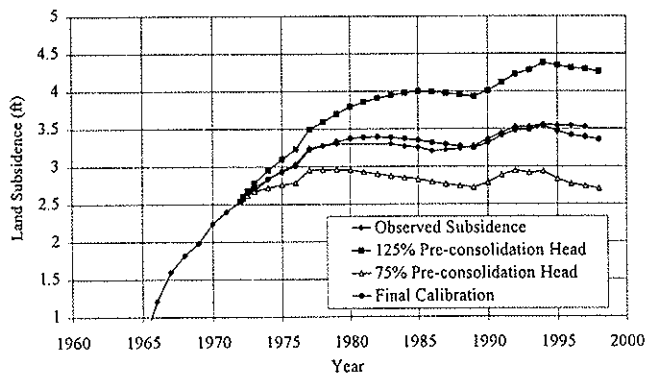

C - Extensometer 3

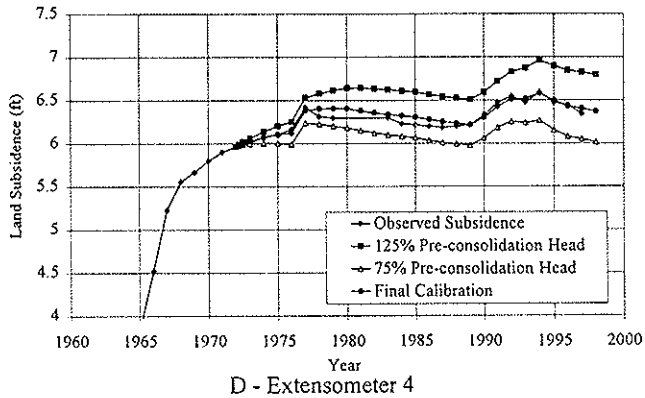

D - Extensometer 4

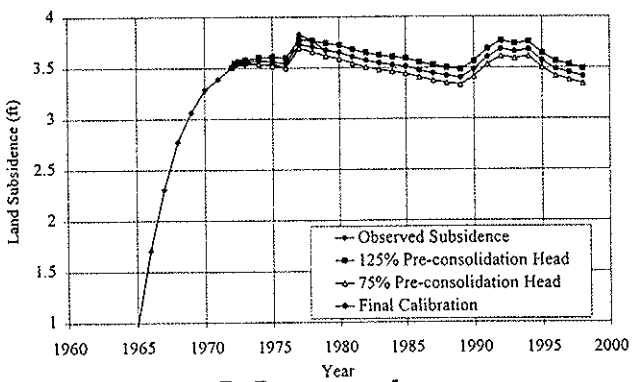

E - Extensometer 5

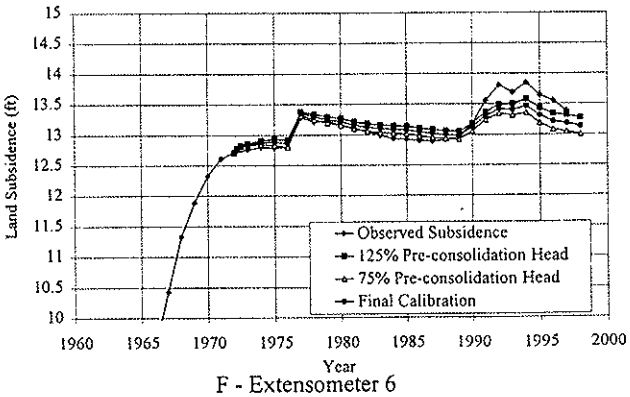

F - Extensometer 6

Figure 32A-F - Simulated Subsidence for 125, 100 and 75 Percent of Final Calibrated Value of Residual Pore Pressure at Six Extensometer Locations

the sum of 40 percent of the current year's April-July unimpaired runoff, 30 percent of the October-March unimpaired runoff, and 30 percent of the previous year's SFRI. A cap of 10 MAF is placed on the previous year's index to account for required flood control releases during wet years (California DWR, 1998).

Figure 33 shows the best fit relationship between the SFRI and the CVP delivery rates for years classified by the California Department of Water Resources as "below average," "dry," or "critical." The relationship is mathematically described ($R^2 = 0.7264$) as:

$$\Phi_s = 2 \times 10^{-7} (SFRI)^{2.2839} \tag{5}$$

in which Φ_s is the percent of contracted CVP surface water and SFRI is in million acre-feet.

Historical records of the SFRI are available from 1906 to present. Although this is still not enough data to provide any strong conclusion regarding the statistical distribution of the population, there are enough samples to generate future scenarios using the bootstrap method. The bootstrap method is based on the assumption that a sample set adequately represents the entire population and that new scenarios can be generated by sampling with replacement from the original set. The major restriction of this method is that all sample points must be independent. Although the SFRI has an obvious one-year lag dependency, the yearly unimpaired runoff reveals no temporal correlation. Thus, the bootstrap method may be used to generate unimpaired runoff scenarios. Sampling from the original set using randomly generated uniform deviates produces potential runoff scenarios. Each thirty-year realization represents an equally likely runoff scenario for the forecast period, 1999-2028. Each runoff scenario is then transformed to a SFRI scenario using the 40-30-30 procedure outlined earlier.

The severity of a drought forecast can be measured in several ways. Two such ways suggested by Shen and Tabios (1996) are average drought severity and cumulative deficit.

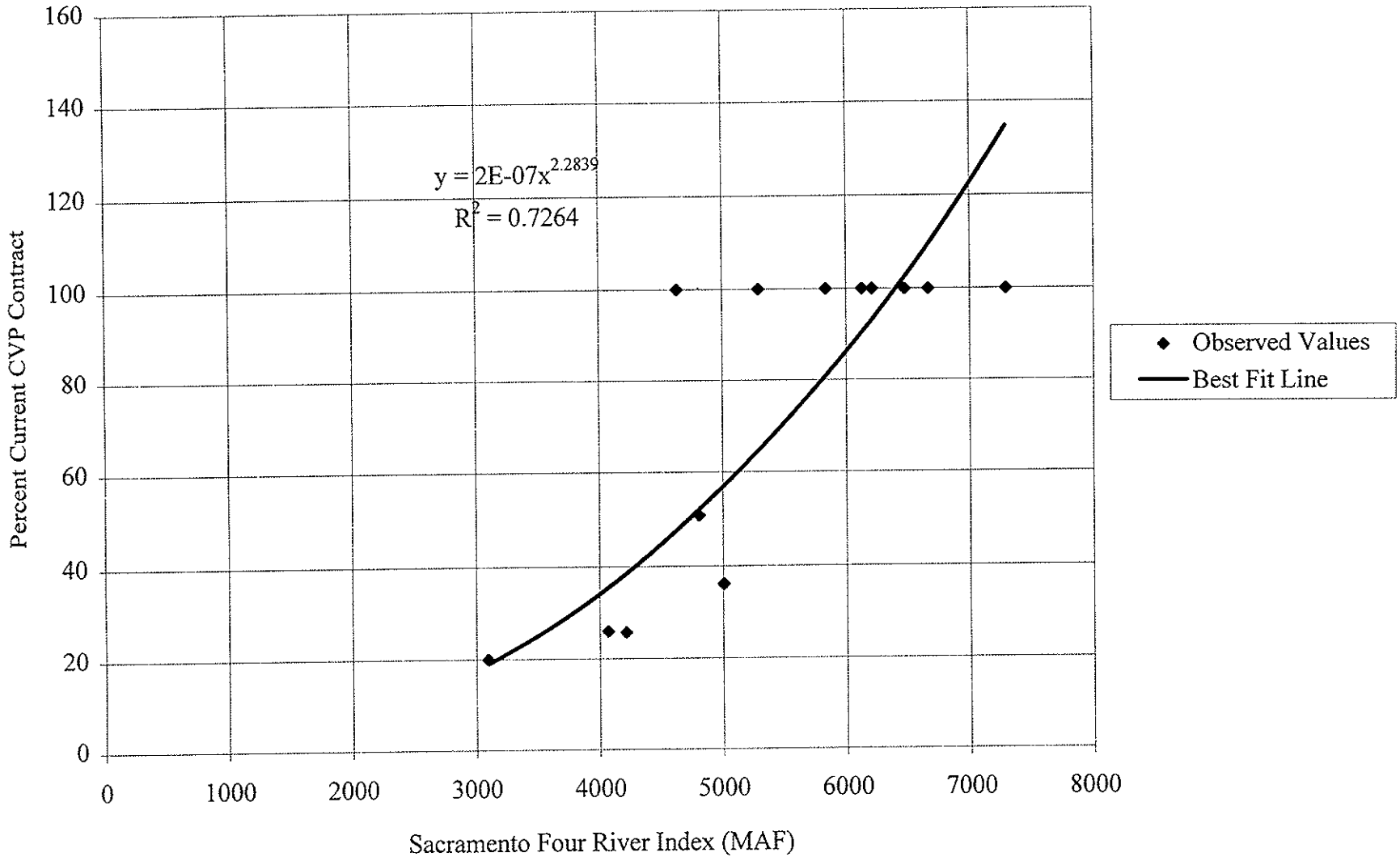

Figure 33 - Best-Fit Delivery Rates for "Below Average," "Dry," and "Critical" Water Years

Average drought severity averages the shortfall for all "drought years" occurring in the forecast. For this purpose, a drought year is defined as any year in which less than 100 percent of the CVP contract water is available. This criterion identifies forecasts with severe drought events but does not consider the number of drought events. Conversely, cumulative deficit sums the shortfall for all years that fall below the critical level, giving increased weight to forecasts with additional years of drought. The disadvantage of this criterion is that forecasts with many years of minor drought are indistinguishable from forecasts with fewer years of severe drought. Years of severe drought cause proportionally more subsidence and thus, are of greater interest for this study.

Figures 34 and 35 show the cumulative distribution functions for the average drought and cumulative deficit criteria, respectively. The distribution functions were created using the drought measurements of five hundred scenarios generated using the bootstrap method. Because both criteria have advantages, a drought scenario with a five percent probability of exceedance for both categories is considered. Table 4 summarizes the SFRI and corresponding CVP delivery rates for the selected scenario.

4.2 Potential Management Alternatives

Figure 36 is a graphical representation of the alternatives considered in this study. Alternative A is the current best-fit relationship between surface water delivery rates and SFRI found in figure 33. In essence, this alternative represents maintaining current management practices. For reasons given previously (section 2.1), however, it is probably unreasonable to expect current surface water supplies to remain undiminished. Additionally, drainage problems documented by Belitz and Phillips (1995) indicate some change in water management is needed

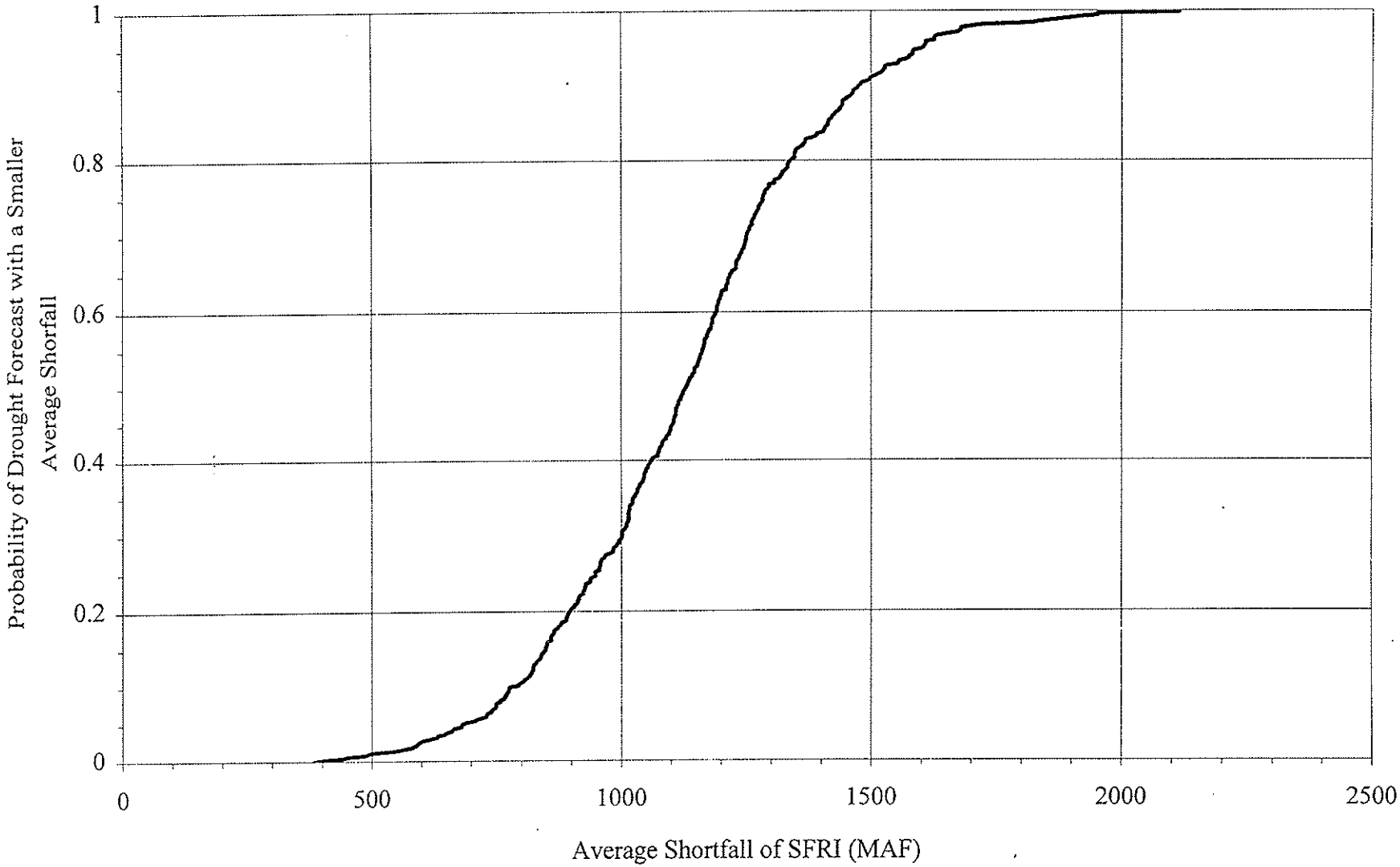

Figure 34 - Distribution Function of Average Shortfall

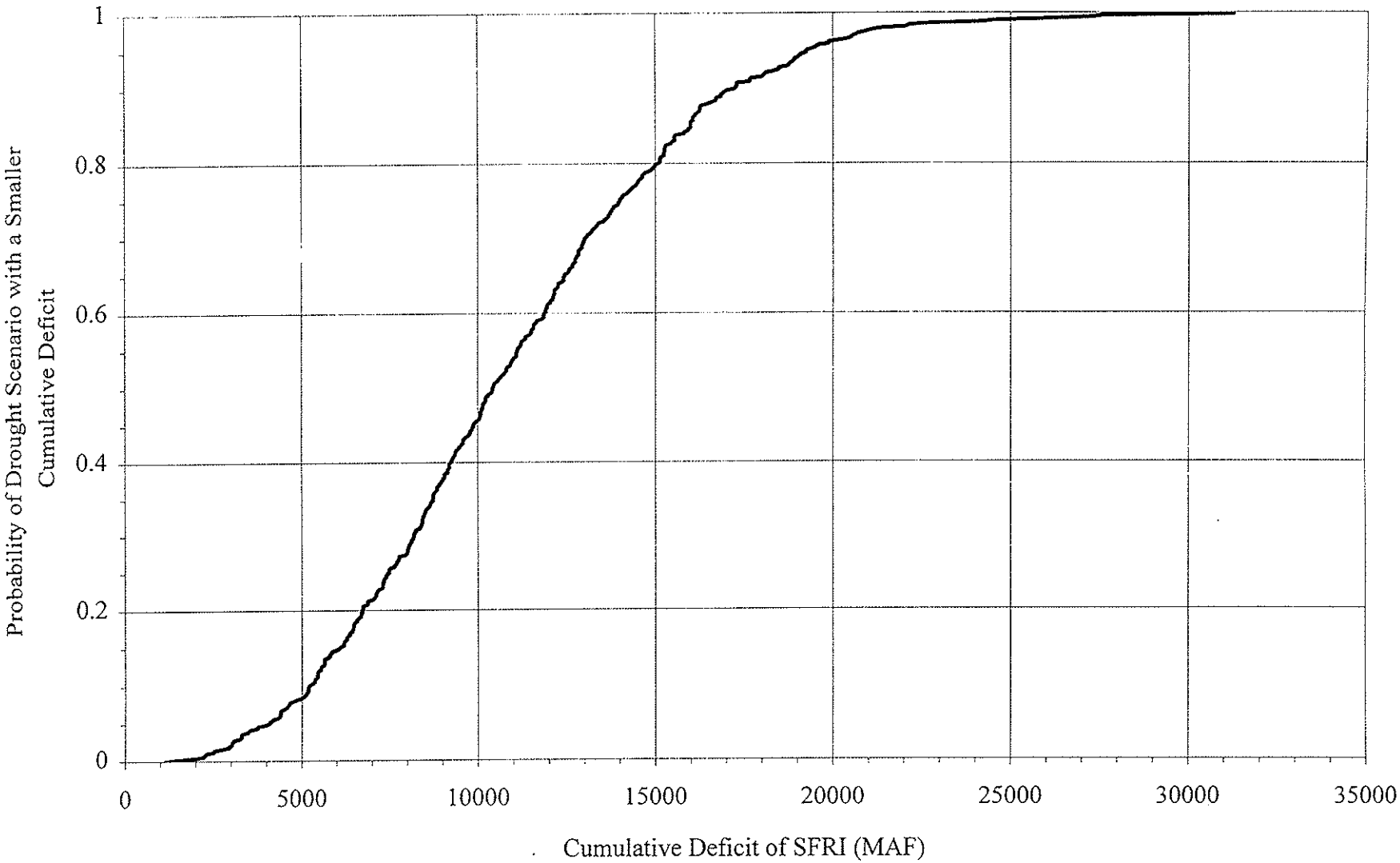

Figure 35 - Distribution Function of Cumulative Deficit

Table 4 - Future Water Delivery Scenario

Year	SFRI (MAF)	CVP Delivery Rate	CVP Delivery Rate Alternative C
1999	5,806	79%	64.7%
2000	4,325	40.3%	33.4%
2001	4,599	46.4%	38.3%
2002	9,363	100%	100%
2003	9,023	100%	100%
2004	7,084	100%	100%
2005	9,776	100%	100%
2006	5,379	66.3%	54.5%
2007	5,984	84.6%	69.3%
2008	4,241	38.5%	31.9%
2009	3,958	32.9%	27.3%
2010	10,129	100%	100%
2011	9,768	100%	100%
2012	8,686	100%	100%
2013	5,455	68.5%	56.3%
2014	9,909	100%	100%
2015	4,727	49.5%	40.8%
2016	7,971	100%	100%
2017	6,725	100%	90.1%
2018	11,795	100%	100%
2019	4,754	50.0%	41.3%
2020	5,381	66.4%	54.6%
2021	3,368	22.8%	19.0%
2022	9,000	100%	100%
2023	13,262	100%	100%
2024	6,754	100%	91.0%
2025	10,257	100%	100%
2026	7,162	100%	100%
2027	6,526	100%	84.2%
2028	7,615	100%	100%

Average Shortfall (Percentile) = 1607.4 (95.6%)
Cumulative Drought (Percentile) = 19,290 (95.2%)

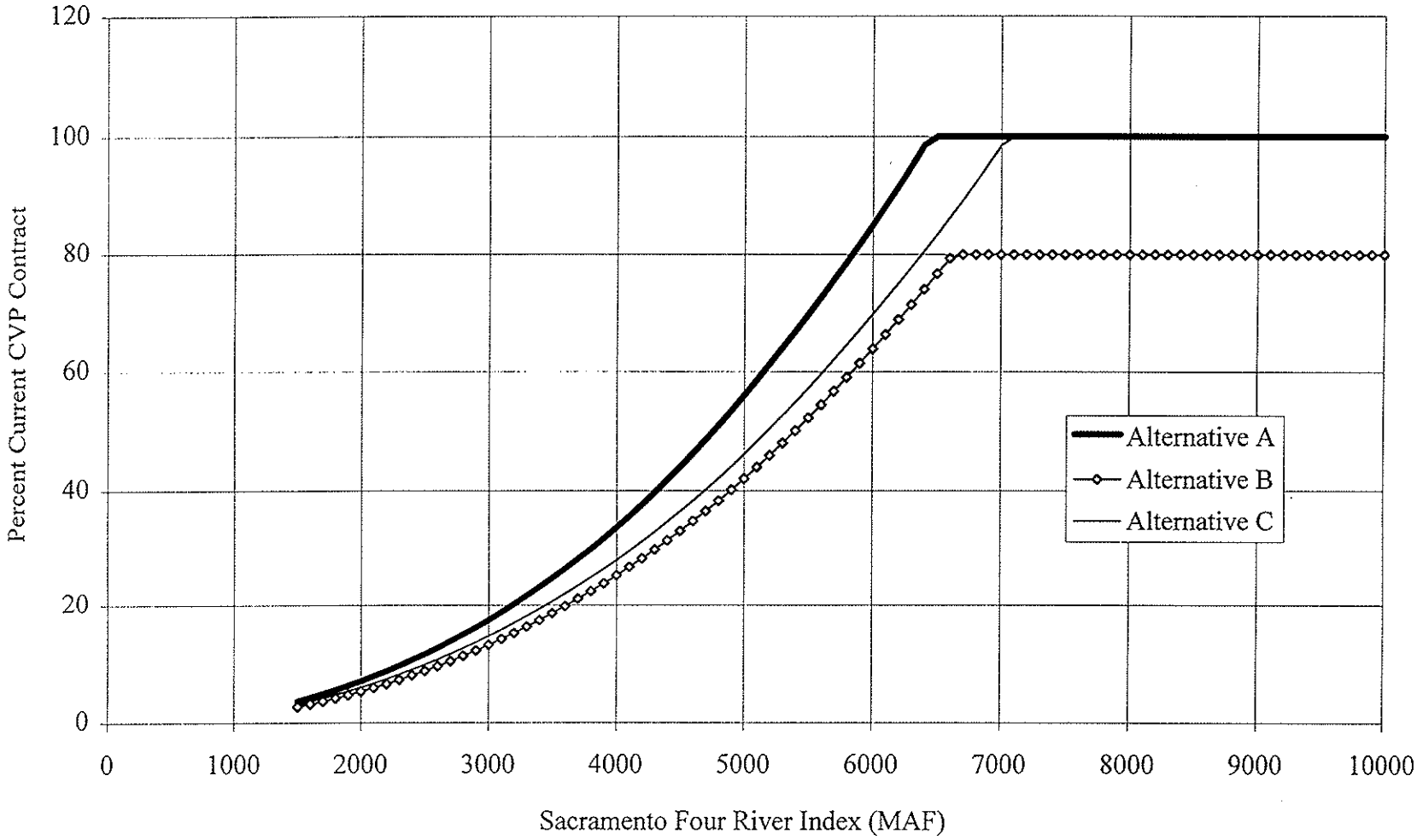

Figure 36 - Management Alternatives

for agriculture to remain viable in the Los Banos-Kettleman City region. Two additional alternatives addressing these issues are also considered.

As one possible solution to the drainage problems in the region, Belitz and Phillips (1995) proposed a combination of increased ground water pumpage and reduced recharge. Their proposal is considered as alternative B and is summarized by the water budget given in Table 5. It is an attractive alternative because it would reduce many of the drainage problems in the region. It would also require only minimal investment, as all increases in pumping would occur at existing wells. It is assumed that the relationship between percent CVP delivery rates and SFRI remains the same as in Alternative A, but that the 100 percent delivery rate is reduced to the rate proposed by Belitz and Phillips (1995).

Alternative C reduces surface water demand not by changing the total contracted amount of surface water, but by changing the relationship between percent delivery rate and SFRI. By increasing the SFRI required to result in a 100 percent CVP delivery rate, Alternative C reduces the surface water used during drought years. During wet years there is no reduction in total surface water use. During drier years, however, surface water use is reduced up to 20 percent for years of moderate drought, with more modest reductions during years of severe drought. (see figure 36) Although this alternative would provide a reduction of up to 153,000 acre-feet of surface water during years of drought, it does little to address the drainage and water quality problems facing the region.

4.3 Optimization Model

A linear optimization model was formulated to find the maximum increase in ground water withdrawal without causing any inelastic compaction during the 30-year planning horizon. In order to eliminate the nonlinearity associated with subsidence, heads are allowed to fluctuate

Table 5 - Alternative B Proposed Water Budget
(From Belitz and Phillips, 1995)

Subarea	Area (mi^2)	Surface Water Delivery (ft/yr)	Ground Water Pumpage (ft/yr)	Ground Water Recharge (ft/yr)
Firebaugh	73	1.85	0.5	0.47
Panoche	48	1.58	0.5	0.56
Broadview	16	1.99	0.5	0.52
Tranquility	30	1.88	0.8	0.71
San Luis	30	1.24	0.9	0.67
WestLands				
Depth to Water < 10 ft	97	1.33	0.9	0.39
10 ft < Depth to Water < 20ft	42	1.58	0.96	0.63
Depth to Water > 20 ft				
with suface water	163	1.79	0.75	0.8
without surface water (1980)	30	1.23	1.23	0.86

only within the region of elastic compaction. This is accomplished by setting the preconsolidation head as the lower bound for ground water levels in the confined aquifer. For simplicity in computation and implementation, the optimization model assumes uniform pumping over each pumping subarea and heads are only monitored at one characteristic location in each subarea.

A response function approach (Gorelick, 1983; Yeh, 1992) is used in the model formulation. In this approach, the calibrated simulation model is used to generate response coefficients. The model is first allowed to reach a steady state under normal-year pumping conditions. Each pumping subarea is then separately subjected to a unit impulse of additional pumpage in the first period with no disturbance thereafter, and the system response to each excitation is monitored over the entire planning period. All the responses are then assembled in a response matrix. This response matrix can subsequently be used in the formulation of the following optimization model.

The objective function of the optimization model maximizes the total ground water withdrawal at all production wells during the forecast period:

$$Max\ Z = \sum_{n=1}^{NTS} \sum_{k=1}^{NOW} Q(k,n) \tag{6}$$

in which Z is the value of the objective function (L); Q(k,n) is volume of water withdrawn from the k^{th} well field (L^3/T); NTS is the total number of periods; NOW is the total number of well fields; and n is the time index.

The constraint set of the model includes the following conditions and specifications:

1. The projected additional ground water demand above the normal year demand, GWD(n), needs to be met:

$$\sum_{k=1}^{NOW} Q(k,n) \geq GWD(n) \qquad \forall n \qquad (7)$$

2. Ground water withdrawals are related to drawdowns through the response function coefficients:

$$s(l,n) = \sum_{n=1}^{NTS} \sum_{k=1}^{NOW} \beta(l,k,n-i+1) \cdot Q(k,n) \qquad \forall l, \forall n \qquad (8)$$

in which s(l,n) is the drawdown at the l^{th} observation point; and β(.) are the response coefficients.

3. Drawdown cannot exceed the maximum permissible drawdown (difference between the initial water level and the preconsolidation head level), and minimum and maximum pumpage rates at the production wells need to be satisfied:

$$s(l,n) \leq s_{MAX}(l) \qquad \forall n \qquad (9)$$

$$Q_{MIN}(k) \leq Q(k,n) \leq Q_{MAX}(k) \qquad \forall n \qquad (10)$$

Maximum pumpage rates are set at 1.3 ft/year for all subareas. This bound was chosen to both limit the amount of pumping from any one subarea and to reflect number of existing wells.

The total area and maximum allowable drawdown for each water budget subarea are given in Table 6. Two different sets of maximum allowable drawdown are used in the optimization model in wet and dry periods. The maximum allowable drawdown in wet years corresponds to the preconsolidation head in the bottom sub-layer of the clay interbed unit. This

Table 6 - Maximum Drawdowns and Areas for Pumping Subareas

	Water Budget Subareas								
	1	6	8	9	10	11a	11b	11c	11d
S_{max}-dry (feet)	141.6	124.8	152.8	172.5	225.2	153.1	168.4	195.3	269.7
S_{max}-wet (feet)	95.9	83.4	97.5	109.6	175.8	98.8	105.4	116.9	214.2
Area (mi^2)	73	30	48	16	30	98	41	148	45

is the maximum preconsolidation head for any compressible layer. Because of the low conductivity of the clay layer, however, piezometric head levels in the confined aquifer may drop below this value for short periods without causing inelastic subsidence. To take advantage of this additional capacity, the maximum allowable drawdown during dry years corresponds to the preconsolidation head in the outermost layer of the clay interbed unit. This adjustment provides for additional drawdown during periods of drought, but sustains long-term head levels above all values of preconsolidation head.

The calibrated MODFLOW (McDonald and Harbough, 1992) model was used to derive the response coefficients. The optimization model formulated above is a linear programming model and was solved using GAMS (Brook et al., 1992). The pumping rates calculated by the optimization model were then returned to the simulation model to estimate land subsidence.

4.4 Results

Figures 37-42 present the model predictions of total subsidence for the years 1999 to 2028 at the six extensometer locations used for calibration. Contour maps of land subsidence across the entire study area are shown as Figures 43-45.

Alternative A causes very little subsidence. Although there is some elastic compaction during years of drought, the overall trend is toward rebound. Alternative B causes significant subsidence, especially in the northwest corner of the model. At extensometers 13/12-20D1, 15/13-11D2, and 16/15-34N1, subsidence occurs predominantly during periods of drought. At the other extensometer locations, subsidence continues during normal water years as well. Alternative C produces subsidence similar to that of alternative A. In general, the compaction is elastic and long-term subsidence is minimal. A small increase in inelastic compaction during periods of drought accounts for the difference between the two alternatives. The optimization

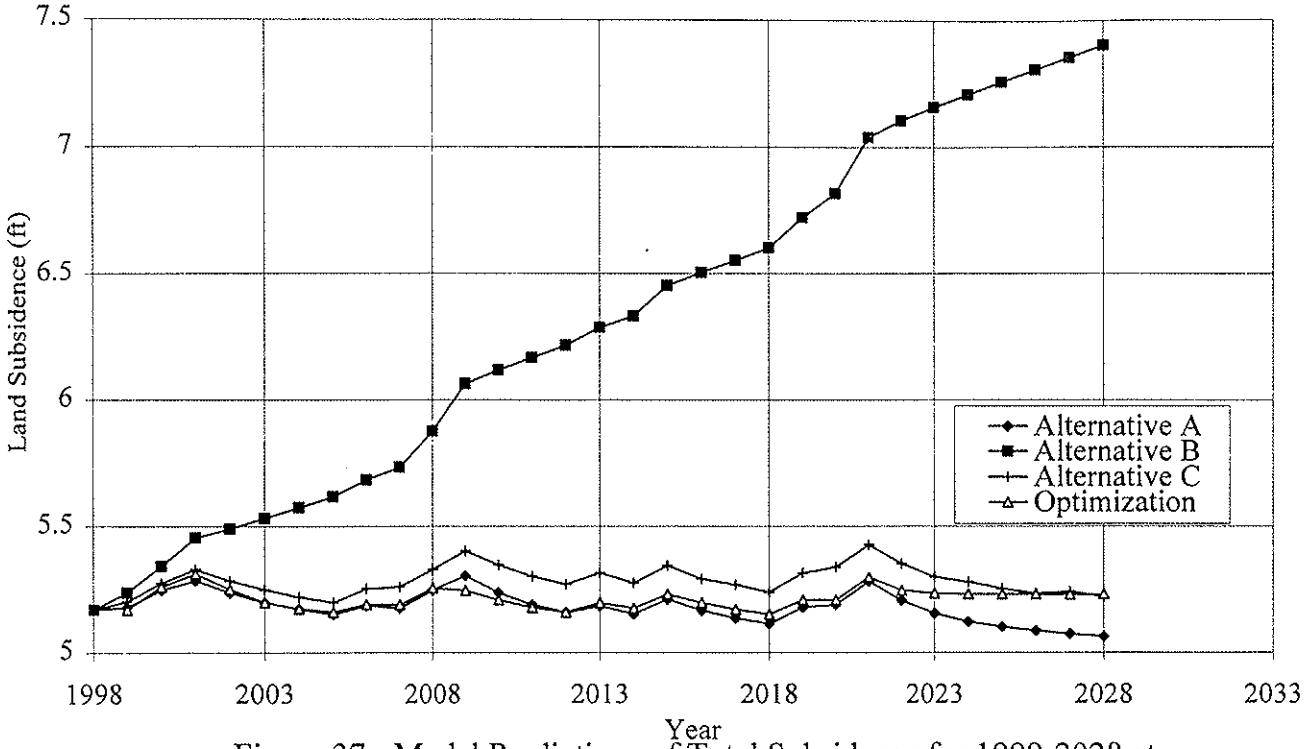

Figure 37 - Model Predictions of Total Subsidence for 1999-2028 at Extensometer 1

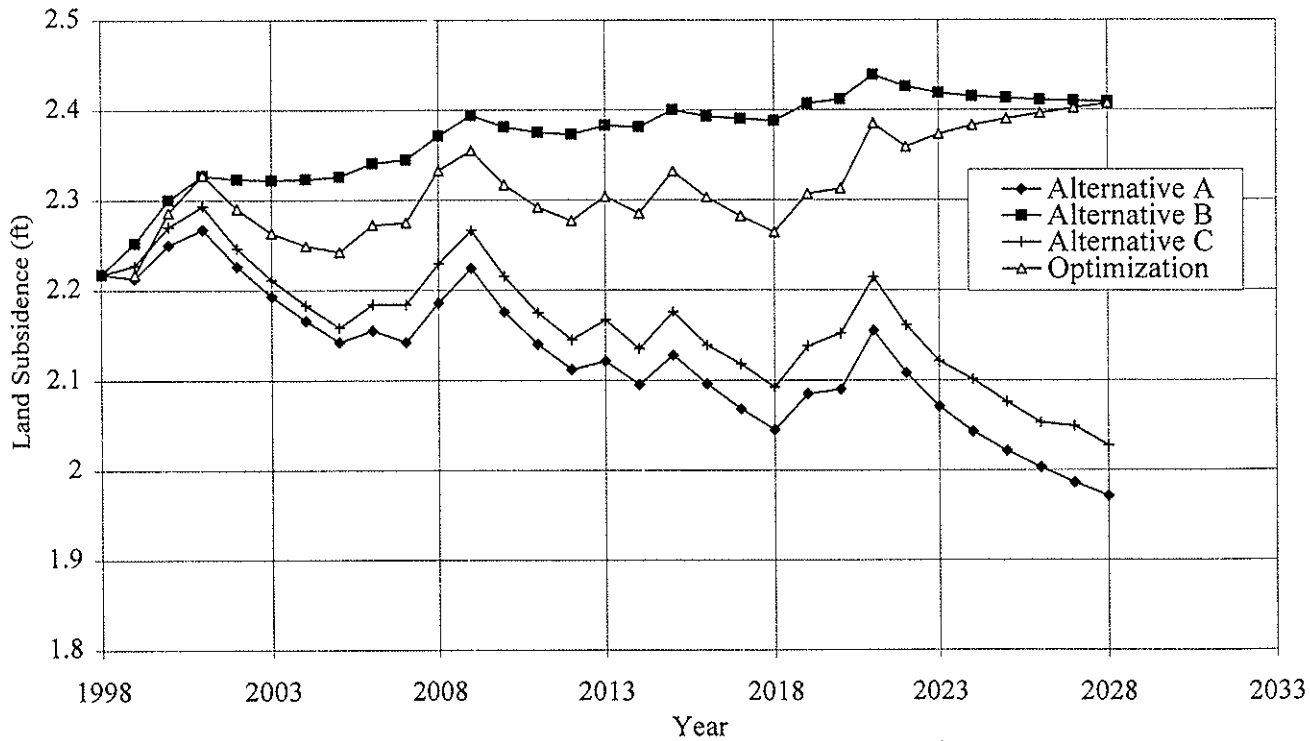

Figure 38 - Model Predictions of Total Subsidence for 1999-2028 at Extensometer 2

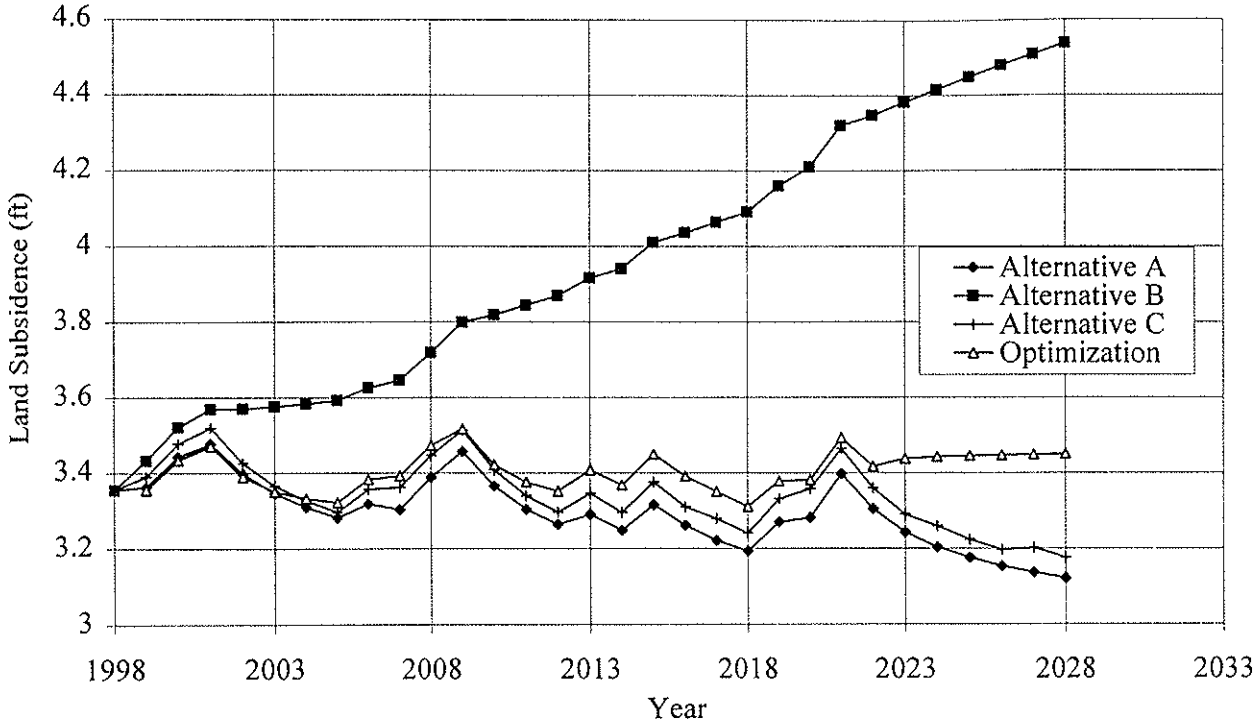

Figure 39 - Model Predictions of Total Subsidence for 1999-2028 at Extensometer 3

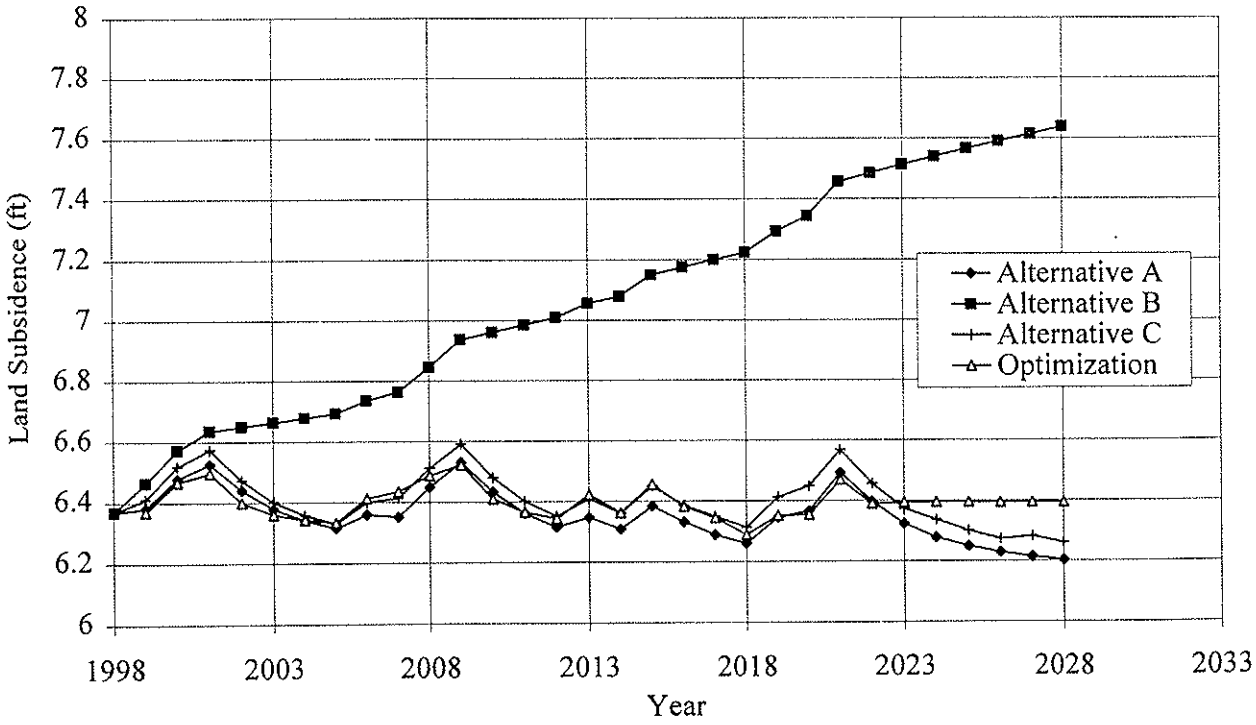

Figure 40 - Model Predictions of Total Subsidence for 1999-2028 at Extensometer 4

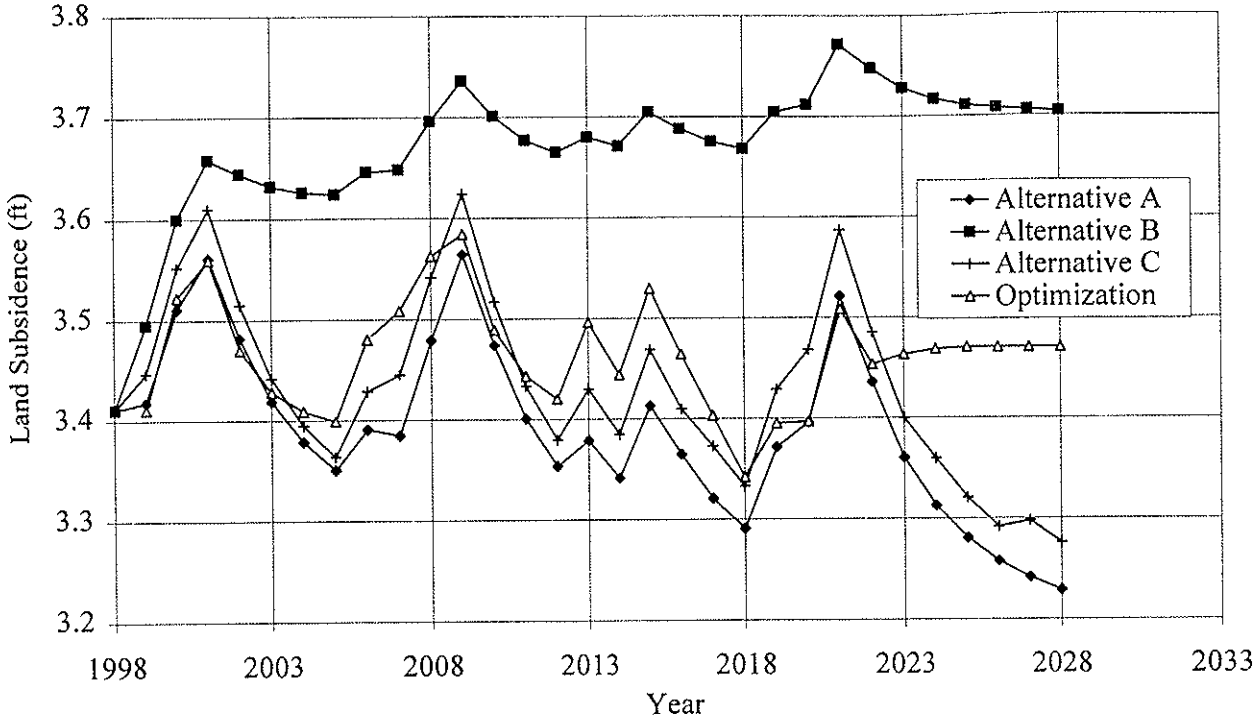

Figure 41 - Model Predictions of Total Subsidence for 1999-2028 at Extensometer 5

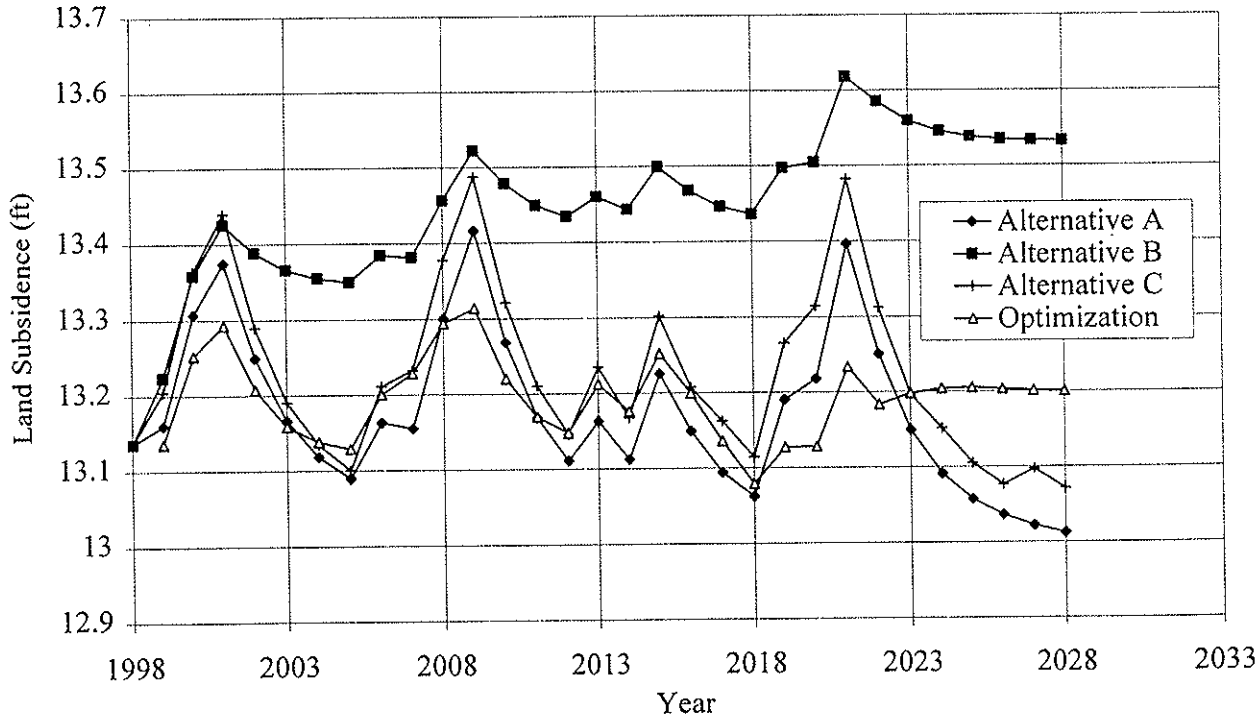

Figure 42 - Model Predictions of Total Subsidence for 1999-2028 at Extensometer 6

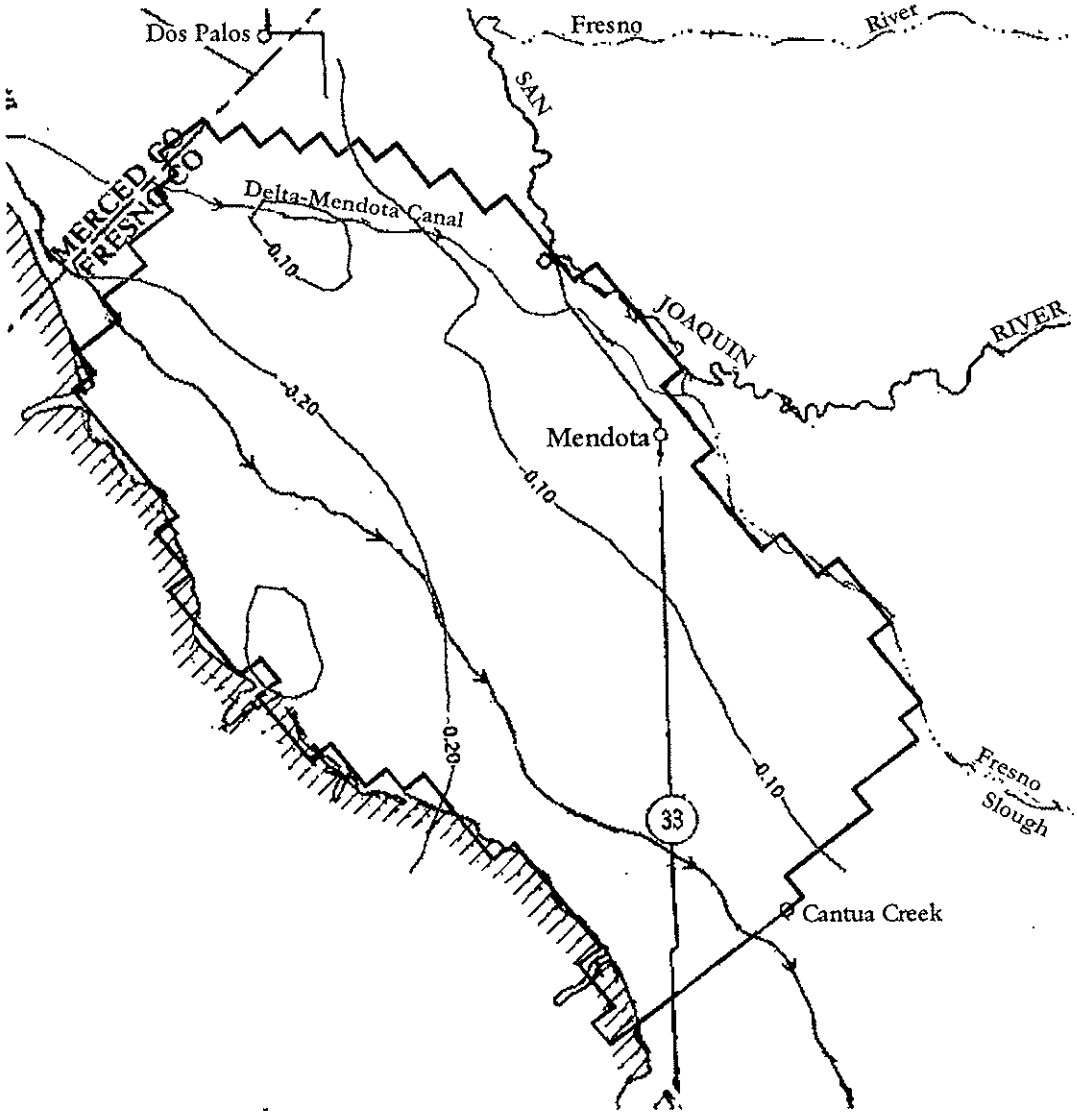

Figure 43 - Simulated Subsidence, 1999-2028 (Alternative A)

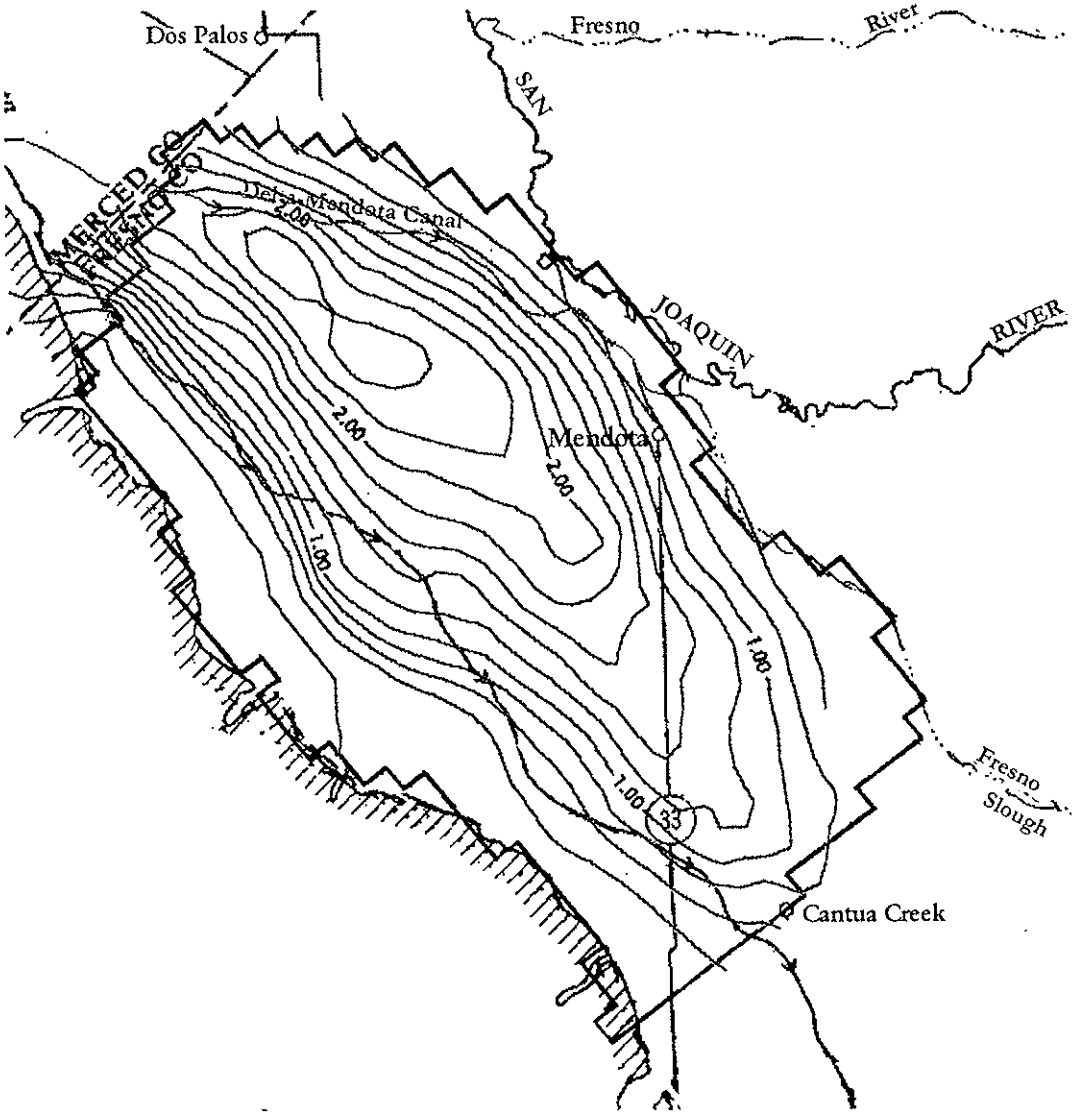

Figure 44 - Simulated Subsidence, 1999-2028 (Alternative B)

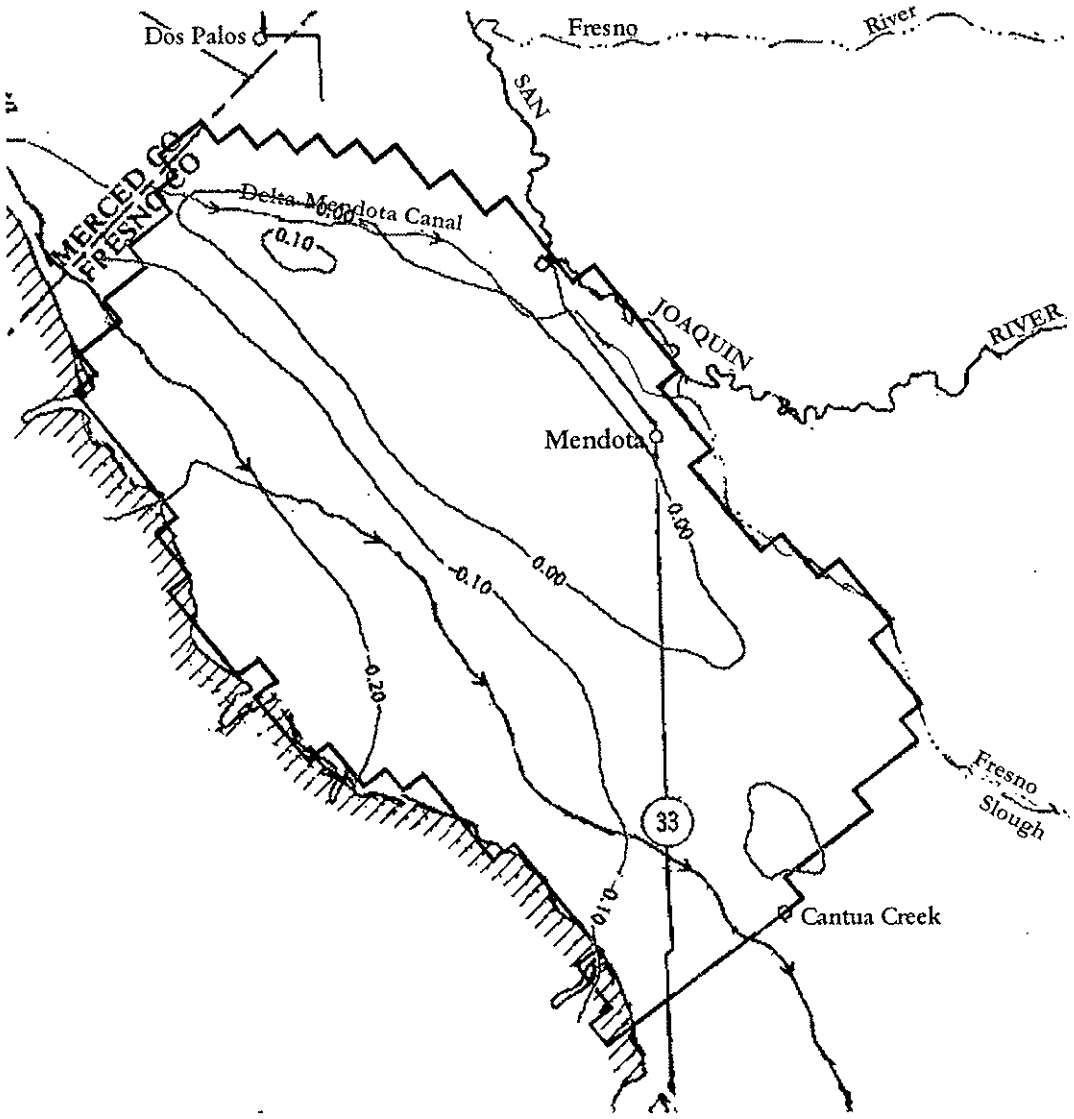

Figure 45 - Simulated Subsidence, 1999-2028 (Alternative C)

results produce subsidence similar to that of Alternatives A and C. The only major difference is a period of little change during the final seven years while Alternatives A and C show significant rebound.

The maximum ground water withdrawal for each water budget subarea found in the optimization model is shown in Fig. 46. Ground water withdrawal can be significantly increased without causing any inelastic compaction in subareas 1 (Firebaugh) and 6 (Tranquillity). These subareas are located along the river in the eastern side of the basin. In contrast, withdrawals cannot be increased above the minimum required rate over the next two decades without leading to inelastic subsidence in subareas 10 and 11 along the no-flow boundary to the west. Ground water supplies are intensely operated in almost all of the subareas during the last years of the future scenario. This is the result of one of the major assumptions of the optimization model. Since the optimization model has perfect foresight, following the final drought period it must no longer plan for future drought and can increase pumping until ground water levels reach the point of maximum drawdown. In general, from the standpoint of land subsidence, there is greater potential for increased withdrawal of ground water supplies on the eastern side of the basin than on the western side.

5. CONCLUSIONS AND RECOMMENDATIONS

For the foreseeable future, land subsidence will remain a concern for water managers in the San Joaquin Valley. To avoid the costly and serious damage associated with land subsidence, it is vital to consider the effects of all proposed water use alternatives. The ground water-subsidence model presented herein provides a method for evaluating each alternative.

The success of a model is mainly measured by its ability to reproduce observed data. Although it cannot represent the complex ground water system in its entirety, the Los Banos-

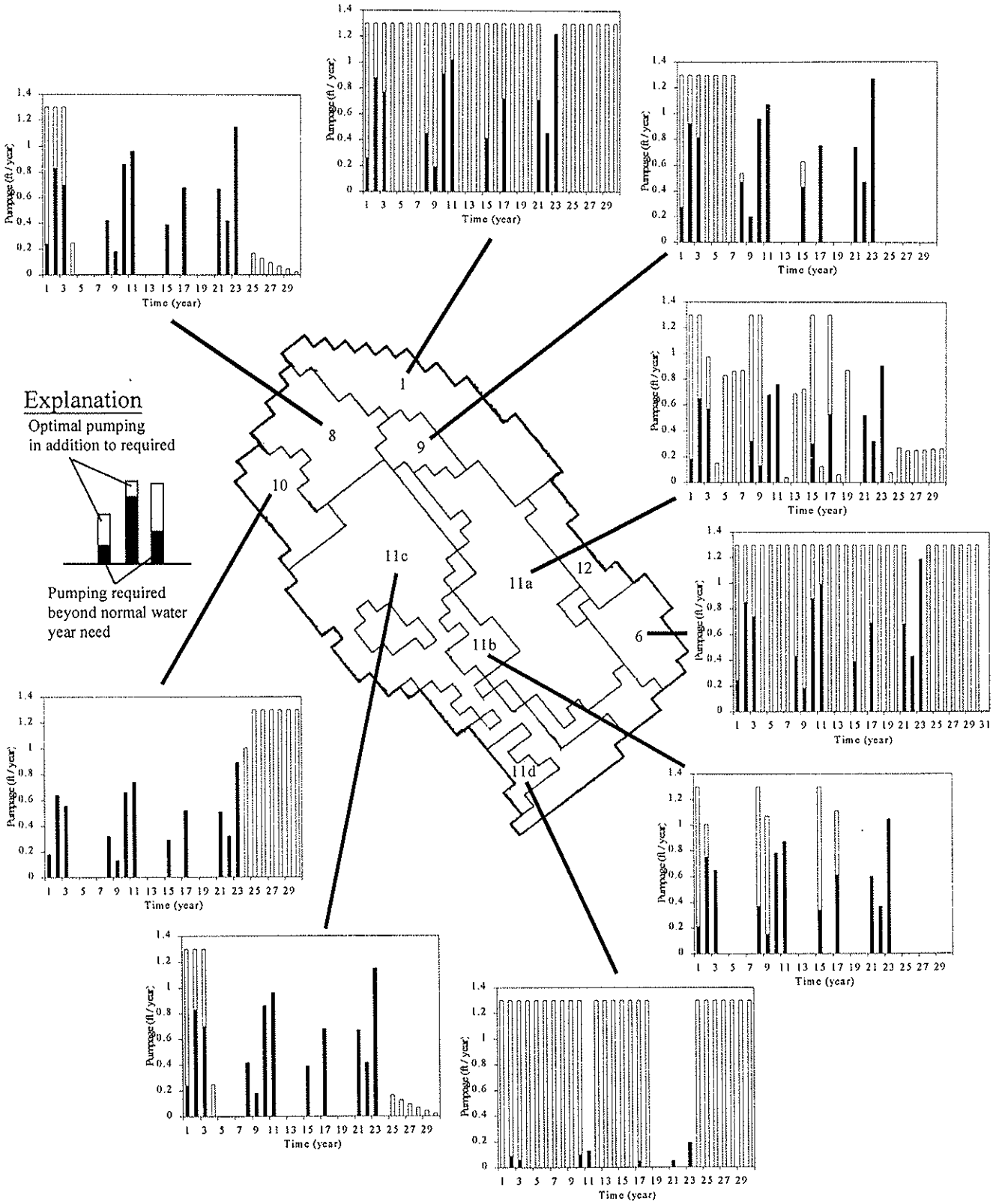

Figure 46 - Maximum Ground Water Withdrawal from Optimization Model

Kettleman City model is a simplified conceptual model that successfully matches observed head and subsidence values. Because of the limited amount of data available and the corresponding large number of calibration variables, however, it is possible that other model parameters could produce equally appropriate matches to the observed data. Although the model is probably not unique, the current calibrated model appears to be sufficient for the evaluation of future water management alternatives.

If present practices can be sustained for the Los Banos-Kettleman City area, land subsidence will not be a serious problem in the next thirty years. Although head levels are significantly reduced and some elastic compaction does occur during periods of drought, there is enough storage in the underlying aquifers to prevent most non-recoverable subsidence. However, with the continued growth of urban populations to the south and concerns over the ecological implications of water exportation from the north, there seems to be little hope of sustaining current practices.

The alternative water budget proposed by Belitz and Phillips (1995) achieves a reduction in surface water dependency by increasing irrigation efficiency and ground water pumping. This proposal is also meritorious for its positive effect on drainage problems in the region. Unfortunately, this alternative produces significant inelastic subsidence during the future scenario considered in this report.

There are two possible reasons the Belitz and Phillips report (1995) did not recognize the proposed water budget's potential for subsidence. First, in their analysis, subsidence was assumed to occur only when the piezometric head in the confined aquifer falls below its past minimum. This neglects the presence of residual pore pressure, which will cause inelastic compaction to begin at heads much greater than the past aquifer minimum. Second, in the water

budget used by Belitz and Phillips (1995), the surface water delivery rate was assumed to be constant for the next 45 years. Much of the predicted subsidence would be eliminated using the same assumption for our model. The proposed water budget lowers head values just enough, however, that when drought years are included, there is not enough storage to prevent subsidence from occurring.

The final alternative examined was a shift in the relationship between available surface water (SFRI) and the amount of CVP water used in the region. Like Alternative A, this alternative limits subsidence to an acceptable rate. Although it does not reduce the surface water required during wet years, it reduces the area's dependence on surface water during years of drought. This or any other alternative that involves an increase in pumping is potentially limited by water quality problems (e.g., TDS, salinity). Although the modest increases in pumpage included here are probably acceptable (Belitz and Phillips, 1995), additional work would be required to determine the long-term impact of such changes on water quality.

A linear optimization model was constructed to predict the maximum potential ground water pumpage from each subarea above the predicted water demands for the next 30 years. Although perfect foresight limits the implementation of the optimization model in practice, the model indicates that ground water supplies of certain subareas in the eastern portion of the study area can be operated far above the target demand rates without leading to inelastic compaction. In contrast, little increase in ground water withdrawal is possible for subareas on the western side.

There are at least three areas in which further work could improve the quality of the model. First, the thickness of the layer representing the interbeds was assumed to be uniform across the study area. Additional field data regarding the composition of the confined aquifer

may allow for a better estimation of the spatial distribution of interbed thickness. Second, the model only considers yearly stress periods. Some detail is lost as pumping is averaged over the entire year. A seasonal or monthly model may capture more accurately the ground water fluctuations leading to subsidence. Finally, the time delay of compaction was adequately captured using the IBS1 package (Leake, 1991) by sub-dividing the compressible layers. However, equally valid and numerically more efficient results may also be attainable using a package which analytically considers time delay, such as the IDP package (Shearer and Kitching, 1994).

REFERENCES

American Farmland Trust. 1995. *Alternatives for Future Urban Growth in California's Central Valley: The Bottom Line for Agriculture and Taxpayers*. Washington, D. C., U.S.A.

Belitz, K., and Heimes, F.J. 1990. *Character and evolution of the ground water flow system in the central part of the western San Joaquin Valley, California*. U.S. Geological Survey Water-Supply Paper 2348: 28p.

Belitz, Kenneth, Phillips, S. P., and Gronberg, J. M. 1992. *Numerical Simulation of Ground-Water Flow in the Central Part of the Western San Joaquin Valley, California*. U. S. Geological Survey Open-File Report 91-535: 71 p.

Belitz, Kenneth and Phillips, Steven P. 1995. *Alternatives to Agricultural Drains in California's San Joaquin Valley: Results of a Regional-Scale Hydrogeologic Approach*. U. S. Geological Survey Open-File Report 91-535: 71 p.

Brooke, A., Kendrick, D., and Meeraus, A. 1992. Release 2.25 GAMS (General Algebraic Modeling System) A User's Guide. Boyd & Fraser Publishing Company, Danvers, Massachusetts, p. 289.

Bull, W. B., and Miller, R. E. 1975. *Land subsidence due to ground water withdrawal in the Los-Banos Kettleman City area, California. Part 1, Changes in the hydrologic environment conducive to subsidence*. U.S. Geological Survey Professional Paper 437-E: 71p.

Bumb, A. C., Mitchell, J. I., and Gifford, S. K. 1997. Design of a ground-water extraction/re-injection system at a superfund site using MODFLOW. *Ground Water* 35(3):400–408.

California Department of Water Resources. 1998. *Compaction Recorded by Extensometer-Wells Since 1984 in the West San Joaquin Valley, California.* Sacramento, California.

California Department of Water Resources. 1999. *California Water Plan Update*, Bulletin 160-98, v. 1

Casagrande, A. 1932. The Structure of Clay and its Importance in Foundation Engineering, *Journal of the Boston Society of Civil Engineers*, April; reprinted in *Contributions to Soil Mechanics 1925-1940*, BSCE:72-113

Gorelick, S. M. 1983. A review of distributed parameter ground-water management modeling methods. Water Resources Research. v. 19, no. 2, pp. 305-319.

Gronberg, J. M. and Belitz, Kenneth. 1992. *Estimation of a Water Budget for for the Central Part of the Western San Joaquin Valley, California*. U. S. Geological Survey Water-Resources Investigation Report 91-4192: 22 p.

Holtz, Robert D. and Kovacs, William D. 1981. *An Introduction to Geotechnical Engineering.* Prentice Hall, Englewood Cliffs, New Jersey: 733 p.

Holzer, T. L. 1989. State and Local Response to Damaging Land Subsidence in United States Urban Areas. *Engineering Geology* 27:449-466.

Hua, Z., Tiezhu, L., and Xinhong, L. 1993. Economic benefit risk assessment of land subsidence in Shanhai. *Environmental Geology* 21:208-211.

Hubbell, J. M., Bishop, C. W., Johnson, G. S., and Lucas, J. G. 1997. Numerical ground-water flow modeling of Snake river plain aquifer using superpostion technique. *Ground Water* 35(1):59-66.

Ireland, R. L., Poland, J. F. and Riley, F. S. 1984. *Land Subsidence in the San Joaquin Valley, California, as of 1980.* U. S. Geological Survey Professional Paper 437-I: 93p.

Ireland, R. L. 1986. *Land subsidence in the San Joaquin Valley, California, as of 1983.* Prepared in cooperation with the California Department of Water Resources, Sacramento, California. U.S. Geological Survey, Denver, CO: 50 p.

Johnson, A. I., Moston, R. P., and Dorris, D. A. 1968. *Physical and hydrologic properties of water-bearing materials in subsiding areas in the central California.* U.S. Geological Survey Professional Paper 497-A: 71p.

Laudon, J., and Belitz, K. 1991. Texture and depositional history of Late Pleistocene-Holocene alluvium in the central part of the western San Joaquin Valley, California. *Bulletin of the Association of Engineering Geologist* 28(1):73-88.

Leake, S. A. 1990. Interbed storage changes and compaction in models of regional ground water flow. *Water Resources Research* 26:1939-1950.

Leake, S. A., and Prudic, D. E. 1991. *Documentation of a computer program to simulate aquifer-system compaction using the modular finite-difference ground water flow model.* U.S. Geological Survey Techniques of Water Resources Investigation, Book 6, Chapter A2: 68 p.

Leake, S. A. 1991. Simulation of vertical compaction in models of regional ground-water flow. pp. 565-574. In: *Proceedings of the fourth international symposium on land subsidence, May 1991.* IAHS Publication no. 200.

Lofgren, B. E. 1979. Changes in Aquifer-system Properties with Ground Water Depletion. pp. 26-46. In: *Procedings, International Conference on Evaluation and Prediction of Land Subsidence, Pensacola, December 1978.* American Society of Civil Engineers.

McDonald, M. G., and Harbaugh, A. W. 1988. *A modular three-dimensional finite-difference ground-water flow model.* U. S. Geological Survey Techniques of Water Resources Investigations, Book 6, Chapter A1: 586 p.

Miller, R. E., Green, J. E., and Davis, G. H. 1971. *Geology of the compacting deposits in the Los Banos-Kettleman City Area, California.* U.S. Geological Survey Professional Paper 497-E: 46p.

Onta, P. R., and Gupta, A. D. 1995. Regional management modeling of a complex ground water system for land subsidence control. *Water Resources Management* 9:1-25.

Page, R. W. 1986. *Geology of the fresh ground water basin of the Central Valley, California, with texture maps and sections.* U.S. Geological Survey Professional Paper 1401-C: 54p.

Phillips, Steven P. and Belitz, Kenneth. 1991. Calibration of a Texture-Based Model of a Ground-Water Flow System, Western San Joaquin Valley, California. *Ground Water* 29(5):702-715

Poland, J.F., Lofgren, B.E., Ireland, R.L., and Pugh, R.G. 1975. *Land Subsidence in the San Joaquin Valley, California, as of 1972.* U.S.G.S. Professional Paper #437-H. U.S. Government Printing Office, Washington D.C., U.S.A.

Poland, J. F. 1981. *The Occurrence and Control of Land Subsidence Due to Ground-Water Withdrawal with Special Reference to the San Joaquin and Santa Clara Valleys, California.* Ph.D.–Dissertation, Stanford University, Palo Alto, California

Reynolds, J. W., and Spruill, R. K. 1995. Ground-water simulation for management of a regulated aquifer system: A Case study in the North Carolina Coastal Plain. *Ground Water* 33(5):741-758.

Shearer, T. R., and Kitching, R. 1994. *A numerical model of land subsidence caused by ground water abstraction at Hangu in the peoples of republic of China.* British Geological Survey, Technical report WC/94/46

Shearer, T. R. 1998. A numerical model to calculate land subsidence, applied at Hangu in China. *Engineering Geology* 49:85-93.

Shen, H. W. and Tabios, G. Q. 1996. *Modeling of Precipitation-Based Drought Characteristics Over California.* Technical Completion Report. Water Resources Center, Contribution No. 204. Water Resources Center. University of California, Davis

Sophocleuos, M., and Perkins, S. P. 1993. Calibrated models as management tolls for stream-aquifer systems: the case of central Kansas, USA. *Journal of Hydrology* 152:31–56.

Terzaghi, K. 1925. Principles of soil mechanics: IV Settlement and consolidation of clay. In: Eng. News-Rec, McGraw-Hill, New York:874-878.

Williamson, A. K., Prudic, D. E., and Swain, L. A. 1989. *Ground water flow in the Central Valley, California.* U.S. Geological Survey Professional Paper 1401-D: 127 p.

Wilson, A. M., and Gorelick, S. 1996. The effects of pulsed pumping on land subsidence in the Santa Clara Valley, California. *Journal of Hydrology* 174:375-396.

Yeh, W-G. W. 1992. System analysis in ground-water planning and management. Journal of Water Resources Planning and Management, ASCE. v. 118, no: 3, pp. 224-237.

APPENDIX

	1	2	3	4	5	6	7	8	9	10	11	12	13	14	15	16	17	18	19	20
1	--	--	--	--	--	--	--	--	--	--	--	--	--	--	--	--	--	--	--	--
2	--	--	--	--	--	--	--	--	--	--	101	102	--	--	--	--	--	--	--	--
3	--	--	--	--	--	--	--	--	--	104	101	101	102	--	--	--	--	--	--	--
4	--	--	--	--	--	--	--	118	112	107	103	101	101	102	--	--	--	--	--	--
5	--	--	--	--	--	151	138	119	111	106	105	101	102	102	103	--	--	--	--	--
6	--	--	--	-18	152	150	128	115	108	105	104	102	102	102	103	104	--	--	--	--
7	--	--	-21	-19	160	149	119	107	103	100	102	102	101	102	103	104	105	--	--	--
8	--	--	-22	-21	145	142	114	101	96	94	97	99	101	101	103	104	105	--	--	--
9	--	--	-24	-23	135	128	110	98	93	90	92	97	99	101	102	104	105	106	--	--
10	--	--	-28	-27	121	109	102	97	94	91	93	97	99	100	102	103	105	106	--	--
11	--	--	-31	93	103	94	93	92	90	91	93	97	98	99	101	103	105	105	106	--
12	--	--	-36	89	92	84	82	82	80	84	89	95	97	98	100	102	104	105	106	--
13	--	-44	-42	72	79	70	71	72	71	76	83	90	93	96	98	101	103	105	106	--
14	--	-46	77	65	66	57	59	61	64	70	78	86	90	93	96	99	102	104	105	--
15	-51	-48	68	53	55	51	51	55	60	66	74	82	87	91	94	98	101	103	104	99
16	-53	101	72	61	49	44	48	51	57	63	71	78	84	88	92	95	99	102	103	101
17	-54	136	76	58	45	42	47	50	55	62	68	75	81	85	89	93	98	101	102	101
18	-55	95	58	40	36	40	45	49	54	60	65	73	78	83	87	91	96	100	102	98
19	--	66	18	6	26	36	43	48	54	58	64	70	76	80	85	89	95	98	101	97
20	-58	48	-11	-9	17	30	40	47	53	57	63	69	73	79	84	88	93	97	99	--
21	-57	28	-32	0	9	22	35	45	53	58	63	68	73	79	84	88	92	97	100	--
22	60	39	26	3	3	11	28	42	51	57	62	67	73	79	84	88	91	95	99	--
23	--	80	32	8	3	9	25	39	49	54	59	65	71	77	81	85	90	94	--	--
24	--	79	32	12	9	14	28	38	46	52	56	61	68	73	78	83	88	93	--	--
25	--	--	34	17	16	25	34	39	45	50	55	60	66	71	77	82	88	92	--	--
26	--	--	--	12	19	30	39	42	45	50	54	60	65	70	76	82	88	92	--	--
27	--	--	--	11	17	31	41	44	44	49	54	60	66	71	77	82	87	91	94	--
28	--	--	--	24	17	29	41	45	46	49	54	60	66	71	76	81	85	89	93	--
29	--	--	--	18	2	23	41	48	50	51	55	60	65	70	75	80	83	87	91	95
30	--	--	--	--	8	16	39	48	53	53	56	59	63	68	73	78	82	86	90	94
31	--	--	--	--	6	12	35	46	53	54	57	59	63	67	73	78	82	85	90	95
32	--	--	--	--	1	14	32	46	53	56	57	60	64	68	73	78	82	85	90	--
33	--	--	--	--	-13	18	38	47	54	58	59	62	66	69	74	78	81	82	84	--
34	--	--	--	--	-24	15	36	47	54	58	61	63	67	70	74	78	81	80	79	--
35	--	--	--	-5	-5	14	31	45	54	59	62	64	68	72	75	78	80	81	--	--
36	--	--	--	-25	5	12	29	43	55	61	64	65	69	73	78	--	--	--	--	--
37	--	--	-49	-24	9	5	24	41	57	63	67	--	--	--	--	--	--	--	--	--

Preconsolidation Heads - Layer 6

	1	2	3	4	5	6	7	8	9	10	11	12	13	14	15	16	17	18	19	20
1	--	--	--	--	--	--	--	--	--	--	--	--	--	--	--	--	--	--	--	--
2	--	--	--	--	--	--	--	--	--	--	57	62	--	--	--	--	--	--	--	--
3	--	--	--	--	--	--	--	--	--	44	50	58	64	--	--	--	--	--	--	--
4	--	--	--	--	--	--	--	33	32	37	45	52	62	65	--	--	--	--	--	--
5	--	--	--	--	--	37	29	23	26	29	41	47	61	63	67	--	--	--	--	--
6	--	--	--	-46	27	30	19	15	18	27	36	46	58	61	67	71	--	--	--	--
7	--	--	-52	-49	28	22	5	4	11	18	33	45	53	58	65	70	75	--	--	--
8	--	--	-57	-52	17	10	-10	-7	2	11	28	42	50	56	63	69	74	--	--	--
9	--	--	-62	-60	3	-12	-21	-21	-6	7	23	40	47	54	61	67	72	76	--	--
10	--	--	-70	-69	-18	-24	-25	-24	-11	4	21	36	44	50	58	64	71	75	--	--
11	--	--	-81	-32	-32	-36	-32	-27	-18	--	15	32	41	48	56	63	70	73	77	--
12	--	--	-96	-45	-42	-43	-40	-33	-27	-9	9	28	37	45	53	61	68	72	77	--
13	--	-118	-114	-64	-56	-51	-46	-38	-34	-17	0	22	32	43	49	58	67	71	76	--
14	--	-124	-71	-76	-72	-67	-54	-47	-38	-24	-7	15	28	39	46	55	64	69	75	--
15	-131	-128	-80	-90	-91	-80	-64	-53	-41	-28	-12	8	24	35	43	52	61	67	74	75
16	-136	-72	-88	-99	-110	-99	-72	-55	-44	-32	-16	2	18	30	39	47	58	64	70	75
17	-140	-64	-91	-100	-113	-99	-71	-57	-46	-33	-20	-3	12	24	34	43	53	62	66	73
18	-145	-86	-100	-106	-106	-89	-68	-55	-46	-34	-24	-8	5	19	31	39	50	59	64	67
19	--	-98	-117	-116	-98	-78	-61	-53	-44	-35	-24	-11	1	13	26	37	48	55	61	62
20	-152	-106	-129	-121	-99	-79	-61	-51	-44	-35	-25	-12	0	12	26	36	46	54	60	--
21	-152	-114	-137	-120	-107	-85	-63	-50	-40	-31	-21	-9	4	16	28	37	45	52	58	--
22	-102	-108	-113	-121	-111	-97	-68	-51	-39	-28	-18	-6	7	17	28	36	43	49	56	--
23	--	-90	-109	-115	-108	-96	-69	-53	-41	-31	-20	-8	5	15	22	30	39	47	--	--
24	--	-89	-105	-105	-101	-90	-64	-53	-42	-31	-23	-14	-2	8	17	24	35	45	--	--
25	--	--	-100	-98	-91	-75	-59	-50	-40	-32	-24	-15	-3	3	13	23	36	45	--	--
26	--	--	--	-97	-84	-70	-56	-48	-39	-30	-22	-12	-3	5	16	28	39	46	--	--
27	--	--	--	-97	-84	-70	-56	-48	-40	-30	-19	-8	2	11	20	32	40	46	52	--
28	--	--	--	-92	-85	-72	-58	-48	-40	-28	-17	-6	5	12	22	32	40	46	52	--
29	--	--	--	-95	-92	-73	-61	-49	-39	-27	-15	-6	4	12	21	31	38	44	51	58
30	--	--	--	--	-93	-82	-64	-53	-38	-27	-16	-8	2	10	18	28	37	44	52	59
31	--	--	--	--	-102	-89	-70	-58	-43	-31	-19	-10	-1	9	18	28	36	45	52	61
32	--	--	--	--	-123	-94	-79	-63	-47	-32	-23	-12	-1	9	21	32	39	46	55	--
33	--	--	--	--	-140	-98	-76	-65	-49	-36	-23	-10	2	11	23	34	40	45	52	--
34	--	--	--	--	-151	-101	-74	-67	-51	-38	-22	-9	3	13	24	34	41	45	51	--
35	--	--	--	-169	-141	-103	-80	-66	-50	-36	-22	-9	4	14	25	35	43	45	--	--
36	--	--	--	-180	-135	-102	-81	-64	-46	-33	-21	-8	5	16	27	--	--	--	--	--
37	--	--	-210	-178	-127	-103	-81	-58	-37	-28	-20	--	--	--	--	--	--	--	--	--

Preconsolidation Heads - Layer 7

	1	2	3	4	5	6	7	8	9	10	11	12	13	14	15	16	17	18	19	20
1	--	--	--	--	--	--	--	--	--	--	--	--	--	--	--	--	--	--	--	--
2	--	--	--	--	--	--	--	--	--	--	28	38	--	--	--	--	--	--	--	--
3	--	--	--	--	--	--	--	--	--	4	15	31	42	--	--	--	--	--	--	--
4	--	--	--	--	--	--	--	-21	-21	-10	6	20	38	44	--	--	--	--	--	--
5	--	--	--	--	--	--	-25	-35	-39	-30	-25	-3	11	36	40	47	--	--	--	--
6	--	--	--	-60	-40	-37	-47	-50	-43	-27	-12	7	30	36	46	54	--	--	--	--
7	--	--	-69	-65	-42	-51	-66	-65	-53	-39	-16	6	21	31	43	51	58	--	--	--
8	--	--	-76	-69	-53	-69	-90	-80	-63	-48	-21	3	17	28	40	49	57	--	--	--
9	--	--	-83	-80	-71	-98	-106	-104	-75	-52	-27	1	12	24	36	45	54	61	--	--
10	--	--	-93	-94	-100	-105	-110	-106	-84	-58	-31	-5	8	19	31	42	51	59	--	--
11	--	--	-110	-102	-112	-117	-115	-109	-93	-64	-40	-11	4	15	28	39	50	56	62	--
12	--	--	-133	-122	-122	-124	-120	-113	-104	-76	-47	-17	-2	12	23	36	48	54	61	--
13	--	-161	-160	-145	-139	-129	-124	-115	-109	-85	-59	-25	-8	8	18	32	45	52	60	--
14	--	-171	-157	-161	-160	-149	-131	-124	-112	-92	-69	-34	-14	4	14	28	42	50	59	--
15	-175	-177	-167	-179	-188	-168	-145	-129	-115	-97	-74	-44	-18	-1	10	22	36	46	57	61
16	-180	-168	-184	-200	-219	-200	-157	-131	-117	-101	-79	-52	-27	-10	4	16	32	42	51	60
17	-189	-178	-193	-201	-221	-201	-156	-133	-119	-101	-83	-59	-36	-18	-3	10	25	37	44	57
18	-198	-191	-196	-199	-202	-180	-148	-129	-117	-102	-88	-64	-46	-26	-9	4	20	34	39	48
19	--	-194	-201	-195	-181	-156	-134	-124	-112	-100	-87	-68	-52	-35	-15	1	17	26	35	39
20	-207	-196	-204	-194	-177	-153	-131	-119	-111	-99	-87	-69	-53	-35	-15	0	14	25	35	--
21	-207	-198	-206	-198	-184	-157	-130	-115	-102	-92	-78	-63	-45	-28	-12	2	14	22	31	--
22	-195	-197	-199	-202	-187	-170	-132	-114	-99	-85	-72	-57	-38	-25	-11	1	10	19	29	--
23	--	-192	-199	-195	-180	-166	-129	-114	-101	-87	-73	-58	-41	-28	-19	-8	4	15	--	--
24	--	-191	-192	-179	-171	-157	-121	-111	-99	-86	-77	-67	-50	-37	-27	-18	-2	13	--	--
25	--	--	-183	-170	-159	-137	-116	-107	-94	-86	-77	-69	-52	-44	-31	-18	1	13	--	--
26	--	--	--	-165	-149	-133	-114	-105	-93	-83	-73	-62	-51	-41	-26	-10	7	15	--	--
27	--	--	--	-165	-148	-133	-116	-105	-94	-81	-69	-56	-43	-31	-19	-2	10	17	24	--
28	--	--	--	-166	-150	-136	-120	-107	-95	-79	-65	-52	-38	-28	-14	-1	10	19	26	--
29	--	--	--	-170	-154	-136	-126	-111	-96	-79	-63	-51	-38	-27	-16	-2	8	17	27	35
30	--	--	--	--	-160	-147	-131	-118	-98	-81	-64	-54	-41	-30	-19	-6	8	18	28	38
31	--	--	--	--	-176	-157	-139	-125	-107	-88	-71	-58	-45	-31	-18	-4	7	20	30	42
32	--	--	--	--	-212	-169	-153	-134	-113	-91	-78	-61	-46	-30	-13	4	14	24	34	--
33	--	--	--	--	-231	-177	-150	-139	-118	-98	-79	-59	-42	-27	-8	8	18	25	36	--
34	--	--	--	--	-242	-178	-146	-142	-120	-102	-78	-57	-39	-24	-7	9	20	26	37	--
35	--	--	--	-279	-233	-179	-152	-138	-118	-98	-77	-57	-38	-22	-6	10	23	26	--	--
36	--	--	--	-283	-225	-173	-152	-133	-112	-93	-75	-54	-35	-20	-5	--	--	--	--	--
37	--	--	-316	-279	-211	-170	-149	-121	-95	-85	-73	--	--	--	--	--	--	--	--	--

Preconsolidation Heads - Layer 8

	1	2	3	4	5	6	7	8	9	10	11	12	13	14	15	16	17	18	19	20
1	--	--	--	--	--	--	--	--	--	--	--	--	--	--	--	--	--	--	--	--
2	--	--	--	--	--	--	--	--	--	--	19	31	--	--	--	--	--	--	--	--
3	--	--	--	--	--	--	--	--	--	-9	4	22	35	--	--	--	--	--	--	--
4	--	--	--	--	--	--	--	-38	-37	-25	-7	10	30	37	--	--	--	--	--	--
5	--	--	--	--	--	-45	-55	-58	-48	-41	-17	-1	28	32	40	--	--	--	--	--
6	--	--	--	-65	-62	-59	-68	-70	-62	-43	-26	-5	21	28	39	48	--	--	--	--
7	--	--	-74	-70	-65	-74	-88	-87	-73	-57	-31	-7	11	23	36	45	53	--	--	--
8	--	--	-82	-74	-76	-94	-115	-103	-84	-66	-36	-9	7	19	32	42	51	--	--	--
9	--	--	-90	-87	-95	-125	-134	-129	-97	-70	-42	-11	1	15	28	38	48	56	--	--
10	--	--	-100	-102	-127	-131	-137	-132	-106	-77	-47	-18	-3	9	23	34	45	53	--	--
11	--	--	-120	-124	-138	-143	-141	-134	-116	-84	-57	-25	-8	5	19	31	43	50	57	--
12	--	--	-144	-147	-148	-149	-145	-137	-127	-97	-65	-32	-14	1	14	28	41	48	56	--
13	--	-175	-175	-172	-165	-153	-149	-138	-132	-105	-78	-39	-21	-3	8	24	38	46	55	--
14	--	-186	-185	-188	-188	-175	-155	-147	-135	-113	-88	-49	-27	-7	4	19	35	43	54	--
15	-190	-193	-195	-207	-218	-196	-170	-153	-137	-118	-94	-60	-32	-12	-1	13	29	39	51	57
16	-195	-200	-215	-232	-253	-231	-184	-154	-139	-122	-99	-69	-41	-22	-7	6	24	34	45	55
17	-205	-215	-225	-233	-254	-232	183	-156	-141	-122	-103	-76	-51	-31	-15	-1	16	30	37	51
18	-215	-225	-227	-229	-232	-209	-173	-152	-139	-122	-108	-82	-62	-39	-21	-7	11	26	32	41
19	--	-226	-228	-220	-207	-180	-156	-146	-134	-121	-107	-86	-68	-50	-28	-11	7	17	27	32
20	-225	-226	-228	-217	-201	-176	-153	-140	-132	-119	-106	-87	-69	-49	-28	-11	4	16	27	--
21	-225	-226	-228	-223	-209	-180	-151	-135	-122	-111	-96	-79	-60	-42	-24	-9	4	13	23	--
22	-225	-226	-227	-228	-211	-193	-152	-133	-118	-102	-89	-72	-53	-38	-23	-10	--	9	20	--
23	--	-224	-227	-220	-203	-188	-148	-133	-119	-105	-89	-73	-56	-42	-32	-20	-7	5	--	--
24	--	-224	-220	-203	-193	-178	-139	-130	-117	-103	-93	-83	-65	-51	-40	-31	-13	3	--	--
25	--	--	-210	-193	-180	-157	-134	-125	-112	-103	-93	-85	-67	-59	-45	-31	-10	3	--	--
26	--	--	--	-187	-170	-153	-133	-123	-110	-100	-89	-77	-66	-55	-40	-22	-3	6	--	--
27	--	--	--	-187	-168	-153	-135	-124	-112	-98	-84	-70	-57	-44	-31	-13	0	8	16	--
28	--	--	--	-190	-170	-156	-140	-126	-113	-96	-81	-66	-51	-41	-26	-11	1	10	18	--
29	--	--	--	-194	-173	-155	-146	-131	-115	-96	-78	-65	-51	-40	-27	-12	-1	9	19	28
30	--	--	--	--	-181	-167	-152	-138	-117	-97	-80	-68	-55	-43	-31	-16	-1	10	21	31
31	--	--	--	--	-200	-179	-161	-146	-127	-105	-87	-72	-59	-44	-29	-14	-2	13	22	35
32	--	--	--	--	-239	-192	-176	-156	-134	-109	-95	-76	-60	-43	-23	-6	5	16	27	--
33	--	--	--	--	-259	-202	-174	-162	-139	-118	-96	-74	-56	-39	-18	-1	10	18	30	--
34	--	--	--	--	-271	-203	-168	-165	-142	-122	-95	-73	-53	-36	-16	1	13	19	32	--
35	--	--	--	-314	-262	-203	-175	-161	-140	-117	-94	-72	-51	-34	-15	2	16	20	--	--
36	--	--	--	-316	-254	-195	-174	-155	-132	-112	-92	-69	-48	-31	-15	--	--	--	--	--
37	--	--	-349	-311	-238	-192	-170	-141	-114	-103	-90	--	--	--	--	--	--	--	--	--

Preconsolidation Heads - Layer 10

	1	2	3	4	5	6	7	8	9	10	11	12	13	14	15	16	17	18	19	20
1	--	--	--	--	--	--	--	--	--	--	--	--	--	--	--	--	--	--	--	--
2	--	--	--	--	--	--	--	--	--	--	21	32	--	--	--	--	--	--	--	--
3	--	--	--	--	--	--	--	--	--	-5	8	24	36	--	--	--	--	--	--	--
4	--	--	--	--	--	--	--	-34	-32	-20	-3	13	32	38	--	--	--	--	--	--
5	--	--	--	--	--	-44	-52	-53	-43	-35	-12	3	29	34	41	--	--	--	--	--
6	--	--	--	-65	-62	-57	-64	-64	-56	-38	-21	-1	23	29	40	48	--	--	--	--
7	--	--	-74	-70	-65	-72	-83	-80	-66	-51	-26	-3	14	25	37	45	53	--	--	--
8	--	--	-82	-74	-75	-90	-108	-95	-76	-59	-31	-5	10	21	34	43	51	--	--	--
9	--	--	-90	-87	-93	-120	-126	-120	-89	-63	-36	-7	4	17	29	39	48	56	--	--
10	--	--	-100	-101	-123	-126	-129	-124	-98	-70	-41	-14	0	11	24	35	46	53	--	--
11	--	--	-119	-122	-134	-138	-133	-126	-108	-76	-51	-20	-5	7	21	33	44	50	57	--
12	--	--	-142	-144	-144	-143	-137	-129	-118	-88	-58	-27	-10	4	16	30	42	48	56	--
13	--	-173	-172	-167	-160	-147	-141	-130	-123	-97	-70	-35	-17	0	10	25	39	47	55	--
14	--	-183	-181	-183	-181	-167	-147	-138	-126	-105	-80	-44	-23	-4	7	21	36	44	54	--
15	-189	-190	-191	-201	-209	-187	-161	-144	-128	-110	-86	-54	-28	-9	2	15	30	40	51	57
16	-195	-198	-210	-224	-242	-220	-173	-145	-130	-114	-91	-63	-36	-18	-4	9	25	36	46	55
17	-203	-211	-219	-225	-243	-220	-172	-147	-132	-114	-95	-69	-46	-26	-11	2	18	31	38	52
18	-213	-221	-221	-221	-222	-198	-163	-144	-131	-114	-100	-75	-56	-34	-17	-3	14	28	34	43
19	--	-221	-222	-213	-199	-172	-148	-138	-126	-113	-99	-79	-62	-45	-23	-7	10	19	29	34
20	-223	-221	-222	-211	-194	-168	-145	-132	-124	-112	-99	-80	-63	-44	-23	-7	7	18	29	--
21	-223	-221	-222	-216	-201	-173	-144	-128	-116	-105	-90	-73	-55	-37	-19	-5	7	16	25	--
22	-222	-221	-221	-221	-204	-185	-146	-127	-112	-97	-84	-67	-48	-33	-19	-6	3	12	22	--
23	--	-219	-220	-213	-197	-181	-143	-128	-114	-100	-84	-68	-51	-37	-27	-16	-3	8	--	--
24	--	-218	-214	-197	-187	-173	-135	-125	-112	-98	-88	-77	-60	-46	-35	-26	-9	6	--	--
25	--	--	-204	-188	-175	-152	-131	-121	-107	-98	-88	-79	-62	-54	-40	-26	-6	6	--	--
26	--	--	--	-182	-165	-148	-129	-119	-105	-95	-84	-72	-61	-50	-35	-18	0	9	--	--
27	--	--	--	-182	-164	-148	-131	-119	-107	-93	-79	-65	-52	-39	-27	-10	3	10	18	--
28	--	--	--	-184	-165	-152	-135	-121	-108	-91	-76	-62	-46	-37	-22	-8	3	12	20	--
29	--	--	--	-187	-168	-150	-141	-126	-110	-91	-73	-60	-46	-36	-23	-9	1	11	21	29
30	--	--	--	--	-175	-161	-146	-133	-112	-92	-75	-64	-50	-39	-27	-13	1	12	22	33
31	--	--	--	--	-192	-172	-155	-140	-121	-100	-82	-67	-54	-40	-26	-11	--	14	24	36
32	--	--	--	--	-229	-184	-169	-150	-128	-104	-89	-71	-55	-39	-21	-4	7	17	28	--
33	--	--	--	--	-248	-194	-167	-156	-133	-112	-90	-69	-51	-36	-16	0	11	19	30	--
34	--	--	--	--	-260	-195	-162	-158	-136	-116	-90	-68	-49	-33	-15	2	13	19	32	--
35	--	--	--	-303	-253	-197	-169	-155	-134	-112	-90	-68	-47	-31	-14	3	16	20	--	--
36	--	--	--	-306	-246	-190	-168	-149	-127	-107	-88	-65	-45	-29	-13	--	--	--	--	--
37	--	--	-339	-302	-233	-187	-165	-137	-110	-99	-87	--	--	--	--	--	--	--	--	--

Preconsolidation Heads - Layer 11

	1	2	3	4	5	6	7	8	9	10	11	12	13	14	15	16	17	18	19	20
1	--	--	--	--	--	--	--	--	--	--	--	--	--	--	--	--	--	--	--	--
2	--	--	--	--	--	--	--	--	--	--	28	36	--	--	--	--	--	--	--	--
3	--	--	--	--	--	--	--	--	--	7	17	30	39	--	--	--	--	--	--	--
4	--	--	--	--	--	--	--	-22	-18	-6	10	22	36	41	--	--	--	--	--	--
5	--	--	--	--	--	-43	-44	-38	-27	-19	2	14	34	37	43	--	--	--	--	--
6	--	--	--	-65	-62	-52	-53	-48	-37	-21	-6	11	29	34	42	49	--	--	--	--
7	--	--	-74	-70	-64	-64	-69	-61	-46	-32	-10	9	22	30	40	46	53	--	--	--
8	--	--	-81	-74	-72	-80	-89	-74	-55	-40	-14	7	19	27	37	44	52	--	--	--
9	--	--	-88	-86	-88	-104	-103	-95	-66	-44	-19	4	13	23	33	41	49	55	--	--
10	--	--	-100	-99	-112	-110	-106	-98	-75	-49	-24	-2	9	18	30	38	47	53	--	--
11	--	--	-115	-117	-122	-121	-111	-101	-83	-55	-32	-8	5	15	26	36	45	51	57	--
12	--	--	-136	-135	-132	-126	-116	-104	-92	-65	-39	-14	0	12	22	34	44	49	56	--
13	--	-167	-162	-155	-145	-129	-120	-106	-97	-72	-49	-20	-6	8	18	31	42	48	55	--
14	--	-175	-171	-169	-161	-145	-124	-113	-100	-80	-57	-28	-11	4	15	27	39	46	54	--
15	-187	-182	-180	-184	-184	-161	-135	-117	-102	-84	-62	-37	-16	0	11	22	34	43	52	57
16	-194	-190	-195	-202	-210	-186	-143	-119	-104	-89	-68	-44	-23	-7	6	17	31	40	49	56
17	-200	-201	-203	-203	-210	-184	-141	-121	-106	-90	-72	-51	-31	-13	0	12	25	36	42	54
18	-206	-208	-204	-200	-194	-168	-136	-119	-106	-91	-77	-56	-39	-20	-4	7	21	33	39	47
19	--	-209	-205	-194	-176	-148	-125	-115	-103	-91	-78	-60	-44	-28	-10	4	18	27	35	39
20	-216	-209	-205	-193	-173	-147	-124	-111	-103	-92	-79	-61	-45	-28	-10	4	16	26	35	--
21	-215	-208	-204	-197	-180	-152	-124	-110	-97	-87	-72	-56	-39	-23	-7	5	16	24	31	--
22	-214	-207	-203	-200	-183	-164	-128	-110	-96	-82	-68	-52	-34	-21	-7	4	12	20	29	--
23	--	-203	-201	-193	-178	-162	-129	-112	-98	-84	-69	-52	-37	-24	-14	-3	7	17	--	--
24	--	-200	-195	-180	-171	-156	-124	-111	-97	-83	-72	-60	-44	-31	-21	-12	2	15	--	--
25	--	--	-186	-172	-160	-140	-121	-108	-94	-84	-72	-61	-45	-37	-25	-13	4	15	--	--
26	--	--	--	-166	-151	-136	-119	-107	-93	-81	-69	-55	-45	-35	-21	-6	9	17	--	--
27	--	--	--	-165	-149	-135	-120	-107	-94	-79	-65	-50	-38	-26	-15	0	11	18	25	--
28	--	--	--	-166	-150	-137	-122	-108	-95	-77	-62	-47	-33	-24	-12	1	11	19	26	--
29	--	--	--	-167	-151	-135	-126	-112	-96	-77	-60	-46	-34	-24	-13	-1	9	17	26	33
30	--	--	--	--	-156	-143	-130	-117	-97	-78	-61	-49	-37	-27	-17	-4	8	17	26	36
31	--	--	--	--	-170	-152	-137	-124	-104	-84	-66	-53	-40	-28	-16	-4	7	18	28	39
32	--	--	--	--	-199	-162	-148	-131	-110	-87	-72	-56	-41	-28	-13	1	10	20	31	--
33	--	--	--	--	-216	-170	-148	-137	-115	-94	-74	-55	-38	-26	-10	4	12	20	30	--
34	--	--	--	--	-228	-174	-145	-140	-117	-98	-74	-55	-38	-24	-9	5	14	20	31	--
35	--	--	--	-271	-226	-178	-151	-137	-116	-96	-75	-56	-37	-23	-9	5	16	20	--	--
36	--	--	--	-277	-224	-175	-152	-133	-110	-93	-76	-55	-36	-22	-8	--	--	--	--	--
37	--	--	-312	-276	-217	-174	-149	-122	-98	-88	-78	--	--	--	--	--	--	--	--	--

Preconsolidation Heads - Layer 12

	1	2	3	4	5	6	7	8	9	10	11	12	13	14	15	16	17	18	19	20
1	--	--	--	--	--	--	--	--	--	--	--	--	--	--	--	--	--	--	--	--
2	--	--	--	--	--	--	--	--	--	--	39	43	--	--	--	--	--	--	--	--
3	--	--	--	--	--	--	--	--	--	25	33	40	44	--	--	--	--	--	--	--
4	--	--	--	--	--	--	--	-4	5	16	28	35	42	44	--	--	--	--	--	--
5	--	--	--	--	--	-41	-32	-15	-2	7	24	31	41	43	46	--	--	--	--	--
6	--	--	--	-65	-61	-45	-37	-22	-9	4	18	29	39	41	45	49	--	--	--	--
7	--	--	-75	-69	-63	-53	-46	-32	-15	-4	15	28	35	39	44	48	53	--	--	--
8	--	--	-80	-75	-68	-63	-59	-41	-22	-10	12	24	32	36	42	46	52	--	--	--
9	--	--	-87	-84	-79	-80	-67	-55	-31	-13	8	21	28	32	40	45	51	54	--	--
10	--	--	-100	-95	-95	-86	-71	-59	-38	-18	3	16	24	29	37	43	49	53	--	--
11	--	--	-110	-108	-104	-96	-77	-62	-45	-22	-3	11	19	27	35	42	48	52	56	--
12	--	--	-126	-122	-114	-99	-83	-66	-52	-29	-9	7	15	24	32	40	47	51	56	--
13	--	-157	-146	-136	-122	-102	-87	-68	-56	-34	-16	2	11	21	29	38	46	50	55	--
14	--	-162	-155	-147	-131	-112	-88	-73	-59	-41	-21	-4	7	16	27	36	43	49	54	--
15	-185	-169	-162	-157	-144	-120	-94	-76	-61	-45	-27	-10	3	14	24	34	41	47	53	58
16	-192	-178	-172	-168	-159	-134	-96	-78	-64	-50	-32	-16	-2	10	22	30	39	46	52	58
17	-194	-185	-176	-168	-159	-129	-94	-80	-66	-52	-37	-21	-7	7	18	26	35	43	49	57
18	-196	-190	-177	-167	-150	-120	-92	-80	-67	-55	-42	-27	-12	3	14	23	33	42	48	53
19	--	-190	-178	-165	-141	-110	-89	-79	-67	-58	-45	-30	-16	-3	11	21	31	39	45	48
20	-206	-190	-178	-165	-141	-113	-90	-78	-70	-62	-48	-31	-17	-3	11	21	29	38	44	--
21	-203	-187	-176	-166	-147	-120	-94	-80	-69	-59	-45	-30	-14	-2	12	20	29	36	41	--
22	-201	-185	-175	-167	-151	-132	-100	-83	-70	-58	-43	-28	-13	-1	11	20	27	33	39	--
23	--	-178	-171	-163	-150	-132	-106	-88	-74	-60	-45	-28	-15	-3	7	15	23	30	--	--
24	--	-173	-166	-153	-144	-131	-107	-89	-74	-60	-48	-33	-19	-8	2	9	19	29	--	--
25	--	--	-159	-147	-137	-121	-105	-90	-74	-61	-48	-34	-20	-12	-1	8	20	28	--	--
26	--	--	--	-142	-130	-117	-104	-89	-74	-59	-45	-30	-20	-11	0	12	23	29	--	--
27	--	--	--	-140	-127	-116	-102	-88	-75	-58	-43	-27	-16	-7	4	15	23	30	35	--
28	--	--	--	-138	-126	-115	-101	-88	-74	-56	-41	-25	-14	-6	4	15	23	30	35	--
29	--	--	--	-137	-126	-112	-102	-90	-74	-55	-39	-25	-14	-6	3	13	21	27	35	40
30	--	--	--	--	-127	-116	-104	-93	-73	-56	-39	-27	-16	-8	-1	9	18	26	33	41
31	--	--	--	--	-135	-121	-109	-98	-77	-59	-42	-30	-18	-10	-1	9	17	25	34	42
32	--	--	--	--	-153	-127	-116	-103	-82	-62	-45	-33	-19	-11	-1	8	16	24	34	--
33	--	--	--	--	-167	-135	-118	-108	-87	-67	-47	-32	-19	-10	0	8	14	21	30	--
34	--	--	--	--	-178	-142	-119	-110	-88	-70	-49	-34	-20	-10	-1	9	15	22	30	--
35	--	--	--	-222	-185	-150	-124	-109	-88	-71	-53	-37	-21	-10	-1	9	16	20	--	--
36	--	--	--	-232	-189	-152	-126	-106	-85	-71	-58	-40	-22	-12	-1	--	--	--	--	--
37	--	--	-268	-235	-193	-153	-125	-100	-79	-71	-64	--	--	--	--	--	--	--	--	--

Preconsolidation Heads - Layer 13

	1	2	3	4	5	6	7	8	9	10	11	12	13	14	15	16	17	18	19	20
1	--	--	--	--	--	--	--	--	--	--	--	--	--	--	--	--	--	--	--	--
2	--	--	--	--	--	--	--	--	--	--	54	52	--	--	--	--	--	--	--	--
3	--	--	--	--	--	--	--	--	--	50	53	54	50	--	--	--	--	--	--	--
4	--	--	--	--	--	--	--	21	35	45	54	54	50	49	--	--	--	--	--	--
5	--	--	--	--	--	-39	-15	17	32	42	53	54	50	50	49	--	--	--	--	--
6	--	--	--	-65	-60	-35	-14	13	29	38	50	54	52	50	49	50	--	--	--	--
7	--	--	-75	-68	-61	-38	-15	8	27	34	49	53	53	51	49	50	53	--	--	--
8	--	--	-78	-75	-63	-41	-18	4	22	31	46	48	50	49	49	50	53	--	--	--
9	--	--	-84	-82	-67	-47	-19	-1	17	28	44	44	47	45	49	49	53	53	--	--
10	--	--	-100	-91	-72	-54	-23	-6	11	25	40	40	43	44	48	49	52	53	--	--
11	--	--	-103	-96	-79	-61	-31	-10	6	22	35	37	39	42	46	49	51	53	55	--
12	--	--	-112	-103	-89	-63	-39	-14	3	20	31	34	36	40	45	49	51	53	55	--
13	--	-144	-126	-110	-91	-65	-43	-18	-1	17	28	32	34	39	44	49	51	53	55	--
14	--	-145	-134	-116	-89	-66	-40	-19	-4	11	27	29	31	33	43	49	49	52	54	--
15	-181	-151	-139	-120	-90	-65	-39	-21	-6	8	22	27	28	33	43	48	50	53	55	58
16	-190	-163	-141	-122	-91	-64	-33	-24	-10	3	16	22	26	33	42	47	50	54	57	60
17	-186	-164	-141	-122	-90	-55	-29	-25	-12	-1	10	18	25	33	41	46	50	53	58	60
18	-182	-164	-141	-123	-90	-56	-34	-27	-15	-6	6	13	24	33	40	45	49	53	59	61
19	--	-165	-141	-125	-93	-59	-40	-30	-19	-12	0	11	22	31	39	44	48	54	58	60
20	-192	-165	-141	-127	-98	-68	-45	-34	-26	-20	-5	9	21	30	38	43	48	53	56	--
21	-188	-160	-139	-125	-103	-78	-52	-41	-31	-21	-8	6	19	27	38	41	47	52	55	--
22	-183	-155	-137	-124	-108	-88	-62	-46	-35	-26	-9	4	15	25	36	41	46	50	54	--
23	--	-144	-131	-121	-112	-92	-75	-55	-41	-27	-14	4	15	25	35	41	44	49	--	--
24	--	-136	-127	-116	-109	-96	-84	-60	-43	-29	-15	4	14	24	33	37	42	48	--	--
25	--	--	-122	-114	-106	-95	-85	-64	-47	-30	-15	4	14	22	31	36	41	47	--	--
26	--	--	--	-109	-101	-92	-83	-64	-48	-30	-14	4	14	21	29	36	42	46	--	--
27	--	--	--	-106	-97	-89	-78	-63	-48	-30	-12	5	14	20	29	36	40	45	50	--
28	--	--	--	-100	-95	-85	-74	-61	-47	-28	-12	5	13	20	26	34	38	45	48	--
29	--	--	--	-95	-92	-81	-70	-60	-45	-26	-11	4	12	19	24	31	36	41	46	49
30	--	--	--	--	-88	-79	-69	-61	-41	-25	-10	3	12	17	21	28	33	38	42	48
31	--	--	--	--	-88	-79	-71	-63	-41	-26	-10	1	11	15	20	25	31	34	42	47
32	--	--	--	--	-92	-81	-74	-65	-45	-27	-9	-2	10	13	15	18	24	29	39	--
33	--	--	--	--	-102	-86	-77	-69	-49	-30	-12	-1	8	10	13	15	18	24	30	--
34	--	--	--	--	-112	-98	-83	-71	-50	-33	-16	-6	4	9	11	14	17	24	28	--
35	--	--	--	-157	-130	-112	-87	-72	-51	-37	-23	-12	1	8	10	13	16	20	--	--
36	--	--	--	-171	-143	-121	-91	-71	-51	-42	-34	-19	-3	3	9	--	--	--	--	--
37	--	--	-210	-180	-161	-125	-92	-70	-54	-48	-45	--	--	--	--	--	--	--	--	--

Preconsolidation Heads - Layer 14